University of Glasgow

Auditory sensory attenuation effect in emerging psychosis

Lingling Hua (MSc)

Submitted in fulfilment of the requirements for the Degree of Doctor of Philosophy

School of Psychology
Institute of Neuroscience & Psychology
College of Science and Engineering
University of Glasgow

September 2020

Abstract

Sensory consequences of one's own voluntary action are perceived as less intense than externally initiated sensations. This process is referred to as sensory attenuation. This sensory attenuation has been identified in humans and animals across various modalities, including visual, auditory and somatosensory domains. The auditory sensory attenuation is explored by comparing the auditory N/M100 amplitude between self- and external-initiated conditions. The focus of auditory sensory attenuation is mainly on the primary auditory cortex and the superior temporal cortex, while emerging evidence indicates that the sensory attenuation is present in broader brain area. Moreover, the generation of sensory attenuation relies upon the precise coordination of the motor system with sensory areas. However, sensory attenuation across the whole brain and the underlying neural interaction between brain areas remain underexplored. Importantly, failure in sensory attenuation is considered to play a role in clinical psychotic symptoms, such as auditory hallucination and illusion. This has been confirmed in chronic schizophrenia (ScZ), possibly resulting from disrupted frontal-temporal coordination during generating sensory attenuation. However, it currently remains unclear whether deficits in sensory attenuation emerge before the prodromal phase of psychosis, as well as what aberrant neural mechanism underlie emerging psychosis.

Given previous studies based on electroencephalogram(EEG) technology, the current thesis aimed to employ magnetoencephalography (MEG) to examine auditory M100 sensory attenuation. MEG-data were collected from 48 healthy controls (HC), 110 clinical high-risk psychosis (CHR), and 26 first-episode psychosis (FEP) participants during an auditory task in which pure tones were either elicited through a button press or passively presented. Auditory M100 event-related fields (ERFs) were recorded to assess auditory M100 sensory attenuation at the sensor- and source-level. The first aim was to map the sensory attenuation effect across the whole brain and further explore the association between motor-related activity and auditory sensory attenuation. Dynamic causal modelling (DCM) was also employed to determine the top-down and bottom-up modulation to determine the underpinning neural mechanism during sensory attenuation generation (Chapter 3). Subsequently, we focused on the auditory regions to address the sensory attenuation characteristics in emerging psychosis and its association with clinical features and cognitive functions. The goal was to address whether the sensory attenuation deficit could be regarded as a potential biomarker for early identification of psychosis

(Chapter 4). Finally, DCM was employed to explore the alteration of neural interactions across the sensory attenuation network in emerging psychosis and investigate the aberrant neural mechanism of sensory attenuation (Chapter 5).

The findings in Chapter 3 revealed that auditory M100 sensory attenuation was present in spatially distributed brain areas, involving various subcortical-cortical areas. In addition, the current results supported the modulation of motor-related activity with auditory sensory attenuation. The results from DCM further indicated the role of both top-down and bottom-up modulation of a thalamo-cortical network in generating auditory sensory attenuation. The results in Chapter 4 demonstrated impaired auditory M100 sensory attenuation in FEP and indicated that aberrant sensory attenuation emerged in the prodromal phase of psychosis. Moreover, the sensory attenuation effect in the auditory cortex was linearly associated with clinical symptom severity and cognitive performance. Finally, the DCM results in Chapter 5 suggested that the impaired sensory attenuation in FEP-participants originated from imprecise top-down control and subsequently enhanced bottom-up input (prediction error). The deficits in top-down control in CHR-individuals were not strong, while CHR participants were characterized by increased bottom-up inputs, which was intermediate between HC and FEP. Collectively, the results of this thesis suggested impaired auditory sensory attenuation in emerging psychosis, resulting from aberrant top-down and bottom-up interaction. This provides evidence that the auditory M100 sensory attenuation could be a potential candidate for the early detection of psychosis.

Table of Contents

Contents

List of Tables

List of Figures

List of Accompanying Material

List of Publications

The findings presented in Chapter 3:

Hua, L., Recasens, M., Grent‐'T‐Jong, T., Adams, R. A., Gross, J., & Uhlhaas, P. J. (2020). Investigating cortico‐subcortical circuits during auditory sensory attenuation: A combined magnetoencephalographic and dynamic causal modeling study. *Human brain mapping*.

Acknowledgment

First of all, I would like to thank my supervisor Professor Peter Uhlhaas for guiding me to perform research critically and scientifically. Your enthusiastic and prudent attitude on research will always inspire me. Thanks for providing me a supporting platform to challenge, push, and improve myself. Special thanks for your patience and huge support during my thesis writing-up.

I would also like to thank particularly to Dr Marc Recasens for always keeping your door open and training my independence to analysis data, as well as your black humour. Although words are weak and pale, special appreciation should be given to Dr Tineke Grent-t'Jong for sharing your professional knowledge and skills during your practical teaching, which really benefits a lot. Thanks a lot for your enormous support, encouragement, and patience in all forms to get through my last two years.

Great thanks to my colleague Dr Thune Hanna and Dr Emmi Mikanmaa. It was such an enjoyable journey to work together with you. I appreciate for your companion and cheer-up throughout my PhD study. Thanks to Dr Frauke Schultze-Lutter, Kelly Chung, Dr Thune Hanna, and Dr Emmi Mikanmaa for teaching me how to perform clinical assessments. Thanks to Gavin Paterson and Frances Crabbe for training me as a MEG operator. I would like to thank all other colleagues and interns for these lovely memories during my PhD study. Finally, I would also like to thank all the participants I have met.

I would like to thanks my previous officemates Dr Keith Anne and Dr Domenica Veniero for having me together with lots of activities, making me feel welcome and warm in UK. Thanks a lot for my chocolate-girl Kate to have you alongside. I would also like to thank my Glasgow friends Wei Liu, Chaona Chen, Jingjing Liu (Machester), Xuhong Liu, Guopeng Yu, Guoshuai Li, Keyu Zhai, for your together time during my PhD journey. I also need to thank my remote friends Minxing Fang, Yi Xie in China for all your ears with my ups and downs. Lastly, I sincerely thank my lovely roommates Xiaofei Cao, Shuqi Rao for your family-like companion when I was thousands of miles away from home. I am fortunate to meet you and share loads of joyful memory with you during this journey.

I especially thank my family, particularly thanks to my mom for your endless love and to my dad for your always support on my way. Special thanks to my brother and sister-in-law, for your care and bringing me lovely niece Xi Hua.

Last but not the least, I would like to thank the support from the Chinese Scholarship Council (CSC) for offering me this opportunity. Great thanks to my master supervisor Prof Zhijian Yao and Prof Lu Qing for paving me the path to pursue my study, as well as my previous hospital, Nanjing Brain Hospital, for permitting me to study abroad. I would also like to thank Haiteng Jiang for your encouragement during this wonderful and precious Journey.

Definitions/Abbreviations

ACC	Anterior Cingulate Cortex
AD	Axial Diffusivity
APS	Attenuated Psychotic Symptoms
AUC	Areas Under the Curve
BACS	Brief Assessment of Cognition in Schizophrenia
BLIPS	Brief Limited Intermittent Psychotic Symptoms
BS	Basic Symptoms
BSABS	Assessment of Basic Symptoms
BSIP	Basel Screening Instrument for Psychosis
CAARMS	Comprehensive Assessment of At-Risk Mental State
CCNi	Centre for Cognitive Neuroimaging
CHR	Clinical High-risk Psychosis
CNB	Penn Computerized Neurocognitive Battery
COGDIS	High-risk criterion Cognitive Disturbances
COPER	Cognitive-Perceptive Basic Symptoms
CRB3	Lobe III of Cerebellum
CRB45	Lobe IV, V of Cerebellum
DA	Dopamine
DCM	Dynamic Causal Modelling
DMN	Default Mode Network
DSM	Diagnostic and Statistical Manual of Mental Disorders
DTI	Diffusion Tensor Imaging
EEG/MEG	Electro/Magnetoencephalography
ERP/ERF	Event-Related Potential/Field
FA	Fractional Anisotropy
FDR	False Discovery Rate
FEP	First-episode Psychosis
GAF	Global Assessment of Functioning
GRD	Genetic Risk and Deterioration Syndrome
HC	Healthy Control
HES	Heschl's Gyrus
ICA	Independent Component Analysis
ICD	International Statistical Classification of Diseases and Related Health Problems
IPL	Inferior Parietal Cortex
ISI	Inter-stimulus Interval
LCMV	Linear Constraint Minimum Variance
MINI	Mini International Neuropsychiatric Interview
MMN	Mismatch Negativity
MRC	Medical Research Council
MRI	Magnetic Resonance Imaging
MRMFs	Movement‐related Magnetic Fields
PANSS	Positive and Negative Syndrome Scale
PAS	Premorbid Adjustment Scale

PCA	Scale of Perceptual and Cognitive Anomalies
PCC	Posterior Cingulate Cortex
PET	Positron Emission Tomography
PoCG	Postcentral Gyrus
PQ-16	16-item Prodromal Questionnaire
PreCG	Precentral Gyrus
RD	Radial Diffusivity
RMS	Root Mean Square
ROI	Regions of Interest
ROL	Rolandic Operculum
RT	Reaction Time
SCID-I	Structured Clinical Interview for DSM-IV-TR AXIS I disorders
ScZ	Schizophrenia
SIPS	Structured Interview for Prodromal Syndromes
SOA	Stimulus Onset Asynchrony
SOPS	Scale of Prodromal Symptoms
SPECT	Single-photon Emission Computed Cosmography
SPI-A	Schizophrenia Proneness Instrument, adult version
ST	Superior Temporal Cortex
SVD	Singular Value Decomposition
TMS	Transcranial Magnetic Stimulation
TOM	Theory of Mind
UHR	Ultra-high Risk
UTC	Unusual Thought Content
VIF	Variance Inflation Factor
Your-study	Youth Mental Health Risk and Resilience Study

Chapter 1 A general introduction to schizophrenia and clinical high-risk psychosis

1.1 Introduction

Schizophrenia (ScZ) is a chronic and disabling mental disorder affecting 20 million people worldwide (James et al., 2018). The lifetime prevalence of ScZ is approximately 1% with a peak onset during adolescence or early adulthood in males and 3-4 years later in females (Gore et al., 2011). Quantitative and qualitative analyses revealed that sustained recovery for at least 2 years in ScZ was about 13.5% (8.1%–20.0%). Less than 20% of ScZ patients were employed in Europe (Marwaha et al., 2007) and data from the USA suggested that 20% of ScZ patients became homeless after a one-year follow-up (Folsom et al., 2005). Consequently, ScZ causes significant social and economic costs (Cloutier et al., 2016). In 2010, psychotic disorders cost the UK and EU economies €16,717 and €93,927 respectively (in million € purchasing power parity (PPP)) (Gustavsson et al., 2011).

ScZ was first described as 'dementia praecox' (Kraepelin, 1971) and Bleuler coined the name ScZ in the early twentieth century (Bleuler, 1950). The International Classification of Diseases (ICD) and the Diagnostic and Statistical Manual of Mental Disorders (DSM) categories the symptoms of ScZ into positive and negative symptoms (Association, 2013). Positive symptoms include hallucinations and delusions, while negative symptoms include affective blunting, alogia (poverty of speech), avolition (an inability to initiate and persist in goal-directed activities), and anhedonia. Additionally, a third cluster has been proposed in DSM-V, a disorganization syndrome, consisting of poor attention, mannerisms and posturing, conceptual disorganization, difficulty in abstract thinking, and disorientation (Brekke, DeBonis, & Graham, 1994; Liddle, 1987). Both negative and disorganization symptoms are more strongly associated with cognitive impairments than positive symptoms (Cuesta & Peralta, 1995).

1.2 Pathogenesis of ScZ

1.2.1 Pathophysiology of ScZ

The pathophysiology of ScZ involves alterations in several neurotransmitter systems. Among these, the dopamine hypothesis has received considerable attention, and medications targeting aberrant dopaminergic activity remain the main pharmacological intervention.

However, during the last two decades, the interaction of the dopamine system with other neurotransmitter systems, such as the glutamate and γ-Aminobutyric acid (GABA) system has given way to a more comprehensive and diverse view on aberrant neurotransmitter-systems in ScZ.

1.2.1.1 **Dopamine hypothesis**

Evidence of dopamine (DA) involvement in ScZ developed in the 1950s with the discovery of reserpine, from the plant Rauwolfia serpentina that was approved for antipsychotic use in 1955 (Hollister, Krieger, Kringel, & Roberts, 1955) and it was soon discovered to block the accumulation of DA (Carlsson, Lindqvist, & Magnusson, 1957). As a result, Carlsson et al (1959) speculated an imbalance in DA release might underlie psychosis. Further support for this hypothesis came from studies with the dopamine agonist amphetamine, which could induce psychotic symptoms similar to those in ScZ (for a review see (Lieberman, Kane, & Alvir, 1987)).

Substantial evidence from genetic, molecular, and post-mortem studies have implicated hyperactivity of dopamine in ScZ, particularly in subcortical brain regions, including striatal areas, ventral tegmental area, and substantia nigra. With the aid of autoradiographic techniques, post-mortem studies revealed altered DA receptors in ScZ patients, located in nucleus caudate, putamen, and nucleus accumbens (Owen et al., 1978), particularly involving D2 receptors (Cross, Crow, & Owen, 1981). Moreover, modifications to the dopamine theory have implicated reduced dopaminergic neurotransmission in the neocortex, particularly in prefrontal regions, to account for the negative symptoms and impairments in cognition (Davis, Kahn, Ko, & Davidson, 1991; Goldman-Rakic, Castner, Svensson, Siever, & Williams, 2004; Tamminga, 2006). Consistent with post-mortem studies, studies using positron emission tomography (PET) and single-photon emission computed tomography (SPECT) confirmed increased D2 receptor density in subcortical areas (e.g., striatum) (Abi-Dargham et al., 1998; Davis et al., 1991; Laruelle, 1998; Laruelle, Abi-Dargham, Gil, Kegeles, & Innis, 1999).

Furthermore, increased dopamine activity in patients with ScZ could result from increased DA synthesis, DA receptors, or DA projection (Howes, McCutcheon, & Stone, 2015). Advanced neuroimaging techniques provided alternative approaches to explore dopamine-related neurochemical features in the DA system. Accumulation of [^{18}F] or [^{11}C]-labelled 3,4-dihydroxyphenylalanine (DOPA) was used to test DA synthesis. Although inconsistent

results of increased dopamine were reported, Lyon et al. (2009) found enhanced accumulation of [^{18}F] DOPA or [^{11}C] DOPA in the striatum, caudate, and putamen of patients providing evidence of increased synthesis (Lindström et al., 1999) and release of dopamine at the presynaptic level (Howes & Kapur, 2009) in ScZ patients. Interestingly, studies revealed increased subcortical synaptic dopamine density and basal dopamine synthesis in participants at clinical high-risk for psychosis (CHR) (Egerton et al., 2013; P Fusar-Poli et al., 2011; Fusar-Poli et al., 2010). Moreover, CHR individuals who converted to psychosis displayed greater dopamine synthesis capacity relative to non-converters (Howes et al., 2011).

1.2.1.2 **Glutamate hypothesis**

In addition to alterations in dopaminergic neurotransmission, aberrant glutamatergic activity has been implicated in ScZ (Olney & Farber, 1995), partly through interactions with other neurotransmitters, such as dopamine and gamma-aminobutyric acid (GABA)(for a review see (Kantrowitz & Javitt, 2010; Poels et al., 2014)).

The principle glutamatergic receptors associated with the pathophysiology of ScZ are NMDA- (Stone, Morrison, & Pilowsky, 2007) and AMPA-receptors (Meador-Woodruff & Healy, 2000). The initial studies with NMDA receptor antagonists phencyclidine and ketamine demonstrated the clinical positive, negative, and cognitive symptoms of ScZ in healthy volunteers (Javitt & Zukin, 1991; Luby, Gottlieb, Cohen, Rosenbaum, & Domino, 1962). PET/SPECT provided an alternative window to examine the NMDA receptors in patients with ScZ, highlighting lower binding rates of specific and nonspecific NMDA receptors (Poels et al., 2014), thus indicating hypofunction of NMDA receptors.

In addition to the involvement of the NMDA-receptors in ScZ, the abnormal functioning of the AMPA-receptors was also noticed. Harrison et al (1991) and Eastwood et al (1995) (1997) reported decreased expression of the mRNA encoding the gluR1 subunit in the medial temporal lobe and hippocampal regions. However, findings for the alteration of AMPA-receptors in cortical (frontal, anterior cingulate cortex) and other subcortical regions (caudate, putamen, and accumbens) have yielded inconsistent results (Healy et al., 1998; Meador-Woodruff & Healy, 2000; Sokolov, 1998).

1.2.2 Genetics hypothesis

Data from family, adoption, and twin studies provided evidence that ScZ is highly heritable (Gejman, Sanders, & Kendler, 2011; Ingraham & Kety, 2000; Franz Josef Kallmann, 1938; Franz J Kallmann, 1946). For example, the offspring of patients with ScZ are 10 times more likely to develop psychosis than the general population (for a review see (Kendler & Diehl, 1993)). Furthermore, twin studies have revealed concordance rates of 40% to 50% for monozygotic twins and 11% (3% to 19%) for dizygotic twins (for a review see (Sullivan, Kendler, & Neale, 2003)). With the advent of molecular genetics in the early 1980s, several candidate genes were identified. These findings, however, based on affected families or a priori-hypotheses, could only test a small number of genes (Risch & Merikangas, 1996), resulting in small effect sizes and difficulties in replications (Gejman et al., 2011). The ability to map and identify millions of common single nucleotide polymorphisms (SNPs) led to the genome-wide association study (GWAS) approach. A recent study with 34,241 cases and 45,604 controls identified 108 genes involved in dopamine synthesis, calcium channel regulation, immune responses, and glutamate receptors (Ripke et al., 2014).

1.2.3 Neurodevelopmental hypothesis

Weinberger et al (1987) and Murray & Lewis et al (1987) proposed that ScZ has its origins in aberrant brain development. This is supported by findings indicating aberrant cytoarchitectural data, altered left-right hemispheric asymmetry, and maternal infection (for reviews see (Rapoport, 2005, 2012).

One important risk factor during the prenatal period is obstetric complications (OCs) which are associated with an odds ratio of 2.0 to develop ScZ (Geddes & Lawrie, 1995; Geddes et al., 1999). Furthermore, maternal exposure to infection also increases the susceptibility to ScZ (Brown & Derkits, 2009; Mortensen et al., 2007; Pedersen, Stevens, Pedersen, Nørgaard-Pedersen, & Mortensen, 2011). In addition, maternal famine during prenatal periods is associated with increased risk (St Clair et al., 2005; Xu et al., 2009). Finally, longitudinal studies investigating early-onset ScZ, and CHR participants revealed alterations of grey matter in frontal, temporal, and subcortical regions, as well as widespread white matter abnormalities prominently in the prefrontal regions(Rapoport, 2012).

1.2.4 Environmental factors

A growing body of evidence has offered a new insight into the important role of environmental factors in ScZ, particularly involving urbanicity, minorities, trauma, and drug abuse. Specifically, there is consistent evidence for a close association between childhood trauma and the development of ScZ. For example, both physically and sexual abuse, as well as neglecting childhood have been associated with psychotic symptoms, such as auditory hallucinations and delusions (Read, van Os, Morrison, & Ross, 2005). In terms of the mediating effect of trauma on psychosis, a model has been proposed which integrates the hypothalamic–pituitary–adrenal (HPA) axis (Nemeroff, 2004; Read, Perry, Moskowitz, & Connolly, 2001) with psycho-social processes (Read, 1997; Read et al., 2005).

Moreover, substance use, including cannabis, alcohol, amphetamine, and cocaine, can induce transient psychotic symptoms. The fact that individuals with ScZ have a high prevalence of substance use raises the question of whether substance abuse is a causative factor for psychosis (Koskinen, Löhönen, Koponen, Isohanni, & Miettunen, 2009; Toftdahl, Nordentoft, & Hjorthøj, 2016). Evidence from a Dutch nationwide sample reported robust evidence that substance abuse increased the overall risk for ScZ, particularly cannabis and alcohol (Nielsen, Toftdahl, Nordentoft, & Hjorthøj, 2017), possibly through increasing striatal dopamine level (Jordaan, Warwick, Nel, Hewlett, & Emsley, 2012). In addition, it has been suggested that cannabis, in particular the psychotropic component delta-9-tetrahydrocannabinol (THC), induces acute psychotic symptoms (D'Souza, Cho, Perry, & Krystal, 2004) and even exacerbates existing psychotic symptoms (Mathers & Ghodse, 1992; Thornicroft, 1990).

Interestingly, early evidence indicated that geographical variation, such as urbanicity, impacts upon the incidence of ScZ (Hare, 1956a, 1956b). Recent evidence has confirmed this association, including several meta-analyses (Kelly et al., 2010; Krabbendam & Van Os, 2005; March et al., 2008). This association remained even after controlling for various confounds, such as social and economic variables (Kelly et al., 2010; Krabbendam & Van Os, 2005; March et al., 2008). Although it is not clear which specific factors mediate the relationship between urbanicity and ScZ, it is conceivable that environmental factors impact childhood and adolescence development in a continuous or repeated exposure pattern (Krabbendam & Van Os, 2005). Building upon this evidence, Van Os et al (2009) proposed the psychosis proneness–persistence–impairment model of psychotic disorders, whereby

exposure to environmental factors shifts individuals from ‘psychosis proneness to ‘psychosis persistence’ and subsequently, repeated exposure results in ‘psychosis impairment’.

Finally, the link between immigration and ScZ was first proposed by Ødegaard (1973) landmark study investigating Norwegian migrants to the USA. Meta-analyses have presented consistency for the correspondence between migration and the risk of ScZ across a wide range of approaches, endpoints, settings, and cultural group definitions (Bourque, van der Ven, & Malla, 2011; Cantor-Graae & Selten, 2005). The mediating effect of migration is not yet explained, although it has been proposed that post-migration factors (e.g. cultural bias, the ethnic density of the areas) (Bourque et al., 2011; Cantor-Graae & Selten, 2005; Veling et al., 2008) and social adversity (Veling et al., 2008) could facilitate the development of ScZ.

1.3 Clinical high-risk for psychosis (CHR)

It has long been acknowledged that the symptoms of ScZ are present before the first psychotic episode(Sullivan, 1927), emerging late adolescence, or early adulthood. The prodromal phase can be up to 5 years, featured by attenuated subthreshold psychotic symptoms (Klosterkötter, Hellmich, Steinmeyer, & Schultze-Lutter, 2001). During the last two decades, the clinical view of psychosis has transitioned to characterize the prodromal phase of psychosis with the aim of early recognition and prevention of psychosis. More specifically, the introduction of high-risk psychosis criteria in the 1996 formed the milestone to operationally identify pre-psychotic phase(Yung et al., 1996), giving rise to ‘at-risk mental state’, ‘ultra-high risk’,’ clinical high-risk’ status. The foundation of criteria facilitates to identify young individuals (14 to 35 years) who have the risk of developing psychosis.

Meta-analysis suggests that the median prevalence of subclinical psychotic symptoms in the general population is about 5% (Van Os, 2009). In comparison, the rate is a little higher among children (9 to12 years old) and adolescents (13 to18 years old) with 17% and 7.5% (Kelleher et al., 2012), respectively. The trajectory of developing first-episode psychosis (FEP) proceeds through the early at-risk psychosis and later at-risk psychosis state (Häfner et al., 2004), which was subsequently refined to the premorbid phase, prodromal phase, and psychotic phase (Fusar-Poli et al., 2013) (Figure 1.1). Specifically, the prodromal phase of psychosis is defined by basic symptom (BS) criteria and ultra-high risk (UHR) criteria, respectively (Fusar-Poli et al., 2013). There is suggestive evidence that BS and UHR are proposed sequence of symptom development in the at-risk phase (Schultze-Lutter,

Ruhrmann, Berning, Maier, & Klosterkötter, 2010). A few studies compared the different characteristics of individuals at various stages of high-risk psychosis, suggestive of individuals with BS displayed intermediate neurocognitive performance between healthy control (HC) and UHR individual (Frommann et al., 2011), as well as the P300 impairment was more pronounced in the later at-risk state than in early at-risk state (Frommann et al., 2008). Furthermore, the BS and UHR criteria were well-accepted to early recognize CHR for the benefit to improve the detection of individuals at risk state of psychosis. Existing evidence from meta-analysis suggested that participants who met both BS and UHR criteria have more risk to convert to psychosis than UHR criteria only(Fusar-Poli, Cappucciati, Bonoldi, et al., 2016).

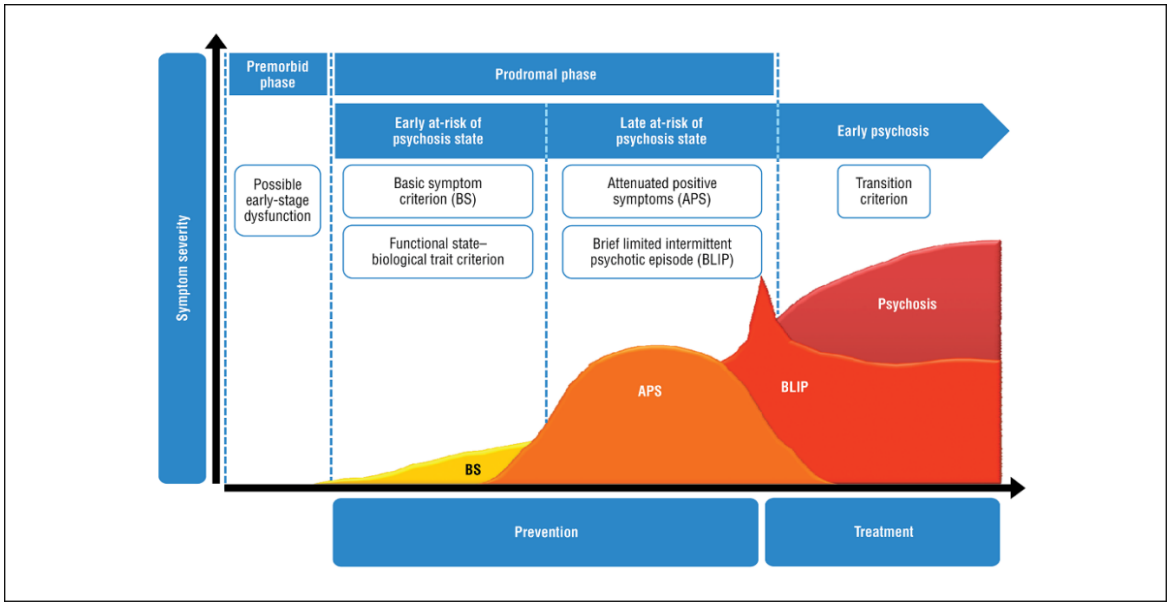

Figure 1.1 The trajectory of psychosis

The higher the line on the y-axis, the higher the symptom severity(Fusar-Poli et al., 2013).

The concept of BS was proposed by Huber and Gross (1989). BS are self-experienced symptoms that involve alterations in perception, thought processes, speech, and attention. The first instrument was the Bonn Scale for the Assessment of Basic Symptoms (BSABS) (Ziermans, Schothorst, Sprong, & van Engeland, 2011), followed by the Schizophrenia Proneness Instrument, adult version (SPI-A)(Schultze-Lutter, Addington, Ruhrmann, & Klosterkötter, 2007). The SPI-A classifies BS criteria into two subsets: 1) Cognitive-Perceptive Basic Symptoms(COPER)(10 cognitive-perceptive BS) and 2) High-risk criterion Cognitive Disturbances(COGDIS)(9 cognitive BS) (Schultze-Lutter, Klosterkötter, Picker, Steinmeyer, & Ruhrmann, 2007)(Table 1.1). For COGDIS criteria, the participant

has at least two of nine cognitive disturbance BS during the last three months. For COPER criteria, the subject has at least one of ten cognitive perceptive BS, which first occurred more than 12 months ago and presented within the last three months(Schultze-Lutter, Addington, et al., 2007).

Table 1.1 COGDIS and COPER criteria of SPI-A

COGDIS Criteria	COPER Criteria
Inability to divide attention	Thought interference
Thought interference	Thought preservation
Thought pressure	Thought pressure
Thought blockages	Thought blockages
Disturbance of receptive speech	Disturbance of receptive speech
Disturbance of expressive speech	Decreased ability to discriminate between ideas/perception, fantasy/true memories
Unstable ideas of reference	Unstable ideas of reference
Disturbances of abstract thinking	Derealisation
Captivation of attention by details of the visual field	Captivation of attention by details of the visual field
	Acoustic perception disturbances

Moreover, UHR-criteria includes attenuated psychotic symptoms (APS), brief limited intermittent psychotic symptoms (BLIPS), and trait vulnerability plus a marked decline in psychosocial functioning (genetic risk and deterioration syndrome, GRD). Several instruments have been developed to examine attenuated psychotic experiences, such as the companion Scale of Prodromal Symptoms (SOPS) (Lencz, Smith, Auther, Correll, & Cornblatt, 2003), the Basel Screening Instrument for Psychosis (BSIP), the Structured Interview for Prodromal Syndromes (SIPS) (McGlashan et al., 2001; Miller et al., 1999) and the Comprehensive Assessment of At-Risk Mental State (CAARMS) (Yung et al., 2005). In addition to the Schizotypal Personality Disorder Checklist, family history questionnaire, and global assessment of functioning scale (GAF), SIPS contains 19 items designed to measure the severity of prodromal symptoms of psychosis, including 5 positive, 6 negative, 4 disorganization, and 4 general symptom items.

1.3.1 Clinical outcome of CHR individuals

The establishment of CHR criteria facilitates to capture CHR in both clinical service and the general public population. However, only a few CHR will eventually develop to psychosis over time. The quantitative studies unveiled approximately 20 to 35% of CHR participants will develop psychosis most likely within 2 years (Fusar-Poli, Bonoldi, et al., 2012; Fusar-Poli, Cappucciati, Borgwardt, et al., 2016; Kempton, Bonoldi, Valmaggia, McGuire, & Fusar-Poli, 2015; Schultze-Lutter et al., 2015b), and the newest transmission rate is about 20% (Fusar-Poli et al., 2016). After two years, the transition risk tends to plateau. For example, the risk to psychosis was about 3.2% from 6 years follow-up onwards for subjects who were referred to secondary mental health services for specialized assessment and treatment (Fusar-Poli et al., 2017), and the overall transition rate was around 35% over a 10 years follow-up (Nelson et al., 2013).

Efforts have been made to explore the predictive factors of the onset of psychosis. Among these factors, the heterogeneity subgroups of CHR may present different transition risk to psychosis. Schultze-Lutter et al. (2015a) suggested that the conversation rate of CHR is relatively similar between those meeting the APS-criteria and the COGDIS subset of SPI-A until 2-year follow-up, while the conversation rate of COGDIS is significantly higher thereafter. Later on, the prognostic validity of BS and UHR was initially investigated by using the areas under the curve (AUC), suggesting that the predictive accuracy of BS for psychosis over three years was beyond mere chance and of UHR criteria was poor (Hengartner et al., 2017). Additionally, the reliability and prediction ability of UHR subgroup criteria was further estimated by meta-analysis. The proportion of CHR individuals meeting APS criteria (85%) was much larger than those meeting BLIPS criteria (10%). There was a higher risk of psychosis in BLIPS groups than APS groups after 24-, 36- and 48- months of follow-up. In contrast, the GRD subgroup is not strongly associated with an increased risk of psychosis relative to APS and BLIPS (Fusar-Poli, Cappucciati, Borgwardt, et al., 2016). Moreover, one crucial consequence of the various criteria of CHR could eventually hinder the identification of reliable clinical biomarkers for clinical practice(Fusar-Poli, 2017). It is thus essential to further explore the risk factor to psychosis in CHR subgroups.

1.3.2 Cognitive impairment in CHR-participants

Cognitive impairment is a core feature of ScZ, involving a broad range of malfunction that encompass deficits in social cognition (Elvevag & Goldberg, 2000) and neurocognition. The importance of cognitive deficits in ScZ is due to their close association with functional outcomes.

Evidence from a large body of work established that disturbances in cognition in patients with ScZ were associated with large effect sizes (d= 0.90–1.08) and in remitted ScZ patients (d = 0.80) (Bora, Yucel, & Pantelis, 2009; Brüne, 2005). Importantly, cognitive deficits encompassing both neurocognition and social cognitive measures are present before the onset of psychosis (Addington, Penn, Woods, Addington, & Perkins, 2008; Thompson, Bartholomeusz, & Yung, 2011), in children who later developed to psychosis (Cornblatt, Obuchowski, Roberts, Pollack, & Erlenmeyer–Kimling, 1999; Jones, Murray, Rodgers, & Marmot, 1994), as well as in the offspring and siblings of individuals with ScZ (Agnew-Blais & Seidman, 2013; Meijer, Simons, Quee, Verweij, & Investigators, 2012; Sitskoorn, Aleman, Ebisch, Appels, & Kahn, 2004; Snitz, MacDonald III, & Carter, 2005)

Neurocognitive deficits are also present in CHR-individuals, involving impairments in attention, executive functions, verbal fluency, and working memory (Fusar-Poli, Deste, et al., 2012), and the effect size was between those observed in ScZ and HC(Giuliano et al., 2012; Pukrop & Klosterkötter, 2010). In addition, longitudinal studies have revealed an association between cognition deficits at baseline and clinical outcomes as well as functional outcomes (Addington & Barbato, 2012; Carrión et al., 2013). Specifically, verbal fluency and memory impairments were linked to conversion to psychosis in CHR-participants (for a review see (Fusar-Poli, Deste, et al., 2012)).

In addition, CHR-participants display moderate deficits in affect recognition and affect discrimination (Edwards, Pattison, Jackson, & Wales, 2001), as well as deficits in Theory of Mind (TOM) (Brüne, 2005). In comparison to neurocognition, a meta-analysis suggests that social cognitive deficits are not strong predictors of conversion to psychosis (Van Donkersgoed, Wunderink, Nieboer, Aleman, & Pijnenborg, 2015). Given the crucial role of cognitive deficits in clinical outcomes as well as social and role function in CHR-participants, several studies have investigated the possibility to target impairments in neurocognition through cognitive remediation (Loewy et al., 2016; Piskulic, Barbato, Liu, & Addington, 2015).

1.3.3 Sensory processing deficits across different stages of psychosis

As aforementioned, various cognitive impairments across different domains were reported in ScZ, while last several decades brought a renewed interest in sensory processing deficits. The sensory processing deficits could affect the sensory experience in individuals with ScZ (Javitt, 2009a). Furthermore, evidence indicated that the early sensory information processing potentially impacts the following cognitive processing (Hamilton et al., 2018). Event-related potentials/fields (ERP/Fs) are time-locked brain response to evoked stimuli, described by its amplitude and latency. ERP/Fs are reflective of the perceptual and cognitive process in neurophysiological mechanism in the brain. Several ERP/Fs components have consistently been found to be abnormal in ScZ, including those involved in early stages of sensory processing (Hornix, Havekes, & Kas, 2018).

The Mismatch Negativity (MMN) does not require attention during tasks, a negative-potential with a peak around 150 to 250 ms after the onset of a deviant stimulus, (Näätänen & Kähkönen, 2009). Although normal MMN amplitude has been reported (Erickson, Ruffle, & Gold, 2016), substantial evidence has highlighted reduced MMN amplitudes in CHR samples in response to duration as well as frequency deviants compared to HC. Furthermore, the reduction of MMN amplitude in CHR who converted to psychosis was larger in comparison to non-converters.

The earlier ERP components, such as the P50 and N100/M100, have also been probed in ScZ. The P50 is a pre-attentive potential and has frequently been studied in the context of sensory gating. Sensory gating is typically explored by a paired-click paradigm in which two consecutive clicks are presented with an inter-stimulus interval (ISI). The difference (S1-S2) in amplitude between the first click (S1) and the second click (S2), or the S2/S1 ratio, provides an index of sensory gating. Besides the P50, the N100, a negative deflection peaking around 100 ms following stimulus onset, is also used to assess sensory gating (Oranje, Geyer, Bocker, Kenemans, & Verbaten, 2006). Although P50 and N100 sensory gating were consistently reduced in ScZ patients, findings in CHR-participants are mixed (Brockhaus-Dumke et al., 2008; Del Re et al., 2015; Hsieh et al., 2012; Shin et al., 2012; Van Tricht et al., 2015). Regarding the N100, several studies reported decreased N100 amplitudes in CHR-participants (Del Re et al., 2015; Gonzalez-Heydrich et al., 2015).

Furthermore, the early auditory sensory component N100 has been used to explore the phenomenon of sensory attenuation, which was estimated by comparing N/M100 amplitude between self-initiated and externally-generated sensation. Theoretically, the N100 amplitude is suppressed during self-induced tone in contrast to externally-initiated tone. The particular interest of sensory attenuation in psychiatry is that it can fundamentally alter the sensory experience of own voluntary action. Currently, the auditory N100 sensory attenuation is elicited by the action-auditory experiment paradigm that comparing N100 amplitude between self-initiated tone (self-talking) and externall-generated tone (Eliades & Wang, 2003; Horváth, 2015).

1.3.4 Dysconnectivity in psychosis

It is noteworthy that sufficient findings from neuroimaging data indicated that ScZ is a disorder of dysconnectivity (Friston, 2002; Stephan, Friston, & Frith, 2009). The abnormal neural circuits underlying task-positive network (Li, Chan, McAlonan, & Gong, 2010; Sheffield & Barch, 2016) and task-negative network (Giraldo-Chica & Woodward, 2017; Shenton, Dickey, Frumin, & McCarley, 2001) have been robustly confirmed in ScZ. Importantly, accumulating evidence proposed that pathophysiological processes in ScZ started before the full-blown of clinical symptoms (Yung & McGorry, 1996), presented with disrupted functional integration (Andreou & Borgwardt, 2020).

A substantial work revealed impaired functional coupling in CHR, including for working memory(Crossley et al., 2009; Schmidt et al., 2013), verbal-related task (Allen et al., 2010; Dauvermann et al., 2013), and resting-state (Du et al., 2018; Satterthwaite et al., 2015; Shim et al., 2010; Yoon et al., 2015). For instance, disrupted frontotemporal and frontoparietal connection have been reported in CHR (Crossley et al., 2009; Schmidt et al., 2013). Of note, such abnormalities were more prominent in CHR converters than CHR non-converters (Cao et al., 2018; Collin et al., 2018). Although various evidence indicated malfunction of neural interaction in CHR, there is no consensus of a comprehensive framework in CHR, possibly due to various tasks and sample heterogeneity(Andreou & Borgwardt, 2020). However, limited research explored the neural substrate of sensory processing deficits in CHR although accumulative evidence revealed the abnormal electrophysiological process in emerging psychosis.

1.4 Sensory attenuation

1.4.1 The concept of sensory attenuation

Conceptually, sensory attenuation can be described as reduced intensity of a sensation caused by voluntary movement compared to externally-generated inputs (Blakemore, Wolpert, & Frith, 1998a). It reflected the suppression of predictable self-initiated sensory consequence. One typical example in our daily lives is that we cannot be tickled by ourselves (Blakemore, Wolpert, & Frith, 2000) because the sensation induced by our voluntary movement was more predictable than externally initiated tickling. One advantage of sensory attenuation enables the brain to work more efficiently to deal with more alarming stimuli in the environment. Moreover, sensory attenuation facilitates the brain to distinguish self and nonself successfully. If we can't precisely identify self-initiated stimuli, this would lead to failure to distinguish internally- and externally-generated stimuli that have been linked to the generation of certain symptoms of psychosis, such as auditory hallucination and delusions (Feinberg, 1978; Feinberg & Guazzelli, 1999).

1.4.2 The sensory attenuation mechanism

Regarding the underlying mechanism of sensory attenuation, several frameworks have been proposed to interpret sensory attenuation. The efference copy model was first put forward by Vol Host and Mittelstaedt in 1950(von Holst & Mittelstaedt, 1950). The theory pointed out that during self-initiated sensation, efference copy of motor command is utilized to inform sensory cortex of the forthcoming sensory consequence of voluntary action, which was used to compare to actual sensory feedback (Von Holst, 1954). If there is a match between predicted and actual sensory outcome, leading to cancellation of afference signal, the organism will perceive the incoming sensation as less intense (Figure 1.2).

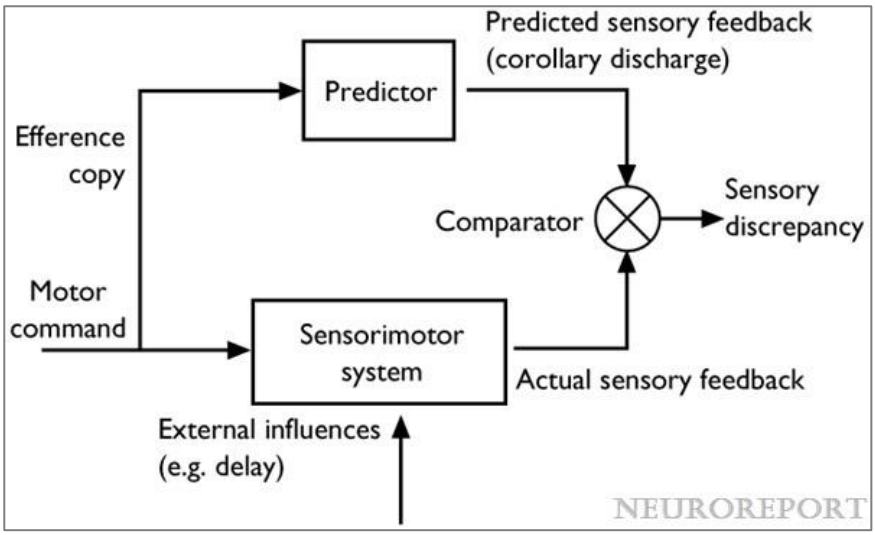

Figure 1.2 A model for determining the sensory consequences of a movement
Refer to (Blakemore et al., 2000).

Meanwhile, Sperry (1950b) independently put forward the corollary discharge to explain the process from the motor-related cortex to the sensory cortex. The fundamental idea of the corollary discharge theory is similar to the efference copy model, and the terms are used interchangeably. The distinction between the two theories is that the corollary discharge (efference copy) signal can arise from all levels of the motor pathway and target different levels of the sensory processing stream (Crapse & Sommer, 2008a, 2008b) (Figure 1.3). The term ‘efference copy’ indicates an actual copy of motor command to target the sensory cortex, while Sperry utilized the ‘corollary discharge’ to imply the signals from the motor cortex to the sensory cortex can be arose from different level of motor control. The efference copy/corollary discharge is interchangeable and has been adapted to interpret different systems in the brain. For example, the concept of an internal model, based on efference copy/corollary discharge frame, was proposed to illustrate the causal interaction between motor actions and their consequences in the human sensorimotor loop (Miall & Wolpert, 1996; Wolpert & Ghahramani, 2000). The efference copy of the motor command is used by the forward model to predict the forthcoming sensory state, and the feedback controller (inverse model) worked to adjust the motor command according to the mismatch between the estimated and real sensory states (Miall & Wolpert, 1996; Wolpert & Ghahramani, 2000).

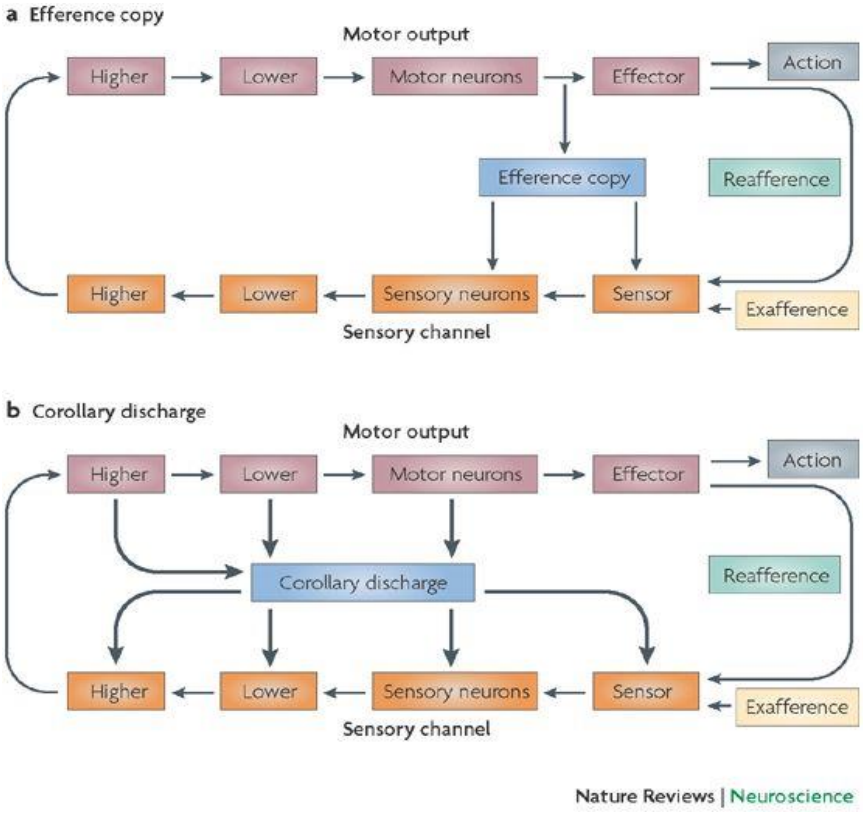

Figure 1.3 A schematic comparison of a sensorimotor circuit between efference copy and corollary discharge

The circuit comprises a sensory pathway (shown in orange) and a motor pathway (shown in brown) in the theory of efference copy and corollary discharge, respectively. Compared to efference copy theory, the motor to sensory signal in corollary discharge can arise from all levels of the motor pathway rather than a specific pathway(Crapse & Sommer, 2008a).

Furthermore, with the development of computational neuroscience, predictive coding account was proposed to explain sensory attenuation within the Bayesian inference principle(Friston & S. Kiebel, 2009; Rao & Ballard, 1999). Predictive coding account on perceptual inference was highlighted by Maher that the failure to integrate sensory input with learned expectation(Maher, 1974). Later, Gray (1991) and Hemsley and Garety(Hemsley & Garety, 1986) first interpreted the Bayesian analysis of delusions that how belief, evidence, and their disrupted interaction contribute to aberrant inference. Embedded in the predictive coding frame is the assumption that the brain is hierarchically organized and that predictions from higher levels are used to predict the sensory outcome of an action. For example, when there is a mismatch between the predicted and real sensory outcome, a prediction error signal is sent to the higher level to update the prediction model. To optimize the prediction, Bayesian inferences estimate the conditional and probabilistic occurrence of an event (posterior probability), which is based on the probability distribution of prior events and the probability that the event occurred given the evidence (likelihood).

In turn, the posterior probability becomes the prior distribution of the next event (Apps & Tsakiris, 2014; Friston & S. Kiebel, 2009). Therefore, it has been suggested that sensory attenuation was associated with an imbalance in a precision shift of the posterior data towards the sensory data and away from prior (Sterzer et al., 2018). One strength of the predictive coding account is that it is compatible with neurobiological data by providing a generic framework.

1.4.3 Sensory attenuation in HC

Sensory attenuation has been confirmed in humans (Blakemore et al., 1998a; Ford & Mathalon, 2004) and in simple and more complex organisms in a variety of modalities (Crapse & Sommer, 2008a), particularly in the auditory, visual, and tactile domains. In humans, behavioural studies related to auditory loudness perception reported a reduction in subjective loudness intensity when tones were self-initiated in comparison to externally generated sounds (Sato, Mengarelli, Riggio, Gallese, & Buccino, 2008) , in line with following studies with better control for predictivity component between two conditions (Sato, Mengarelli, Riggio, Gallese, & Buccino, 2008; Stenner et al., 2014; Weiss, Herwig, & Schütz-Bosbach, 2011). Furthermore, one study found that the reduced tone intensity during self-initiated stimuli was associated with the feeling of controlling over their action consequence (Stenner et al., 2014), in support of the motor origin of attenuated sensation.

In line with behavioural studies, the neuroimage studies demonstrated the sensory attenuation effect. Reduced hemodynamic activation in the temporal cortex was present during self-generated words compared to externally generated words in healthy volunteers(Warburton et al., 1996). The first study from electroencephalography (EEG) reported auditory N100 sensory attenuation in 1973(Schafer & Marcus, 1973), which was repetitively confirmed in the following EEG/magnetoencephalography (MEG) studies (Aliu, Houde, & Nagarajan, 2009; Baess, Horváth, Jacobsen, & Schröger, 2011; Cao, Thut, & Gross, 2017; Eliades & Wang, 2003).

1.4.4 Sensory attenuation in psychosis

As one perspective of sensory attenuation facilitates the brain to distinguish self and nonself, the failure of sensory attenuation was posited to account for clinical psychotic symptoms, such as ScZ patients often report sensory disturbance with the idea of being control or being persecuted. The underlying deficits in sensory attenuation were well-interpreted by the

failure of efference copy/corollary discharge mechanism. In other words, if an efference copy of an intended action(thought) does not produce a precise efference copy/corollary discharge of the expected experience, patients may fail to distinguish between their own thoughts and external generated stimuli, resulting in auditory hallucination or passivity experience (Feinberg, 1978; Feinberg & Guazzelli, 1999).

The dysfunction of corollary discharge in ScZ has been explored in visual and auditory domains during both behavioural and electrophysiological studies. Efference copy/corollary discharge has been confirmed to play an important role in sustaining visual stability during saccadic eye movement by predicting the post-saccadic retinal image(Zaretsky & ROWELL, 1979). Findings suggested that ScZ cannot precisely judge the direction of visual target according to the pre-saccadic visual target location during a saccadic double-step task(Rösler et al., 2015), in line with the findings from Thakkar (2015). Moreover, the disrupted corollary discharge existed in the auditory system in ScZ by employing self-generated speech paradigm, in which they demonstrated the failure to suppress self-initiated auditory N100 in patients with ScZ(Ford & Mathalon, 2004). The underlying neural mechanism of aberrant auditory N100 attenuation was due to disrupted gamma coherence between frontal and temporal areas(Ford, Gray, Faustman, Heinks, & Mathalon, 2005). This was putatively because of the damage to the white-matter (WM) fasciculus connecting the sites of discharge initiation and destination(Whitford et al., 2011). Importantly, the impairment of corollary discharge was associated with psychotic symptom severity(Heinks-Maldonado et al., 2007; Rösler et al., 2015).

In addition, the aberrant corollary discharge is also observed in schizotypy (Oestreich et al., 2015), first-degree relatives of ScZ patients(Ford et al., 2013), patients with schizoaffective disorder (Ford et al., 2013; Ford, Palzes, Roach, & Mathalon, 2014), as well as bipolar disorder patients with psychotic symptoms (Ford et al., 2013). However, there is currently limited evidence whether impairments in sensory attenuation are present before the onset of psychosis, such as in participants meeting clinical high-risk psychosis criteria(Mathalon et al., 2019; Perez et al., 2012; Poletti, Tortorella, & Raballo, 2019; Whitford et al., 2018). First evidence had indicated mixed evidence for impairments in CHR participants with some studies showing intact (Perez et al., 2011; Whitford et al., 2018), while a study from the same group but with a larger sample size did report a deficit in CHP (Mathalon et al., 2019). Therefore, it remains questionable whether sensory attenuation emerged before the full-blown of psychosis. In addition, current studies have utilized the technology of EEG to

investigate the auditory sensory attenuation. While in comparison to EEG, MEG detects the magnetic fields of primary current without deterioration along with the distance or brain tissue. The main advantage of MEG is good spatial resolution in separating cortical sources due to less spatial smearing. Therefore, MEG is suitable for precisely localising in the auditory region and further exploring the underlying neural mechanism in generating sensory attenuation.

1.4.5 Neurobiological mechanism of sensory attenuation

1.4.5.1 The neurobiological mechanism of sensory attenuation in HC

The generation of sensory attenuation involves in the precise coordination of the sensorimotor network. According to the efference copy theory, the efference copy is generated from motor-related areas. Existing evidence from neuroimaging studies implied several regions associated with the origin of efference copy, including the primary motor cortex (Abbasi & Gross, 2020; Chronicle & Glover, 2003), the supplementary motor cortex(SMA) (Haggard & Whitford, 2004), and the premotor cortex (PreM) (Christensen et al., 2007; Ellaway, Prochazka, Chan, & Gauthier, 2004). In particular, the repetitive transcranial magnetic stimulation (rTMS) study found that the alteration of SAM was closely associated with the suppression of sensory attenuation during voluntary action. They interfered the SMA activity by delivering a conditioning pre-pulse over the SMA before motor evoked potential was delivered over the left motor cortex(Haggard & Whitford, 2004), which could give rise to similar effect by intervening PreM with pre-pulse TMS (Christensen et al., 2007; Haggard & Whitford, 2004).

Furthermore, the cerebellum appears to play an important prediction role in the internal forward model during motor learning and motor control (Miall, Weir, Wolpert, & Stein, 1993; Wolpert, Miall, & Kawato, 1998). Accumulating evidence from HC (Blakemore, Frith, & Wolpert, 2001; Blakemore et al., 1998a; Blakemore, Wolpert, & Frith, 1999) and patients with focal cerebellum lesions suggested that the cerebellum was involved in predicting the sensory consequence of the voluntary movement(Knolle, Schröger, Baess, & Kotz, 2012; Knolle, Schröger, & Kotz, 2013; Roth, Synofzik, & Lindner, 2013). Recent evidence investigating the functional connectivity between the cerebellum and the somatosensory cortex indicates that the cerebellum is engaged in sensory prediction during self-generated sensations (Kilteni & Ehrsson, 2019). Moreover, the parietal cortex is also involved in the sensory prediction process through interaction with the cerebellum

(Blakemore & A. Sirigu, 2003; Pollok, Gross, Kamp, & Schnitzler, 2008). According to predictive coding framework, the interaction among sensory attenuation network is hierarchical. However, it remains underexplored regarding the hierarchical neural interaction during generating sensory attenuation in HC.

Apart from areas involving in generating sensory attenuation, researchers were interested in when the efference copy was generated. Existing evidence indicate that the efference copy is sent out during motor execution (Schneider, Nelson, & Mooney, 2014; Stenner, Bauer, Heinze, Haggard, & Dolan, 2015). However, animal studies suggests that vocalization-induced suppression begins several hundred milliseconds before the onset of vocalization (Eliades & Wang, 2003), supported by study from HC (Voss, Ingram, Haggard, & Wolpert, 2006). Furthermore, re-afference stage of motor action has been reported to impact the sensory attenuation (Burin et al., 2017; Kilteni & Ehrsson, 2017a, 2017b). These findings provided a cue that the prediction signal could originate from different stages of motor-related action.

1.4.5.2 The neurobiological mechanism of sensory attenuation in emerging psychosis

As frontal regions are associated with speech generation and responsible for modulating auditory cortex during vocalization (Creutzfeldt, Ojemann, & Lettich, 1989), evidence indicated that HC displayed increased gamma-band oscillations (25-40 Hz) between frontal and temporal regions during self-talking in comparison to passive listening to self-talking(Ford et al., 2005). However, the frontal regulation in temporal cortex was disrupted in ScZ patients during vocalization (Ford et al., 2005). Similarly, the communication between frontal and temporal region in the gamma oscillations was impaired in ScZ patients when there was a distortion between expected and actual sounds during speech, indicating malfunction of top-down control in frontal area(Ford & Mathalon, 2005) (Figure 1.4). Moreover, disturbed frontal-temporal coherence possibly resulted from abnormal myelination in frontal areas of ScZ patients as the N100 sensory attenuation was linearly related to fractional anisotropy of arcuate fasciculus due to delayed propagation of efference copy feedback (Whitford, Ford, Mathalon, Kubicki, & Shenton, 2010; Whitford et al., 2011). However, it remains unknown about the aberrant underlying neural interaction mechanism in CHR during generating sensory attenuation.

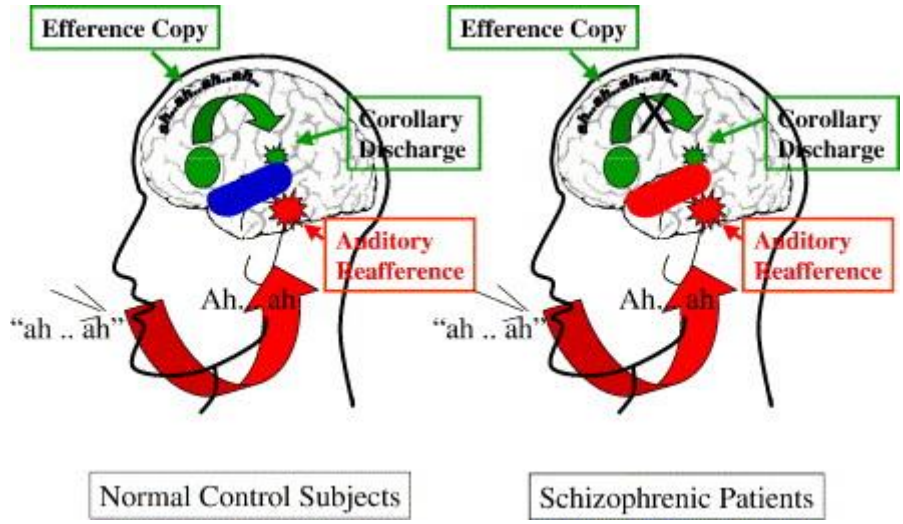

Figure 1.4 The operation of the corollary discharge/efference copy in ScZ

This panel shows the regular operation of the hypothesized efference copy/corollary discharge mechanism during speech (left) and its possible dysfunction in ScZ (right)(Ford & Mathalon, 2005). The speech originates in the frontal areas as shown in green circle. The frontal areas send efference copy (green ribbon) to the auditory cortex where it becomes a corollary discharge (green splash). At the same time, the talking is initiated and the speech sounds arrive at auditory cortex (red ribbon) as the auditory reafference (red splash). If the corollary discharge matches the auditory, then the auditory sensory experience is suppressed (blue). Otherwise, the failure to suppress auditory cortex is marked in red in ScZ patients.

1.4.5.3 Dynamic causal modelling in psychosis

According to the predictive coding account, successful generation of sensory attenuation yielded to the precise top-down and bottom-up modulation among the sensorimotor network. Functional connection estimated the temporal correlation between geographically distributed brain regions, providing insights about the large-scale neural communication(Friston, 2011). One of the functional connection approaches, effective connectivity, was designed to measure the hierarchical interaction between brain areas, including dynamic causal modelling (DCM), granger causal modelling (GCM) and structural equation modelling (SEM). Unlike SEM and GCM, DCM constructed a reasonably realistic neuronal model to estimate the relationship between brain areas.

DCM was first introduced in 2003 (Friston, Harrison, & Penny, 2003). The basic idea behind DCM is that the data could be modelled as a dynamic input-state-output system to estimate the experimental modulation on effective connections as DCM regards an experiment as a designed perturbation of neuronal dynamics are promulgated and distributed throughout the network to produce source-specific responses. In particular, DCM is a model-based approach

to compare numerous competing hypothesis about how observed data were generated by various models based on different connection patterns. Given EEG and MEG are distinctive to measure the excitability of neuronal populations with millisecond (ms) resolution (Uhlhaas et al., 2009), DCM for EEG/MEG are neurobiologically plausible to estimate the neural parameters based on the architecture underlying the neural dynamics.

DCM has been applied to psychiatric disorders to examine the neural mechanism underlying perceptual and cognitive disturbances. The constrained top-down control from the inferior frontal cortex to the occipital cortex was reported within ScZ patients, potentially associated with the malfunction of face perception (Dima, Dietrich, Dillo, & Emrich, 2010a). Similarly, the inability to increase backward modulation from right intraparietal sulcus to temporoparietal was associated with attention deficits in patients with ScZ when attended stimuli changed (Roiser et al., 2013). Regarding predictive processing, finding indicated malfunction of both top-down modulation (increased) and bottom-up input (attenuation) in ScZ during predicting the visual target (Fogelson, Litvak, Peled, Fernandez-del-Olmo, & Friston, 2014). In addition, supporting evidence from the auditory system revealed impaired top-down control from inferior frontal gyrus to superior temporal gyrus in ScZ during generating MMN(Dima, Frangou, Burge, Braeutigam, & James, 2012a). Furthermore, altered effective connectivity strength was associated with clinical psychotic experience in ScZ during the auditory oddball task, featured by impaired intrinsic connectivity between the left primary auditory cortex and the inferior frontal gyrus (Dzafic et al., 2021). Altogether, these results indicated that dysconnectivity in ScZ involves both top-down and bottom-up modulation.

Although a limited study investigated the aberrant effective connection in CHR, a sample of 24 patients with psychosis and 25 of their unaffected relatives displayed similar decreased intrinsic inhibitory self-connectivity in the inferior frontal gyrus. The aberrant intrinsic connectivity was reflective of excitability of the superior pyramidal cell population in the inferior frontal gyrus, indicating that increased prediction error was sent to the prefrontal cortex during generating MMN (Ranlund et al., 2016). One more DCM study investigated the psychotic patients and their unaffected relatives during generating P300, characterized by altered excitability synaptic gain in frontal and parietal sources during generating P300(Diez et al., 2017). These findings suggested that the abnormal neural interaction was presented in patients with psychosis and individuals with a genetic risk of psychosis. However, rare studies studied the disrupted hierarchical interaction of sensory attenuation network in emerging psychosis.

1.5 Research aim and hypothesis

As aforementioned, sensory attenuation deficits contribute to clinical psychotic symptoms, which has been confirmed in chronic ScZ and first-degree relatives of ScZ. However, it remains unanswered whether the impaired sensory attenuation is present before the onset of psychosis. Therefore, our current thesis attempted to investigate the sensory attenuation characteristics as indexed by auditory M100 in a large sample of individuals at clinical high-risk state and a smaller sample of FEP and HC participants. The goal was to examine the impaired sensory attenuation in emerging psychosis and to investigate whether the deficit in sensory attenuation could be a potential biomarker of psychosis. Furthermore, I sought to discuss the neural mechanism underlying the impaired sensory attenuation in psychosis by employing a DCM approach.

Before examining sensory attenuation in clinical samples, the first aim of this thesis was to explore the neurophysiological correlates of auditory sensory attenuation across the whole brain in HC with MEG technology. Given that attenuated brain activity has been observed beyond the sensory cortex, such as the thalamus and the inferior parietal cortex(Blakemore & Sirigu, 2003; Blakemore et al., 1998a), I first explored the sensory attenuation effect in the whole brain at the sensor- and source-level in HC in Chapter 3. In addition, the activity in the motor-related cortex was analysed to examine the association between motor-related activity and auditory sensory attenuation. Finally, DCM was employed to primarily examine the top-down and bottom-up interaction across the sensory attenuation network. I predicted that auditory sensory attenuation in HC involved not only in the auditory cortex, but also in cortical-subcortical areas, including thalamus and inferior parietal cortex. Moreover, I expected that the auditory sensory attenuation would be modulated by motor-related activity and resulting from the precise feedforward and feedback interaction among the sensory attenuation network.

In Chapter 4, my primary goal was to examine auditory sensory attenuation in patients with FEP and a sample of participants meeting CHR-criteria. I sought to investigate whether the impaired sensory attenuation is present before the onset of psychosis, as well as the association between auditory sensory attenuation and clinical psychotic symptoms and cognitive function. In addition, the M100 amplitudes in the active and passive condition were examined across groups to discuss the potential contribution of M100 malfunction to impaired sensory attenuation in emerging psychosis. Moreover, the sensory attenuation difference between CHR subgroups was investigated to address the potential impact of

heterogeneity of CHR-samples on impaired sensory attenuation, for example, different clinical staging and the different clinical outcome at 12 months. According to previous studies in ScZ, I predicted that FEP displayed sensory attenuation deficits, and that the deficits in CHR-individuals were intermediate between HC and FEP. In addition, the impaired sensory attenuation was related to clinical psychotic symptoms and cognitive functioning in emerging psychosis. Importantly, I predicted that impaired sensory attenuation was irrelevant to the basic M100 function, in support of the dysfunction of corollary discharge in ScZ(Ford & Mathalon, 2005).

In Chapter 5, the aim was to examine the aberrant neural interaction underlying sensory attenuation in emerging psychosis. As I primarily explored the dynamic interaction across cortical-subcortical circuits in HC with the DCM approach in Chapter 3, various competing DCM models were again built in Chapter 5 to examine the possible hierarchical interaction among cortical-subcortical areas, followed by Bayesian model selection to determine the winning model. I hypothesized that sensory attenuation deficits in CHR- and FEP-participants would result from disrupted causal interaction among the sensory attenuation network. In particular, the impaired sensory attenuation in FEP-individuals was possibly due to reduced top-down control and enhanced bottom-up input (prediction error), while the impaired interaction among sensory attenuation network in CHR was intermediate between FEP and HC.

Chapter 2 Participants and Methods

2.1 Recruitment

The data of this thesis was collected as part of the Youth Mental Health Risk and Resilience Study (YouR-Study), funded by the Medical Research Council (MRC). This project was approved by the West of Scotland Research Ethics Committee, and supported by community-based services, NHS Greater Glasgow & Clyde (NHS GG& C) and NHS Lothian. The CHR and FEP participants were recruited from clinical referrals and the general population in Glasgow and Edinburgh via email invitations, and public transport advertisements. The HC were enrolled from the subject pool of the School of Psychology at the University of Glasgow.

For CHR- and FEP-individuals, all participants were included between September 2014 and November 2019. Participants were first assessed for risk of psychosis online with: 1) the 16-item Prodromal Questionnaire (PQ-16) (Ising et al., 2012) and 2) a 9-item scale of perceptual and cognitive anomalies (PCA) which was developed to assess basic symptoms. If they met the criteria of PQ-16 or PCA, they were invited to take part in the following procedures.

During their first visit, they were made aware of the research purpose and research procedures of this study before they signed consent forms. The general demographic and treatment information were obtained, including age, education, citizenship, marital status, employment, physical, and mental health history of participants and their family, treatment, and substance use. In particular, suicide and self-harm risk were also assessed to ensure the safety of participants in this study, otherwise, they were suggested to an appropriate referral.

CHR for psychosis was estimated based on two semi-structured scales, the positive symptom items of the CAARMS(Yung et al., 2005) and SPI-A(Schultze-Lutter, Addington, et al., 2007). The initial assessment was carried out by two trained research assistants and/or MSc/PhD researchers, followed by symptom discussion in team-meeting. Additionally, the subjects who met the SPI-A criteria were further verified by Schultze-Lutter. Therefore, the CHR-participants in this study were confirmed to either SPI-A criteria, CAARMS criteria, or both.

The participants were enrolled as CHR-group if they met the following SPI-A criteria: 1) Cognitive Perceptive Basic Symptoms (COPER) or/and 2) Cognitive Disturbances

(COGDIS). Additionally, they were included if they met the following CAARMS criteria: 1) Genetic risk of family history and 30% drop of functional deterioration according to GAF; 2) Attenuated psychosis symptoms (APS); 3) Brief Limited Intermittent Psychotic Symptoms (BLIPS). FEP participants were assessed with the Structured Clinical Interview for DSM-IV and the Positive and Negative Syndrome Scale (PANSS)(Kay, Fiszbein, & Opler, 1987).

The exclusion criteria for all subjects are as follow: an existing neurological disorder, the age is less than 16 years old or larger than 35 years old, metal implants in body parts, pregnancy, and suicidal intent. The exclusion criteria of CHR include: 1) current or past diagnosis with Axis I psychotic disorders; 2) other co-morbid Axis I diagnoses, such as mood or anxiety disorders. The inclusion of the FEP group were participants who met CAARMS criteria for psychosis threshold and the diagnostic criteria for FEP on DSM-IV, as well as the Structured Clinical Interview for DSM-IV-TR AXIS I disorders (SCID-I)(First, Williams, Karg, & Spitzer, 2015). Additionally, HC were assessed by CAARMS and SPI-A during the first visit to exclude CHR for psychosis.

CHR- and HC-samples were assessed with the Premorbid Adjustment Scale (PAS) (Cannon-Spoor, Potkin, & Wyatt, 1982) and the Mini International Neuropsychiatric Interview (MINI)(Sheehan et al., 1998). In addition, all participants were assessed with social and role functioning scales (Cornblatt et al., 2007) and a neuropsychological evaluation, consisting of the Brief Assessment of Cognition in Schizophrenia (BACS)(Keefe et al., 2004) and the Penn Computerized Neurocognitive Battery (CNB) (Moore, Reise, Gur, Hakonarson, & Gur, 2015). After the assessment, 110 CHR- and 26 FEP-participants were included in this study, and 48 age-matched HC-participants were enrolled as a comparison group in Chapter 4 and Chapter 5. Notably, given that we were interested in the association between movement-related potential and auditory sensory attenuation in Chapter 3, we included 35 HC with right handedness to avoid handedness impact on movement-relate activity. The HC in Chapter 4 and Chapter 5 were overlapped with Chapter 3.

Subsequently, CHR participants were further invited to do follow-up at 3, 6, 9, 12, 18, 24, 36 months by CAARMS to estimate their CHR status. In addition, SPI-A and SCID were administrated at 24 and 36 months (refer to the assessment list in the supplementary materials).

2.2 Data Acquisition

MEG data were collected at the Center for Cognitive Neuroimage at the University of Glasgow. Participants were instructed to sit still in magnetically shielded room. MEG-data were acquired with a 248-magnetometers whole-head MEG system (MAGNES 3600 WH, 4-D Neuroimaging) at a sample rate of 1017.25 Hz. Prior to the MEG-recording, the head-shape was digitized using a Polhemus Fastrack digitizer and the head position was digitally registered. Head position was recorded at the beginning and the end of the MEG session using five head position indicator (HPI) coils. Participants with head movement exceeding 1 cm was asked to repeat the block to limit source reconstruction error.

The MRI data were obtained from a Siemens 3T scanner after MEG scanning. A 10-minute duration anatomical T1 weighted magnetic resonance imaging (MRI) scan was recorded to do source reconstruction with parameters: 192 slices, voxel size 1 mm^3, FOV=256*256*176 mm^3, TR=2250 ms, TE=2.6 ms, FA=9°.

2.2.1 Experiment paradigm

The experiment paradigm of this thesis is part of Your-study Project. The whole experiment paradigms were designed to estimate the brain function in emerging psychosis from four perspectives, including the resting-state, visual gamma experiment paradigm, auditory MMN, and auditory steady-state response paradigm. The current experiment paradigm was designed based on 40 Hz auditory steady state response to explore the auditory sensory attenuation.

A 1,000 Hz flat tone of constant intensity (2000 ms duration, 93, dB) and a 40 Hz amplitude‐modulated 1,000 Hz tone (‘ripple’ tone, 2000 ms duration, 87 dB) were presented binaurally in two blocks with 100 trials each: 1) A ‘passive’ condition block compromising of 100 ripple tones and 10 flat tones with a jittered stimulus‐onset‐asynchrony (SOA) between 3,500 and 4,500 ms. Participants were instructed to press a button with their right index finger when a flat tone occurred and 2) A self‐generated condition (‘active’ condition) that required participants to elicit a ripple tone via button press with their right index finger at approximate 4,000 ms SOA. A flat tone was presented if the participant responded earlier than 3,000 ms or later than 5,000 ms SOA (Figure 2.1). Prior to the beginning of the experiment, participants were given practice runs to familiarize themselves with the task.

Figure 2.1 Experiment paradigm

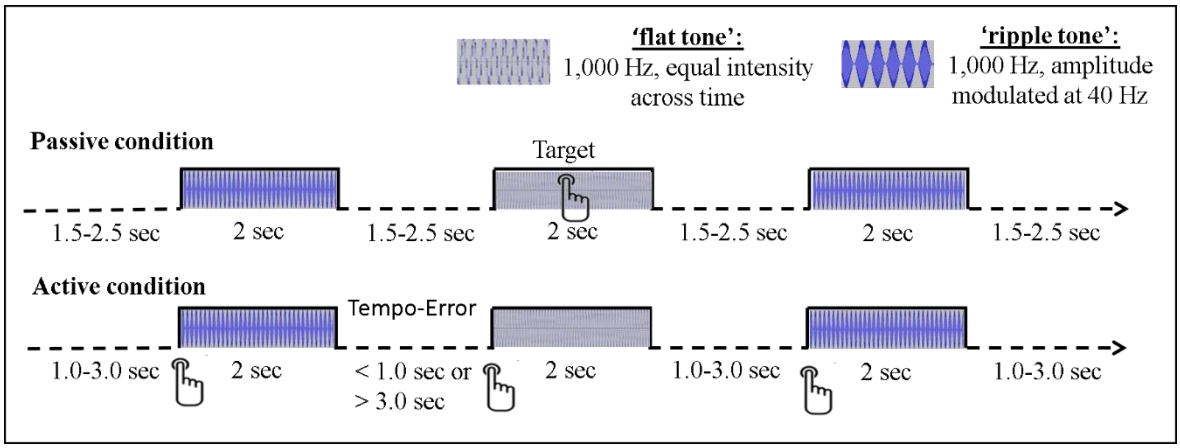

2.2.2 Data pre-processing at the sensor level

All analyses were conducted with the Fieldtrip-toolbox (Oostenveld, Fries, Maris, & Schoffelen, 2011). Only trials that contained a ripple tone were included in sensor- and source- space analysis. For the pre-processing of MEG-data, recordings were filtered to remove line noise in 50, 100, 150 Hz using a discrete Fourier transform filter, and were cut from -1000 ms to 3000 ms. Then trials with artifacts were detected manually and rejected from further analysis. Faulty sensors with large signal variance or whose signals were flat were removed and interpolated using the nearest-neighbor averaging procedure.

Independent component analysis (ICA, runica) was applied to remove variance from artifacts such as heartbeat, saccade and eye blinks. Prior to trial averaging, MEG-data was band-pass filtered from the 1 to 30 Hz with a baseline correction, followed by averaging of individual trials in each condition. Filtered neuromagnetic data were transformed from an axial magnetometer to planar gradient signals (Bastiaansen & Knösche, 2000). For sensor-level analysis, the time window of interest was 110-140 ms according to the grand average ERP data from the combined condition dataset, which covered the peak latency of the M100 component. The detailed process at the sensor level was depicted in individual Chapter when there was a difference.

2.2.3 Data pre-processing at the source level

Source-space (virtual channel) data were extracted based upon the centroids of 116 available AAL atlas regions from BrainNet Viewer software (Xia, Wang, & He, 2013), followed by normalizing the central coordinates into the same template grid with source reconstruction. The linear constraint minimum variance (LCMV) beamformer was used to compute the

source-space data with the covariance matrix based on the time window from pre-stimuli 1000 ms to post-stimuli 3000 ms. The regularization value was set to 5%. Finally, the singular value decomposition (SVD) was used to decompose and extract the data vector representing the dominant source orientation, used to reconstruct the source-space data. Source-space data were averaged across trials to obtain the evoked activity at each individual source areas. The detailed process at the source level was described in individual Chapter.

2.2.4 Dynamic casual modelling (DCM)

DCM was employed to explore the causal interactions between brain regions that explain differences between observed ERFs (David et al., 2006; Friston et al., 2003). Conceptually, the interactions between neural nodes in DCM consist of 1) Structural forward, backward and lateral connections between nodes which convey changes in brain activity elicited by a stimulus (i.e. a driving input) and 2) Modulatory connections which estimate the effect of experimental factors (context-dependent) on neural interactions, including forward and backward connections to investigate whether sensory attenuation was driven by bottom-up message passing, top-down predictions, or both. In addition, self-modulation within each source was added to test the role of intrinsic changes in neural excitability (Kiebel, Garrido, & Friston, 2007) as well as the contribution of lateral connections given their role in auditory processing (Boly et al., 2011; Phillips, Blenkmann, Hughes, Bekinschtein, & Rowe, 2015).

DCM-analysis of evoked responses uses excitatory and inhibitory neuronal subpopulations in a neural mass model which was applied to auditory ERF responses between -100 ms and 200 ms. Source-space data were entered into the DCM analysis and local-field potentials (LFP) were utilized to model ERF data without spatial reconstruction. Given that we were interested in the change in connection strengths during sensory attenuation relative to a baseline condition (auditory input without sensory attenuation), between-condition effects were set to 0 (baseline) and 1. DCM was performed based on Statistical Parametric Mapping 12 (SPM 12,v7487) (https://www.fil.ion.ucl.ac.uk/spm/).

2.2.5 Statistics

For demographic and clinical features, one-way analysis of variance (ANOVA) or an independent t-test was performed to continuous variables, and a chi-square test for categorical variables to test the potential group difference at baseline and follow-up data.

At the sensor level, cluster-based non-parametric permutation from fieldtrip platform was utilized to examine the sensory attenuation effect within group and between groups within interested time window. At the source level, the sensory attenuation effect was investigated by paired t-test or F-test in each individual ROIs within group and between groups, followed by false discovery rate (FDR) correction with 4 auditory regions.

2.2.6 Correlation

To investigate whether the dependent variables were predicted by independent variables, multiple regression model was conducted in SPSS 19.0 version. Spearman correlation was conducted to investigate the association between auditory sensory attenuation and clinical features.

2.3 Demographic information

The features of 35 HC were listed in Chapter 3. The current demographic information was from 48 HC, 110 CHR, 26 FEP for Chapter 4 and Chapter 5. There was no significant difference in age and sex across three groups (Table 2.1).

Of 110 CHR individuals, 30 participants met CAAMRS criteria, 30 subjects met SPI-A criteria and 50 of participants met both criteria. Of those who met CAARMS criteria (80/110), almost all CHR-participants (96.25%, 77 out of 80) were classified into the APS subgroup. Two out of 80 CHR-participants were identified with GRD, and only one CHR-participant was included with the criteria of BLIPS. Regarding those who met SPI-A criteria, 15.18% of them met COGIDS sub-criteria, 44.17% of them met COPER sub-criteria and 43.03 % of them met both COGIDS and COPPER criteria.

Regarding the sub-symptom meeting CAARMS criteria, 42.7% of CHR samples met the inclusion criteria of unusual thought content. 70.9% of the sample experienced non-bizarre ideas, 73.6% of them described perception abnormality experience, and 60.9% of subjects reported disorganized speech symptoms. Of those who were rated as having a psychotic experience, 53.3% of them reported that they were at least moderate distress (> 50% out of 100%) of those symptoms. Furthermore, a total CAARMS severity score was calculated for each participant by multiplying the global score by the frequency score for each of the four symptom groups and calculating the sum of these four numbers(Morrison et al., 2012). There was a significant group effect of total CAARMS severity score and GAF score across three groups ($p < 0.05$).

Table 2.1 Demographic information of subjects

	HC	CHR	FEP	F value	*p*	Post-hoc
Age, mean(SD),y	22.58(3.51)	21.87(4.52)	24.45(3.21)	1.62	>0.05	-
Sex(Male/Female)	15/33	30/80	15/11	1.94	>0.05	-
Education, mean(SD),y	16.70(2.98)	15.36(3.18)	15.75(2.93)	3.07	0.049	-
First-degree relative of ScZ history	0	10	2	-	-	-
Medication	1	57	11	-	-	-
Non-medication	47	53	4	-	-	-
Antipsychotic	0	1	1	-	-	-
Antidepressant	0	27	3	-	-	-
Mood stabilizer	0	1	0	-	-	-
Anti-convulsants	0	0	0	-	-	-
Others	1	13	1	-	-	-
Multiple	0	15	6	-	-	-
GAF_baseline mean(SD)	87.82(6.33)	58.5(13.37)	46.73(12.10)	122.84	<0.05*	HC>CHR CHR>FEP HC>FEP
Total CAAMRS severity mean(SD)	-	29.00(18.29)	81.93(22.48)	-10.12	<0.05*	
SPI-severity mean(SD)	-	0.41(0.43)	0.58(0.44)	-1.40	>0.05	

Note: * $p<0.05$.

2.4 Neuropsychological result

The statistical results of BACS across groups were presented below (Table 2.2).

Table 2.2 The BACS statistical results across the three groups

BACS	HC (mean±SD)	CHR (mean±SD)	FEP (mean±SD)	Levene statistics	Levene's test	F	*p-value*	Post hoc
Working Memory	0±1	-0.23±1.65	-0.27±1.56	4.73	<0.05	0.38	>0.05	-
Motor Speed	0±1	-0.56±1.03	-1.13±1.56	2.51	>0.05	9.20	<0.05*	HC>CHR HC>FEP CHR>FEP
Verbal Memory	0±1	-0.36±1.03	-0.83±1.36	1.97	>0.05	2.87	>0.05	-
Verbal Fluency	0±1	-0.01±1.03	-0.75±1.36	2.41	>0.05	2.09	>0.05	-
Executive Function	0±1	-0.25±1.03	-0.16±1.36	1.56	>0.05	0.41	>0.05	-
Processing Speed	0±1	-4.83±1.03	-1.52±1.36	0.54	>0.05	391	<0.05*	HC>CHR HC>FEP CHR<FEP
BACS Composite	0±1	-0.44±1.03	0.95±1.36	38.19	>0.05	4.52	<0.05*	CHR<FEP

Note: $p < 0.05$*.

Chapter 3 The role of thalamo-cortical circuits and movement-related cortical potentials in auditory sensory attenuation: A combined MEG-DCM Study

3.1 Introduction

An important goal of organisms is to distinguish between sensory information originating from the external environment vs sensations caused by the organism's own actions (Schafer & Marcus, 1973; von Holst & Mittelstaedt, 1950). One example to illustrate this phenomenon is sensory attenuation whereby sensations that are caused by the organism's own action are decreased in intensity compared to externally-generated stimuli (von Holst & Mittelstaedt, 1950).

The first framework to account for sensory attenuation was proposed by von Holst and Mittelstaedt (1950) who suggested that an efference copy of the motor command is used to predict the forthcoming sensory outcome, followed by a comparison with the afferent information (corollary discharge) (Sperry, 1950a). In this framework, sensory attenuation occurs if the predicted sensory feedback matches the incoming sensory stimulus. More recent accounts have highlighted the role of hierarchical inferences in sensory attenuation from a predictive coding perspective (Brown, Adams, Parees, Edwards, & Friston, 2013; Friston & S. Kiebel, 2009).

Sensory attenuation has been observed in tactile, auditory, and visual domains in a range of species (Nelson et al., 2013; Poulet & Hedwig, 2002), including humans (Blakemore et al., 2000; Limanowski, Sarasso, & Blankenburg, 2018; Synofzik, Lindner, & Thier, 2008), suggesting an evolutionarily conserved mechanism. In EEG/MEG recordings, sensory attenuation is characterized by the suppression of the auditory N/M100 ERP/ERF during self-generated speech or tones (Cao, Thut, et al., 2017; Heinks-Maldonado, Nagarajan, & Houde, 2006; Martikainen, Kaneko, & Hari, 2005a). Analysis of the underlying generators through source localization identified the superior temporal cortex (ST) as the primary auditory region contributing to the attenuation of the M100 (Aliu et al., 2009; Martikainen et al., 2005a). Additional brain regions that have been shown to be involved in the sensory attenuation during self-generated speech are the cerebellum (Cao, Thut, et al., 2017; Pollok et al., 2008), the parietal cortex (Pollok et al., 2008), and the anterior cingulate cortex (Simons et al., 2010). Moreover, impaired sensory attenuation has been linked to psychiatric

disorders, such as ScZ (Ford, Gray, Faustman, Roach, & Mathalon, 2007; Ford et al., 2001; Whitford et al., 2017), to account for disturbances in the sense of agency that could potentially underlie the emergence of hallucinations and delusions (Ford & D. H. Mathalon, 2005).

von Holst and Mittelstaedt (1950) proposed that motor areas generate the efference copy that is compared to the incoming sensory signal. This is supported by studies with TMS showing that interference with motor regions is associated with reduced sensory attenuation in the auditory cortex (Haggard & Whitford, 2004). It is currently unclear, however, at which stage motor information impacts sensory processing as this could occur before motor execution (Schneider et al., 2014; Timm, SanMiguel, Keil, Schröger, & Schönwiesner, 2014), during motor action (Schneider et al., 2014; Stenner et al., 2015) or following the re-afference stage of motor action (Burin et al., 2017; Kilteni & Ehrsson, 2017a, 2017b).

An additional question concerns the role of the parietal cortex as well as the thalamus and their interactions with auditory regions during sensory attenuation. There is evidence to suggest that the inferior parietal cortex together with the cerebellum is involved in the prediction of sensory outcomes of actions (Blakemore & A. Sirigu, 2003; Pollok et al., 2008). The thalamus, on the other hand, has been postulated to be involved in the relay of the efference copy generated in motor areas to auditory regions (Sherman, 2016). This hypothesis is supported by findings from visual perception where lesions in the thalamus lead to impaired saccade orientation, possibly through interfering with updating the corollary discharge signal (Bellebaum, Daum, Koch, Schwarz, & Hoffmann, 2005; Sommer & Wurtz, 2004).

In the current study, we aimed to provide novel insights into the contributions of cortical and subcortical regions as well as their interactions toward auditory sensory attenuation through the combination of advanced source reconstruction of MEG data together with computational modelling. To address these questions, we first compared M100 responses during self versus non self - generated 40 Hz amplitude modulated (AM) tones. We then identified movement - related magnetic fields (MRMFs) in order to identify potential efferent motor signal contributions to sensory attenuation. MRMFs have not been investigated within this paradigm, but can be identified and extracted from MEG data (Nagamine et al., 1994). Multiple regression analyses were used to identify the contribution of motor cortical regions towards the attenuation of the M100 amplitude in auditory areas. Finally, we employed DCM (Friston et al., 2003) to study the interactions between sources in the thalamus as well as

auditory and parietal regions to identify the network parameters that capture sensory attenuation in MEG-data.

Based on existing evidence and theoretical models, we predicted that, in addition to the auditory cortex, sensory attenuation would engage in a distributed network, including the thalamus as well as parietal and motor regions. Moreover, we anticipated that this network would involve both bottom-up as well as top-down mediated interactions, providing support for the role of predictive processes in sensory attenuation.

3.2 Methods

Given the potential impact of handedness on movement-related potential, it was noteworthy to mention that 35 HC were selected in the current Chapter with pure right handedness(26 females; mean (SD) age: 22.31±3.10). Handedness was assessed with Edinburgh Handedness Inventory (Oldfield, 1971). The experiment paradigm, data collection, data analysis of auditory M100 and DCM approach were described in Chapter 2.

3.2.1 Movement-related magnetic fields (MRMFs)

In addition to identify the motor areas involved in sensory attenuation, we averaged the source-space data across trials and identified evoked potentials that corresponding to motor-related magnetic fields (MRMFs) through the visual identification of peaks (Jankelowitz & Colebatch, 2002; Nagamine et al., 1994) at each individual source from -100 ms to the onset of tone. These were then used in a regression analysis to examine the relationship with the attenuation of the M100 in auditory regions. Motor-related cortical areas were not used in the DCM analyses as DCM requires the driving input to be the same between experimental conditions (see below).

3.2.2 Statistics

3.2.2.1 Sensory attenuation effect

Sensor-level sensory attenuation effects were examined with a cluster-based non-parametric t-test implemented in Fieldtrip (Maris & Oostenveld, 2007) within a 110-140 ms window aligned to the peak of the M100 component from the grand-average data. The significant clusters were calculated with the Monte Carlo method with 1000 permutations ($p < 0.05$, alpha-level = 0.05, two-tailed).

At the source-space level, dependent sample t-tests were applied to examine the difference between the active and passive condition between 90 and 140 ms as this was the time window in sensory attenuation occurred across sources. A false discovery rate (FDR) was applied to correct for multiple comparisons across 116 source regions (p<0.05, alpha-level = 0.05, two-tailed).

3.2.2.2 **Regression analysis**

A stepwise multiple regression method was employed to identify the relationship between MRMFs and attenuation of the M100 amplitude. The dependent variables were M100 sensory attenuation in the right HES and right ST which was calculated through the root mean square (RMS) of M100 amplitude. Due to the fact that sensory attenuation effects were characterized by negative values, the sign of the effect was reversed and entered into the regression analysis. The independent variables were MRMFs amplitude from motor - related regions, including precentral gyrus, postcentral gyrus, anterior and posterior cingulate cortex, inferior parietal cortex, and cerebellum - related areas. To avoid potential auditory activity in motor - related areas, MRMFs in the active condition were subtracted from the passive condition data using the same time latency of each peak. Two factors of tolerance and the variance inflation factor (VIF) were employed to identify the multicollinearity of independent variables. We confirmed that the predictors in final regression models have no collinearity based on tolerance > 0.1 and VIF <10.

3.2.2.3 **DCM: Bayesian model selection (BMS)**

For DCM model-analysis, fixed-effects Bayesian model selection (FFX-BMS) was used to determine the winning DCM-model. The metric of model performance was the free energy approximation to the model evidence: the probability of the observed data given the model (integrating over all possible parameter values). This free energy metric is improved by model accuracy but penalized by model complexity. Each model inversion also derived the posterior distributions of the parameters given the observed data.

3.3 Results

3.3.1 Sensory attenuation effect

At the sensor level, a smaller amplitude M100 component was observed over temporal and parietal channels in the active condition than in the passive condition (p <0.05, Figure 3.1A). At the source level, M100 sensory attenuation was present in the right thalamus, right HES, right ST, right rolandic operculum (ROL) as well as in parietal regions, located in the right inferior parietal cortex (IPL) and right precuneus(Figure 3.1B).

3.3.2 MRMFs

We observed the following MRMFs: (a) Motor preparation potentials, (b) Motor potential peak, and (c) Motor re‐afference peak. The motor‐readiness potential was not included in the further analysis as it could be confounded by attention, anticipation, and task load (for a review see (Hughes, Desantis, & Waszak, 2013). Given the fact that we observed contralateral (left hemisphere) and ipsilateral (right hemisphere) MRMFs, we identified 4 MRMF‐related peaks, including a contralateral MRMF with a peak latency between -50 and -20 ms (Peak 1) and a similar MRMF in the ipsilateral hemisphere with a peak latency between -25 and 5 ms (Peak 2). Additionally, the re‐afference potential in contralateral and ipsilateral hemisphere constituted Peak 3 and Peak 4 with a time latency from 20 to 50 ms and from 50 to 80 ms, respectively (Figure 3.2). The mean amplitude of each peak within above mentioned time window was entered into the following regression model.

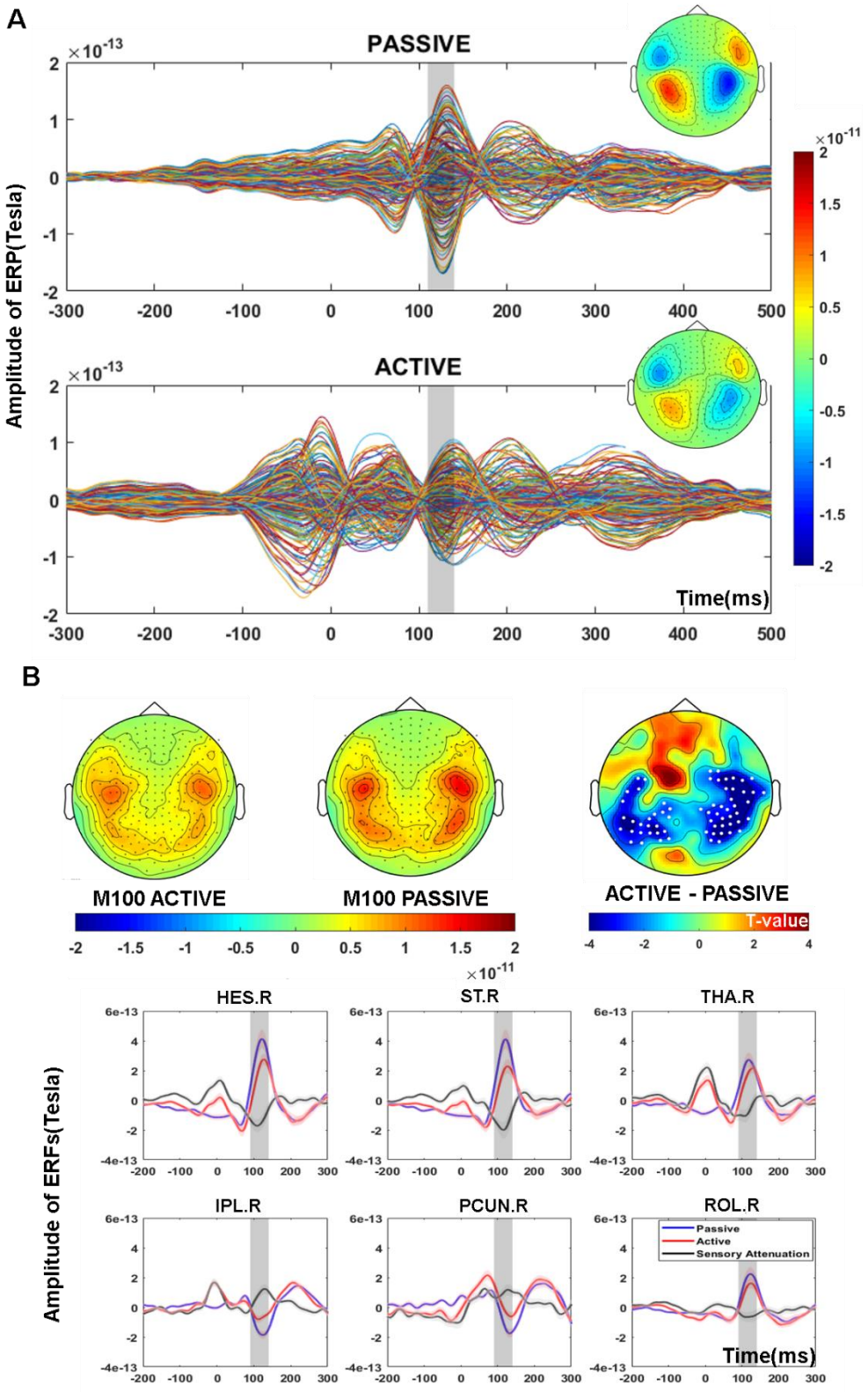

Figure 3.1 Sensory attenuation effect at sensor- and source-space level

Panel A depicts the topographic map of the M100 in the active and passive conditions between 110 and 140 ms. Statistically significant channels are highlighted with white stars. Panel B plotted the mean and standard deviation of auditory ERFs in active and passive condition and attenuation effect in parietal, auditory, and subcortical areas (after FDR correction) at the source-space level. The grey shadow indicates interested statistical time-window between 90 and140 ms. THA: Thalamus; HES: Heschl's Gyrus; ST: Superior

Temporal Cortex; IPL: Inferior Parietal Cortex; PCUN: Precuneus; ROL: Rolandic Operculum; L: Left; R: Right.

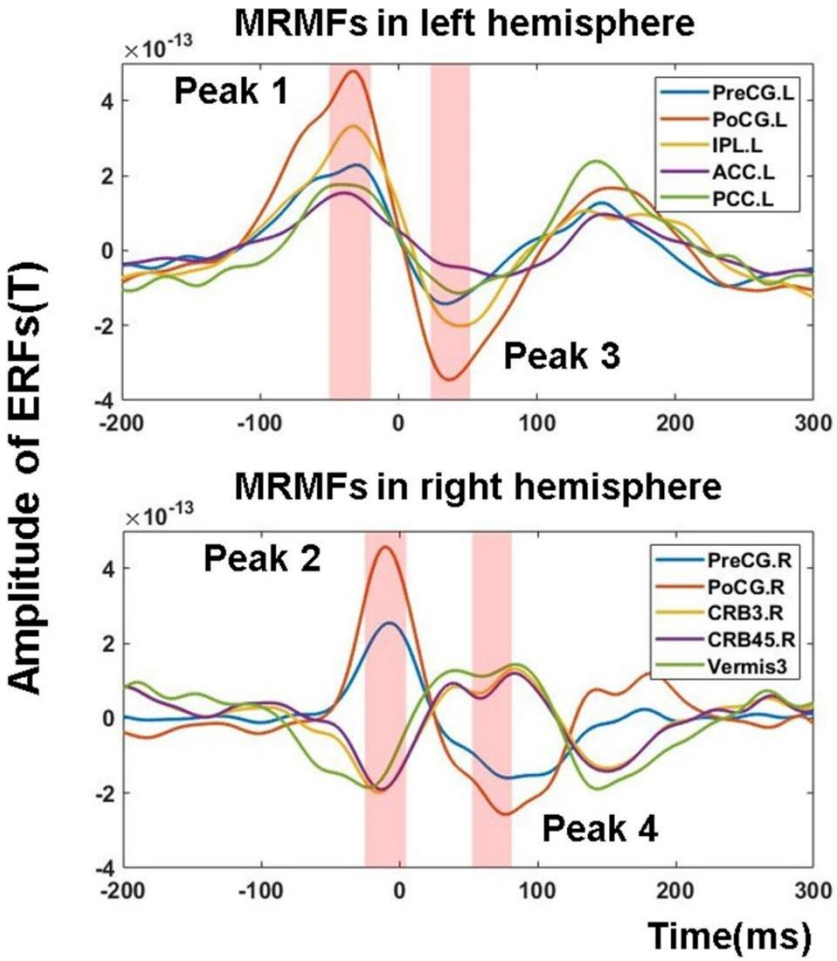

Figure 3.2 MRMFs peaks at the source level

Regions of interest of MRMFs from Peak 1 to Peak 4 and the pink shadows highlight the analysis time windows (Peak 1: -50 to -20 ms; Peak 2: -25 to 5 ms; Peak 3:20 to 50 ms; Peak 4:50 to 80 ms). PreCG: Precentral Gyrus, PoCG: Postcentral Gyrus; IPL, Inferior Parietal Cortex; ACC, Anterior Cingulate Cortex; PCC, Posterior Cingulate Cortex; CRB3, Lobe III of Cerebellum; CRB45, Lobe IV, V of Cerebellum; HES, Heschl's Gryus; ST, Superior Temporal Cortex; L, left; R, right.

3.3.3 Regression Analysis

Table 3.1 Summary of multiple regression results

	Coefficient Std.err	Std.coff beta	t	Sig	Collinearity Torenlence	VIF
Right HES Sensory Attenuation						
Peak2_PoCG.R	0.10	0.42	3.2	0.004*	0.99	1.00
Peak3_PreCG.L	0.19	0.47	3.5	0.001*	0.99	1.00

Right ST Sensory Attenuation						
Peak2_PoCG.R	0.12	0.37	2.6	0.014*	0.96	1.01
Peak3_PreCG.L	0.15	0.40	2.8	0.008*	0.98	1.01

Notes: The dependant variables are the reverse value of sensory attenuation in the right HES, right ST, respectively. The independent variables are movement-related activity at each peak. Sig: Significance; VIF: Variance inflation factor; PreCG: Precentral Gyrus; PoCG: Postcentral Gyrus; Tha: Thalamus; IPL: Inferior Parietal Lobe; HES: Heschl's Gyrus; ST: Superior Temporal Cortex;L: left; R: right. *($p < 0.05$).

3.3.4 DCM results

3.3.4.1 DCM model structures

For the DCM-model, we wished to implement a model as parsimonious as possible and thus concentrated on the following brain regions: 1) Bilateral thalamus 2) Bilateral HES and 3) fright IPL. Bilateral thalamus and HES were included due to the fact that auditory stimuli were presented binaurally. Moreover, we only included HES as the ST is anatomically close to the HES and sensory attenuation in both regions was highly correlated (r= 0.88, p <0.001). Although the attenuation of the M100 was also observed in ROL and precuneus, we did not include these regions into the DCM model because additional brain regions substantially increase the complexity of the DCM exponentially, in particular, if the areas are distant (in hierarchical terms) from the input. Finally, as mentioned previously, MRCPs were not included as DCM requires that the driving input for both experimental conditions is the same. DCM was then used to test the contribution of each brain area (HES, IPL and Thalamus) towards sensory attenuation as well as the interactions between nodes to examine the role of feedback and feedforward message passing as well as the importance of intrinsic connectivity. Family 1 included bilateral thalamus and HES to test whether sensory attenuation was mediated by a thalamo-cortical network. The right IPL was then added into Family 2 to examine the potential role of top-down predictions on auditory areas. In all cases, driving inputs into the bilateral thalamus perturbs the brain and conveyed to higher-order cortex, which is modulated by condition-specific effects on forward, backward or intrinsic connections. Models with or without intrinsic (self-inhibitory) and lateral connections at each level were also included (Figure 3.3).

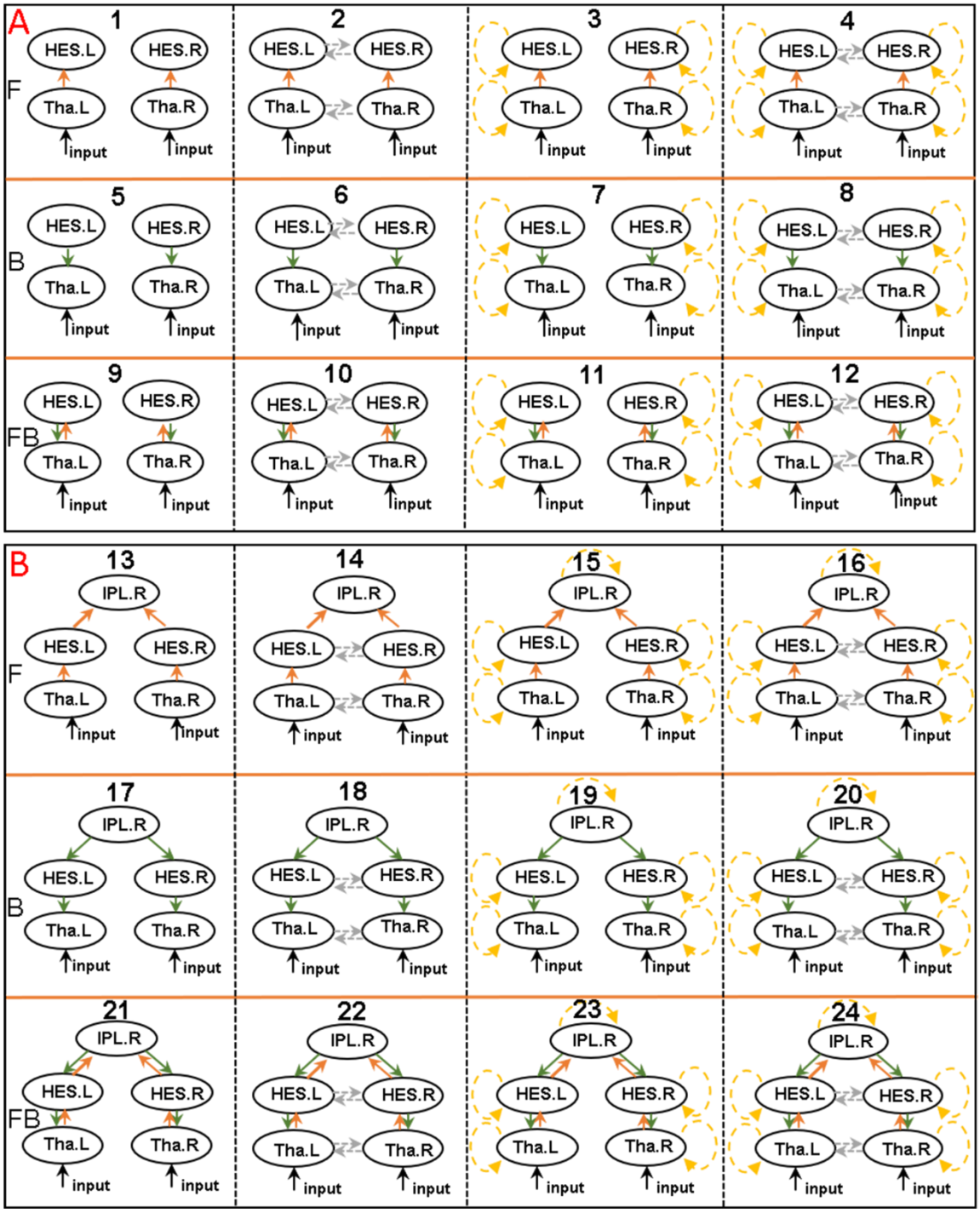

Figure 3.3 DCM-model structures

Panel A displays the structure of Family 1 and panel B shows the structure of Family 2. The rows displays forward (F, orange solid line), backward (B, green solid line), and bi-direction (FB) connection pattern in each family, which are then varied within or without intrinsic and lateral connection. Grey dotted line shows the lateral connection, and the yellow dotted line represents the self-modulated connection. Tha: Thalamus; HES: Heschl's Gyrus; IPL: Inferior Parietal Lobe; L: Left; R: Right.

3.3.4.2 **Fixed effect factors of Bayesian model selection**

At the family level, FFX favoured Family 2 with nodes in IPL, thalamus, and HES. At the model level, Model 23 won with almost 100% posterior probability, involving both bottom-up and top-down modulation connections as well as self-modulation in each node but without lateral connections (Figure 3.4ABC). Additionally, we re-organized the models into three alternative families according to the connections modulated by sensory attenuation in forward, backward, and bidirectional modulation connection patterns. FFX results suggested that the family with both forward and backward modulated connections had the most evidence with 100% probability (Figure 3.4D). The winning model fitted the data well with the observed and predicted waveforms closely aligned in all areas (the exceptions being effects occurring prior to 0 ms (the input onset) which cannot be modelled using this approach) (Figure 3.4E).

Finally, the modulatory parameters were averaged across participants after Bayesian model averaging (BMA) over the winning family in order to identify the connections that were modulated in the sensory attenuation condition. Only connections with a posterior probability (of being modulated during sensory attenuation) of over 95% are reported. For the winning model, the self-inhibition was decreased during sensory attenuation (i.e. implying increased excitability or 'gain') in bilateral thalamus and right HES, and the bottom-up (excitatory) connection strength from right thalamus to right HES was likewise increased. Conversely, the bottom-up connection strength from right HES to right IPL was reduced, and top-down (inhibitory) connection strengths between right IPL, right HES and right thalamus were increased (Figure 3.4C).

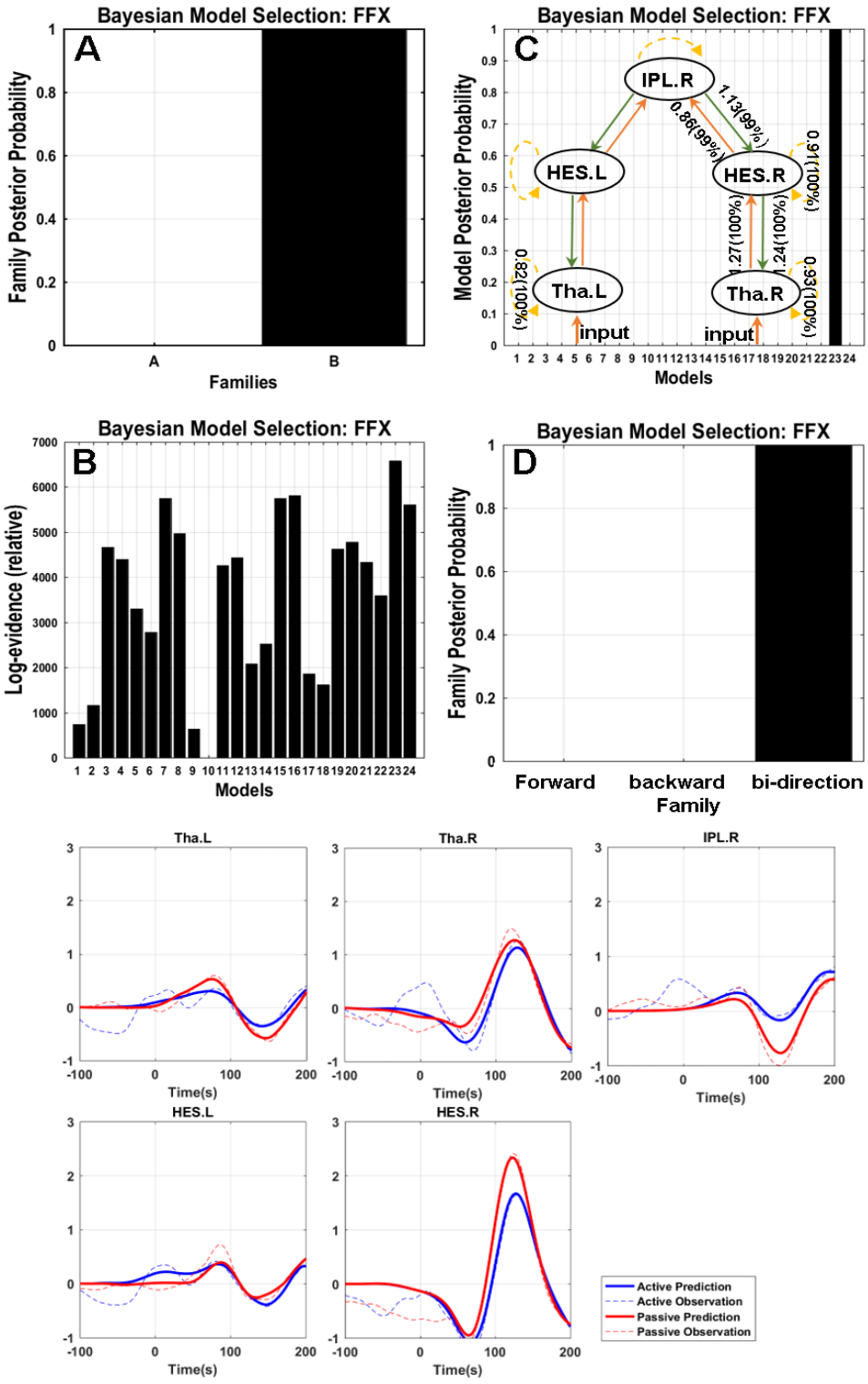

Figure 3.4 Dynamical causal modelling results

BMS results based on fixed effect (FFX) and the grand-average ERF of predicted and observed evoked potential response in five nodes. Panel 5A displays the posterior probability at the family level. Panel 5B displays the log-evidence of individual models. Panel 5C shows the winning models across all the constructed models with almost 100% posterior probability. Simultaneously, condition inference (more than 95% posterior probability) of the modulatory connection of the winning model is marked in panel 5C. The connection parameters are described with the gain coupling and the probability that the coupling is increased (gain coupling >1) or decreased (gain coupling <1) in the active condition. Panel 5D displays the BMS results based

on the forward, backward, bidirectional modulatory connection pattern in each family. Panel 5E plots the grand-average ERFs of predicted and observed evoked potential response in five nodes. The solid and dotted line represents the predicted and observed ERF in the active (red line) and passive condition (blue line). The x-axis is the time (ms), and the y-axis is the ERF amplitude. Tha: Thalamus; HES: Heslchl's Gyrus; IPL: Inferior Parietal Lobe; L:left; R: Right.

3.4 Discussion

The current study aimed to identify the brain regions and network interactions underlying sensory attenuation of the M100 in auditory cortices. Our MEG data show that sensory attenuation was shown in the right HES and ST, ROL and parietal areas as well as in the thalamus. Moreover, our analysis revealed that the motor-related ERFs from right PoCG and the left PreCG positively predicted sensory attenuation in the right HES and ST. Finally, DCM results suggest that the auditory sensory attenuation involved both top-down and bottom-up modulations in a thalamo-cortical network.

The involvement of the HES and ST is consistent with invasive electrophysiological data indicating that sensory attenuation occurs in both primary and secondary auditory cortices (Rummell, Klee, & Sigurdsson, 2016). In contrast, previous MEG studies (Aliu et al., 2009; Martikainen et al., 2005a), only localized sensory attenuation to secondary auditory regions. One reason for these divergent findings may be differences in the source localization approach employed. In the current study, we identified generators with a LCMV beamforming approach while the previous study employed an equivalent current dipole (ECD) technique.

Previous fMRI and EEG/MEG studies have observed reduced parietal cortex (Benazet, Thénault, Whittingstall, & Bernier, 2016; Blakemore, D. M. Wolpert, & C. D. Frith, 1998b; Hughes & Waszak, 2011) and precuneus activity (Cao, Thut, et al., 2017) during self‐induced sensations. The IPL is a core area for the integration of auditory‐motor information (Alain, He, & Grady, 2008) (Hickok, Okada, & Serences, 2009; Pa & Hickok, 2008). Moreover, existing evidence supports that IPL plays an important role through interactions with the cerebellum (Pollok et al., 2008) in the prediction of motor outcomes (Blakemore & A. Sirigu, 2003). Accordingly, the involvement of IPL in the current task may index a role in the mapping of integrated auditory and motor responses.

An alternative explanation is that the IPL reflects the participants' covert analysis of time‐intervals between sounds as a strategy to respond to task demands. In either case, the

observed suppression of IPL activity to self‐generated sounds may be discussed in the context of motor predictive signals, resulting in a suppression of self‐generated auditory‐motor or temporal representations. Future studies assessing the involvement of efferent motor signals during auditory sensory attenuation should therefore further address the role of predictive signals in the attenuation of IPL activity.

A novel observation in our MEG‐study is the presence of sensory attenuation in the thalamus and ROL. Modulation of thalamic activity has been described during sensory attenuation in previous fMRI‐data (Blakemore et al., 1998b; Boehme, Hauser, Gerling, Heilig, & Olausson, 2019; Fu et al., 2005), but the functional role of the thalamus has remained unclear. As previously highlighted, one possibility is that the thalamus underlies the relay of the efference copy generated in motor areas to auditory regions (Sherman, 2016), which is supported by evidence from visual perception (Bellebaum et al., 2005; Sommer & Wurtz, 2004). In contrast, sensory attenuation in the ROL is likely to reflect the role of executive motor functions (Penfield & Roberts, 2014) and somatosensory processing (for a review see (Mălîia et al., 2018)).

Regression analyses highlighted the contribution of the right PoCG and the left PreCG in the modulation of the M100 sensory attenuation in HES and ST. The involvement of the PoCG, a region of the somatosensory cortex, is a novel observation compared to previous evidence that has highlighted the role of motor-related areas influence, including the supplementary motor cortex and premotor cortex, in sensory attenuation (Haggard & Whitford, 2004; Whitford et al., 2018). The contribution of the PoCG, towards sensory attenuation is consistent, however, with emerging evidence that activation of the somatosensory cortex is mediated by motor-related cortex during voluntary movement (Christensen et al., 2007).

Moreover, the left PreCG also positively predicted auditory sensory attenuation. The re-afference potential of the PreCG reflects proprioceptive afferents of motor actions (Naito, 2004) and thus could contribute to body ownership (Walsh, Moseley, Taylor, & Gandevia, 2011). Indeed, it has been proposed that body ownership mediates sensory attenuation via updating the internal body state that in turn provides input to generate sensory prediction (Kilteni & Ehrsson, 2017a). This perspective is in line with the predictive coding account that has highlighted the importance of proprioceptive afferents to guide and predict motor outcomes (Adams, Shipp, & Friston, 2013; Brown et al., 2013).

Finally, DCM analysis in our study revealed that the sensory attenuation involved reciprocal feedforward and feedback loops between the thalamus, HES, and right IPL as well as intrinsic modulation within each source. Notably, Bayesian model selection preferred the family model which involved the right IPL contributed via interactions with bilateral HES. The involvement of the IPL in auditory sensory attenuation supports the view that parietal cortices provide a top-down modulation of sensory regions (Auksztulewicz & Friston, 2015).

In terms of the extrinsic modulation of connections between sources, our DCM parameter supports the enhancement of both top‐down and bottom‐up connections in the active condition, particularly in the right hemisphere. Moreover, the winning DCM model involved modulation of intrinsic (self‐inhibitory) connections, increasing local synaptic gain following the actively produced sound. Taken together, these results imply that the self‐generated stimuli entail an initial amplification of the sensory input through the thalamus that is then suppressed by increased inhibition of this input by top‐down connections. This pattern is consistent with the source‐space data, where the active condition causes a greater deflection than the passive condition in the early right thalamic response (around 70 ms), which is subsequently damped, especially in higher-order auditory areas at around 110 ms. Interestingly, a similar pattern was observed in an auditory oddball paradigm containing manipulations of attention and expectations (Auksztulewicz & Friston, 2015). In this study, attention had an early enhancing effect on the ERP (~50 ms), in part by changing the gain (self‐inhibition) in HES, whereas expectations had a later inhibitory effect on the ERP (~140 ms), accounted for by changes in backward (and forward) connectivity Thus, from a predictive coding account, self‐generated sensations may similarly produce an initial boost (as the precision of the predicted sensations is high) but then a subsequent dampening (as this sensory input is better predicted, reducing the prediction error).

3.5 Limitations

One potential limitation of our findings is the detection of thalamic activity with MEG. However, emerging evidence supports the ability of MEG to detect activity in deeper brain areas, such as the thalamus (Cornwell et al., 2008; Roux, Wibral, Singer, Aru, & Uhlhaas, 2013) and hippocampus (Recasens, Gross, & Uhlhaas, 2018a). In addition, we did not include a motor-only condition as a baseline for the sensorimotor-system. This is because previous studies showed that sensory attenuation remains present after ruling out the motor contamination by subtracting motor activity from motor-auditory activity(Horváth, 2014; Martikainen et al., 2005a).

In addition, the DCM-analysis only compromised a subsection of brain regions that showed sensory attenuation effects. We intentionally selected only the HES, IPL, and Thalamus since a larger number of sources would have increased the complexity of the DCM-model significantly. Secondly, we did not include motor-regions as indicated above as the driving input for both experimental conditions need to be similar in DCM.

3.6 Summary

Taken together, our results provide novel evidence to suggest that auditory sensory attenuation involves a distributed network in cortical (motor, parietal, and auditory regions) as well as subcortical (thalamus) regions. Furthermore, DCM analysis revealed that self-produced sensations are associated with information flow in a thalamo-cortical network that involves bottom-up, top-down, and local self-inhibitory connections. Specifically, the winning DCM model highlights the crucial role of the thalamus in amplifying self-generated sensations, before this activity is then attenuated (in both cortex and thalamus) by top-down projections from auditory and parietal areas. In addition to the relevance for understanding during normal brain functioning, these data provide a potential framework for the investigation of alterations in psychiatric syndromes, such as ScZ, where abnormal sensory attenuation may provide clues to the symptoms of psychosis (Ford & D. H. Mathalon, 2005).

Chapter 4 Sensory attenuation in participants at clinical high-risk for psychosis and in patients with first-episode psychosis

4.1 Introduction

The distinction between self-generated and nonself generated sensations is an important mechanism for establishing a sense of agency(Haggard & Chambon, 2012). One example to illustrate this phenomenon is sensory attenuation whereby self-initiated sensation is decreased in intensity compared with externally-generated stimuli(von Holst & Mittelstaedt, 1950).von Holst and Mittelstaedt (1950) suggested that an efference copy of the motor command is used to predict the forthcoming sensory outcome, followed by a comparison with the afferent information (corollary discharge)(Sperry, 1950a). From this perspective, sensory attenuation occurs if the predicted sensory feedback matches the incoming sensory stimulus.

Sensory attenuation has been explored in ScZ with both behavioural and neuroimage approaches. Evidence from behavioural studies has revealed that ScZ patients were impaired in distinguishing self from nonself generated sensations (Rösler et al., 2015; Thakkar, 2015), particularly in ScZ patients with delusion or auditory hallucinations (Daprati et al., 1997; Franck et al., 2001). The auditory N100 has been utilized to investigate sensory attenuation during a self-generated speech that overt talking suppressed N100 amplitudes compared to passive listening (Eliades & Wang, 2003). Ford and colleagues (Ford & Mathalon, 2004; Ford et al., 2001) primarily examined auditory sensory attenuation in ScZ patients by comparing the N100 amplitude between overt talking and listening to self-generated speech. During normal brain functioning, self-generated auditory input is associated with a reduction in the N100 amplitude compared to passively perceived sounds (Curio, Neuloh, Numminen, Jousmäki, & Hari, 2000; Ford et al., 2001), while the attenuation of N100 is reduced in ScZ (Ford & Mathalon, 2004; Ford et al., 2001).

Abnormalities in sensory attenuation have been observed in schizotypy (Oestreich et al., 2015, 2016), first-degree relatives of ScZ patients (Ford et al., 2013), in patients with schizoaffective disorder (Ford et al., 2013; Ford, Palzes, Roach, & Mathalon, 2014), as well as in bipolar disorder (Ford et al., 2013), indicating that deficits in sensory attenuation occur across the psychosis spectrum. First evidence had indicated mixed findings for impairments in CHR participants with some studies showing intact (Perez et al., 2011; Whitford et al.,

2018), while a study from the same group but with a larger sample size did report a deficit in CHR (Mathalon et al., 2019). However, it is currently unclear whether sensory attenuation could represent a biomarker for early detection and diagnosis.

Of note, it has been suggested that early auditory sensory processing was linked to cognitive functioning, including the social functioning, the global functioning outcome in ScZ patients (Fulham et al., 2014; Kim et al., 2014), in suggestive of the cascade information processing model that early auditory information has a flow-on impact on the following cognitive functioning (Javitt, 2009a). Interestingly, a large sample size of ScZ patients provided robust evidence that impaired early auditory information processing contributed to functional outcome by impacting the cognitive function and negative symptoms, indicating the lower auditory processing influence the higher cognitive processing(Thomas et al., 2017). However, it remains unclear about the potential association between auditory sensory attenuation and cognitive function. Furthermore, it has been suggested that altered auditory sensory attenuation was linked to clinical psychotic symptoms, such as usual thought disorder(Mathalon et al., 2019). However, this result has not been replicated(Perez et al., 2011).

In the current study, I explored sensory attenuation alterations in a sample of CHR participants (n=110) and FEP patients (n=26). We hypothesized that FEP-patients would exhibit impaired sensory attenuation in auditory areas and that CHR-group deficits would be intermediate between HC and FEP. Secondly, the relationship between auditory sensory attenuation and clinical features was examined as existing evidence suggested that sensory attenuation deficits are linked to the auditory hallucination and the formal thought disorder (Feinberg & Guazzelli, 1999).

Furthermore, regarding the intermixed results of neuroimaging studies in CHR, one of the potential factor could be the heterogeneity of CHR(Fusar-Poli, Cappucciati, Borgwardt, et al., 2016). Several researches suggested the different risk of inclusive criteria of CHR to develop psychosis(Fusar-Poli, Cappucciati, Borgwardt, et al., 2016; Schultze-Lutter et al., 2015a), however, limited studies addressed the neural features according to different inclusion criteria. Additionally, different CHR clinical outcomes gave rise to distinct neural features at baseline(Addington et al., 2019; Tang et al., 2020), we primarily explored sensory attenuation features in CHR-participants at baseline according to the different CHR status at 12 months. According to whether the CHR still met the CAARMS criteria at 12 months, the CHR status was defined to CHR-persistent or CHR-nonpersistent state.

4.2 Methods

4.2.1 Participants

Data was collected as part of the Youth Mental Health Risk and Resilience Study (YouR-Study). A sample of 110 CHR, 48 HC, and 26 FEP were included in the present analysis. CHR participants either met criteria of the positive symptoms of CAARMS (Yung et al., 2004), or SPI-A(Schultze-Lutter, Addington, et al., 2007), or both. The criteria of CAARMS was utilized to estimate the ultra-high risk (UHR) of psychosis, and SPI-A is related to BS at an earlier phase of UHR. FEP-participants met the psychosis criteria of the fourth edition of DSM as assessed by SCID-I (First, Spitzer, Gibbon, & Williams, 1995). HC were recruited without an axis I diagnosis or family history of psychosis diagnosis, and HCs in this Chapter were overlapped with Chapter 3. All participants were assessed with the BACS(Keefe et al., 2004).

Following the assessment of CHR, CHR-participants were divided into three subgroups, including meeting only SPI-A (CHR-SPI), only CAARMS (CHR-CAM), or both (CHR-both) criteria. Furthermore, the CHR-participants were followed-up at 3,6,9,12 month by CARRMS. In the current Chapter, we followed up to 12 months and identified the CHR status into a persistent and non-persistent state according to whether CHR met CAARMS criteria at 12 months. Not all the CHR individuals have 12 months data, therefore, the last assessment state within 12 months was used in this Chapter. The follow-up assessment was listed in the supplementary materials.

4.2.2 Neuroimaging data collection

The MEG data collection was depicted in Chapter 2.

4.2.3 MEG-data pre-processing at the sensor level

The MEG data pre-processing was performed as the description in Chapter 2. Following the pre-processing, the available average number of trials did not differ significantly between groups ($p > 0.05$). The mean number of trials in HC for the active condition was 94.1(standard deviation [SD] = 2.9) and for the passive condition was 94.2 (SD=3.0). In the CHR group, the mean number of trials in the active condition was 92.8 (SD=5.6), and in the passive condition was 93.5 (SD = 2.5). The mean value of trials in the active and in the passive conditions was 92.5 (SD = 9.7) and 92.5 (SD = 3.3) for the FEP group separately.

Prior to trial averaging, MEG-data was band-pass filtered from 1 to 30 Hz with a butterworth filter. The filter direction is two-pass and the filter order is set to default value 6. Subsequently, all trials were baseline corrected by subtracting the mean value of the baseline time window from -600 ms to -400 ms. Filtered neuromagnetic data were transformed from the axial magnetometer to planar gradient signals (Bastiaansen & Knösche, 2000). According to the grand-average ERP-data, the time window of interested M100 was 110-140 ms at the sensor level.

4.2.4 MEG-data analysis at the source level

T1-weighted MRI data were manually aligned with MEG data with three anatomical landmarks (the nasion, the left and right ears), followed by the automatic co-registration procedure with the ICP algorithm (Besl & McKay, 1992). The individual MRI data were applied to construct head models after segmenting the individual MRI-data into grey matter, white matter, and the cerebro-spinal fluid (CSF) compartments, followed by normalizing into a template MRI (Montreal Neurological Institute, MNI) to reduce individual differences. A single-shell volume conductor model was utilized to generate a head model.

The LCMV beamformer (Van Veen, Van Drongelen, Yuchtman, & Suzuki, 1997) was applied to reconstruct source-space data with a priori defined central coordinates for the left HES ([-41.99,-18.88,9.9]), the right HES ([45.86,-17.15,10.41]), the left ST ([-53.16,-20.68,7.13]) and the right ST ([58.15,-21.78,6.8]), which were obtained from BrainNet Viewer software (Xia et al., 2013).

Common spatial filters were first generated by the covariance matrices from -1000 ms to 3000 ms, and then applied to generate the wholetime course of each trial in active and passive conditions separately. The covariance matrix was regularized by 5% of its eigenvalues. Finally, the SVD was used to decompose and extract the data vector representing the dominant source orientation. The extracted time series were filtered from 0.1 Hz to 30 Hz and a baseline correction was applied in a time window between -600 ms and -400ms before averaging across trials. The analysis time window for M100 sensory attenuation was determined by a cluster-based non-parametric approach across auditory regions between 50 to 200 ms at the source level. Moreover, given that the spatial orientation of the M100 was flipped in some individuals, the absolute value of M100 amplitude between 90 and 150 ms was averaged for further statistical analysis.

4.2.5 Statistics

For demographic and neuropsychological variables, continuous normal distributed data were analysed with a one-way ANOVA or t-test; otherwise, a non-parametric permutation test was performed. Categorical data were assessed with a chi-squared test. BACS-scores of both CHR- and FEP-groups were standardized (z-scores) by using mean and stand deviation values from the HC group.

Sensor-level sensory attenuation effects were examined with a cluster-based non-parametric Monte Carlo permutation (Maris & Oostenveld, 2007) (permutation=1000, $p < 0.05$, alpha-level = 0.05, two-tailed). At the source level, non-parametric permutation test was employed in regions of interest (left and right HES/ST) (permutation=1000, $p < 0.05$, alpha-level = 0.05, two-tailed). A false discovery rate (FDR) was applied to correct for multiple comparisons across the 4 auditory nodes ($p < 0.05$, alpha-level = 0.05, two-tailed).

Correlations were performed with Spearman's rank correlation to test the association between sensory attenuation in four auditory nodes and clinical features across CHR- and FEP-participants, including GAF, clinical symptoms, and BACS-tests. The total CAARMS severity, total CAARMS distress, total SPI-A severity, and total SPI-A distress were calculated individually based on the mean value of sum scores of each scale.

4.3 Results

4.3.1 Demographic and neuropsychological data

There was a significant difference in years of education across three groups (Table 2.1). Furthermore, group difference in the cognitive dimension of motor speed, processing speed and attention, and BACS composite scores were presented below(Table 2.2). In addition, the demographic information of the different criteria of CHR subgroup was calculated (Table 4.1), as well as the demographic information for CHR-persistent and CHR-nonpersistent state at 12 months (Table 4.2). CHR-both group displayed more severe global functioning and the CAARMS symptom severity than BS-criteria group or UHR-criteria group, while there was no significant group difference in cognitive function across three subgroups (Supplementary Table 1). Regarding the clinical outcome status at 12 months follow-ups, 44.5 % of CHR-participants at 12 months still met the UHR criteria with more severe global functioning and CAARMS symptom severity than individuals with non-persistence of CHR state. CHR-persistent participants displayed more severe CAARMS symptoms and GAF

impairment at baseline than CHR-nonpersistent individuals (Table 4.2), while the cognitive function was similar to CHR-nonpersistent group (Supplementary Table 2).

Table 4.1 Demographic information in subgroups of CHR and HC

	CHR-SPI	CHR-CAM	CHR-both	HC	F value	*p*	Post-hoc
Age, mean(SD),y	21.8(4.1)	21.2(4.2)	22.3(4.9)	22.6(3.5)	-	>0.05[a]	-
Sex(Male/Female)	11/19	5/25	14/36	15/33	-	>0.05	-
Education, mean(SD),y	15.3(2.5)	14.9(3.3)	15.7(3.4)	16.7(3.0)	53.0	<0.05*	HC>CHR-SPI HC>CHR-CAM HC>CHR-both
First-degree relative of ScZ history	0	2	0	0	-	-	-
Non-Medication	15	17	21	1	-	-	-
Medication	15	13	29	47	-	-	-
Antipsychotic	0	1	0	0	-	-	-
Antidepressant	5	7	15	0	-	-	-
Mood stabilizer	0	1	0	0	-	-	-
Anti-convulsants	0	0	0	0	-	-	-
Others	6	2	5	1	-	-	-
Multiple	4	2	9	0	-	-	-
GAF_baseline mean(SD)	63.9(13.7)	61.4(11.0)	53.5(12.4)	87.8(6.3)	-	<0.05*[a]	HC>CHR-SPI HC>CHR-CAM HC>CHR-both CHR-CAM>CHR-both CHR-SPI>CHR-both
Total CAARMS severity mean(SD)	14.5(13.2)	26.2(13.7)	39.4(16.7)	-	-	<0.05*	CHR-SPI<CHR-CAM CHR-CAM<CHR-both CHR-SPI<CHR-both
SPI-severity mean(SD)	0.5(0.3)	0.07(0.09)	0.6(0.5)	-	-	<0.05*[a]	CHR-CAM<CHR-SPI CHR-CAM<CHR-both

Notes: Abbreviations: y: year; SD: Standard Deviation; HC: Healthy Controls; CHR: Clinical High-risk Psychosis; CHR-CAM: CHR subjects who only met the criteria of the Comprehensive Assessment of At-Risk Mental States(CAARMS); CHR-SPI: CHR subjects who only met the criteria of Schizophrenia Proneness Instrument, Adult Version(SPI-A); CHR-both: CHR subjects who met the criteria of both SPI-A and CAARMS. FEP: First-episode Psychosis; ScZ; Schizophrenia; BACS: Brief Assessment of Cognition n Schizophrenia. * $p<0.05$, [a] non-parametric permutation statistics.

Table 4.2 Demographic information in CHR-persistent and CHR-nonpersistent at 12 months

	CHR-non persistent	CHR-persistent	HC	F value	*p*	Post-hoc
Age, mean(SD),y	21.9(4.7)	21.2(4.2)	22.6(3.5)	-	>0.05[a]	-
Sex(Male/Female)	7/29	10/29	15/33	3.63	>0.05	-
Education, mean(SD),y	15.2(3.1)	15.0(3.3)	16.7(3.1)	3.63	<0.05*	HC > CHR-persistent
Non-Medication	17	21	-	-	-	-
Medication	19	18	-	-	-	-
Antipsychotic	2	0	-	-	-	-
Antidepressant	7	12	-	-	-	-
Mood stabilizer	1	0	-	-	-	-
Anti-convulsants	0	0	-	-	-	-
Others	4	3	-	-	-	-
Multiple	5	3	-	-	-	-
GAF_baseline mean(SD)	60.4(12.1)	53.0(12.5)	87.8(6.3)	92.2	<0.05*	HC > CHR-nonpersistent HC > CHR-persistent CHR-nonpersistent > CHR-persistent
Total CAARMS severity mean(SD)	27.2(14.4)	40.1(16.9)	-	-	<0.05	CHR-nonpersistent < CHR-persistent
SPI-severity mean(SD)	0.3 (0.4)	0.5(0.5)	-	-	>0.05	-

Notes: Abbreviations: y: year; SD: Standard Deviation; HC: Healthy Controls; CHR: Clinical High-risk Psychosis; FEP: First-episode Psychosis; ScZ; Schizophrenia. * p<0.05, [a] non-parametric permutation statistics.

4.3.2 MEG-data results

4.3.2.1 Sensory attenuation effect at the sensor Level

At the sensor level, there was a significant M100 amplitude difference between active and passive conditions (p < 0.05, two-tailed) over frontal and temporal-parietal sensors across all participants (Figure 4.1A). The significant clusters between the active and the passive conditions were located over bilateral temporal-parietal and frontal sensors in HC (Figure 4.1B). In CHR-participants, condition differences were identified over frontal and right temporal-parietal sensors. In the FEP group, significant differences between conditions were only found over the right temporal-parietal sensors (Figure 4.1B).

There was no statistically significant group difference in sensory attenuation effect across three groups at sensor level (p > 0.05, two-tailed). Furthermore, M100 amplitudes in active

and passive conditions were separately examined across groups. The results showed no significant group differences in the M100 amplitude in either the active or the passive condition ($p > 0.05$, two-tailed).

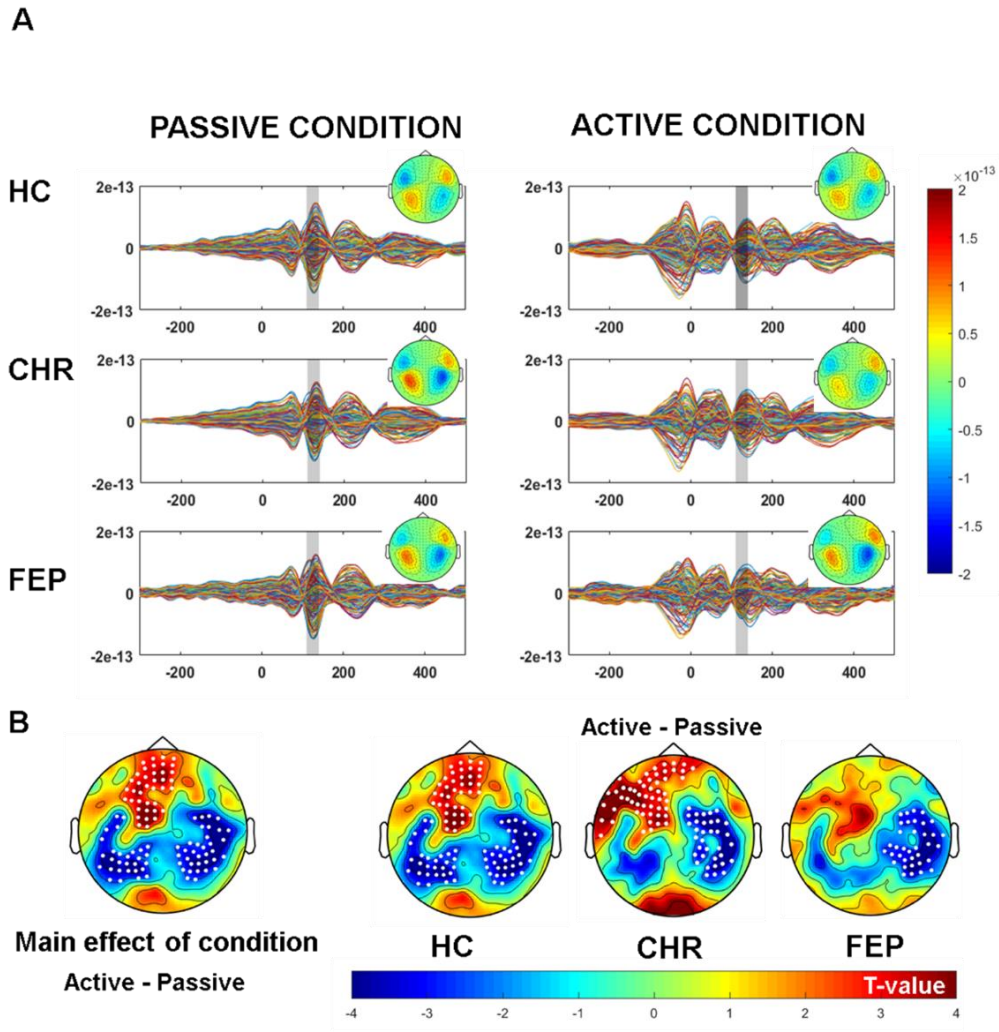

Figure 4.1 Sensory attenuation effect at the sensor level

A) Grand average butterfly ERF time series are computed for all 248 sensors and baselined corrected (-600 and -400 ms) and plot separately for each group. The right top panel of ERFs are topographical distribution plots of the M100 component in axial-magnetometer representation, plotted for data averaged over the 110-140 ms latency window highlighted in grey for the sensory attenuation effect. B) Topographical distributions in planar-magnetometer representation t-values for the SAP effect across and within groups. Significant clusters of sensors ($p < 0.05$, two-tailed) are highlighted with white dots. Abbreviations: HC: Healthy Controls; CHR: Clinical High-risk Psychosis; FEP: First-episode Psychosis.

4.3.2.2 Sensory attenuation effect at the source Level

4.3.2.2.1 Condition effect across groups and within the group

At the source level, there was a significant M100 amplitude difference between active and passive conditions in the left HES, right HES, and right ST across all participants (corrected

p < 0.05, two-tailed, Figure 4.2), indicating a smaller M100 amplitude in the active condition. The condition effect (sensory attenuation effect) in HC involved left HES, right HES and right ST (corrected p < 0.05, two-tailed). In contrast, CHR-participants showed sensory attenuation only in left ST (without correction), while the FEP group showed no significant sensory attenuation effect in both hemispheres (p > 0.05, two-tailed). On the contrary, FEP-participants displayed larger M100 amplitudes in the active condition than in the passive condition in left HES and left ST(corrected p < 0.05,two-tailed) (Table 4.3).

Additional analysis for the CHR subgroup revealed that the condition effect was disappeared in 4 auditory regions in the CHR-both group. In contrast, CHR-SPI and CHR-CAM groups displayed absence of sensory attenuation in part of the auditory cortex (Table 4.4). Moreover, the condition effect (sensory attenuation effect) was disappeared in CHR-persistent and CHR-nonpersistent group at 12 months (Table 4.5).

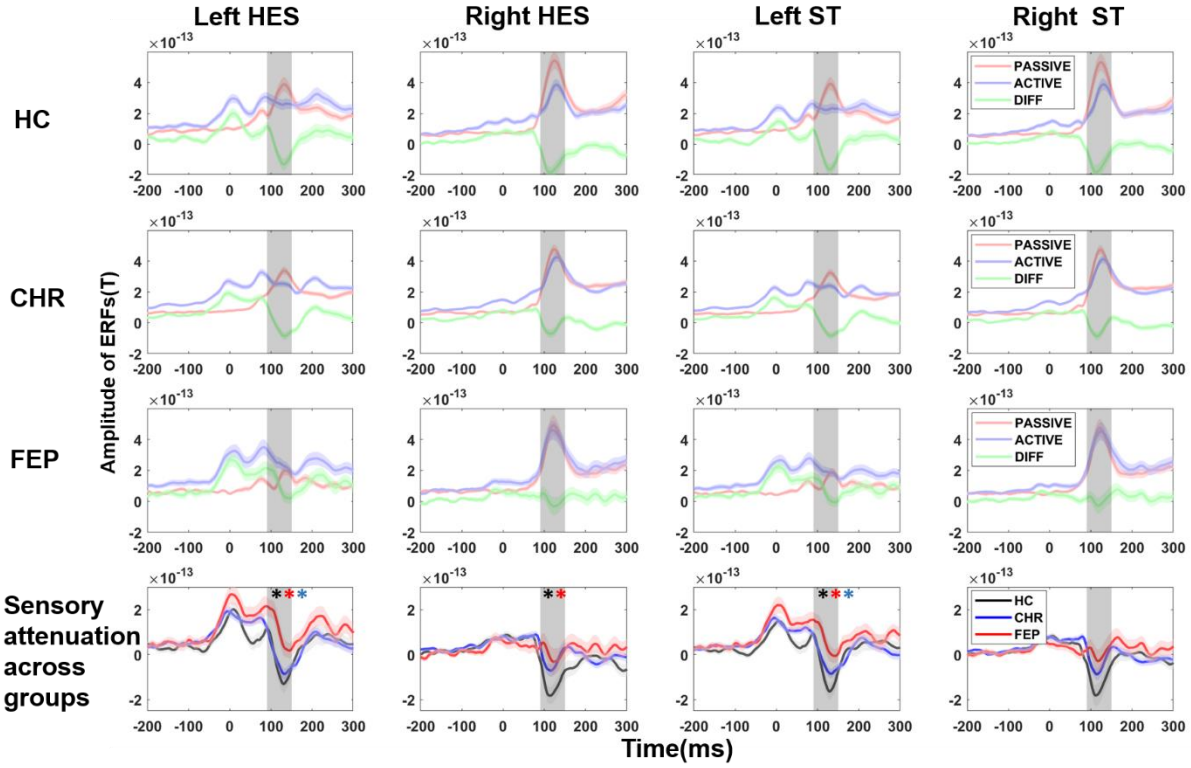

Figure 4.2 Virtual-channel level data

Source-reconstructed grand-average virtual channel ERF traces show separately for the 4 main ROIs (left and right HES and ST) and the sensory attenuation across groups (bottom row). Traces for the active condition are plotted in the red line, passive condition in the blue line, and the difference between two conditions in the green line. The bottom row shows the sensory attenuation effects per virtual channel per group (HC: black, CHR: blue, FEP: red). Shaded error-bars represent the standard error of the mean. Black asterisks mark significant condition effect within each group (false discovery rate corrected) in the top three rows. In the bottom row, black asterisks represent the significant sensory attenuation across the three groups, while the red asterisk

indicates a significant sensory attenuation group effect between HC and FEP, and the blue asterisk a significant sensory attenuation difference between CHR and FEP. The significant statistical *p*-value was 0.05. Abbreviations: HES: Heschl's Gyrus; ST: Superior Temporal Cortex; HC: Healthy Controls; CHR: Clinical High-risk Psychosis; FEP: First-episode Psychosis.

Table 4.3 Condition effect of M100 amplitude across groups and within group at source level for active and passive conditions

		Sensory attenuation Mean(SD)	t-value	*p*	CI-range
Main effect of condition (Active versus Passive)					
Left HES		-1.19E-14(1.98E-13)	-	-	-
Right HES		-6.15E-14(2.26E-13)	t(183)= -3.1	0.005*	[0.0006 0.0094]
Left ST		-3.23E-14(1.71E-13)	t(183)= -2.2	0.018*	[0.0098 0.0262]
Right ST		-6.13E-14(2.29E-13)	t(183)= -3.1	0.003*	[-0.0004 0.0064]
Condition effect within group (Active versus Passive)					
Left HES	**HC**	-3.76E-14(1.76E-13)	-	-	-
	CHR	-1.97E-14(2.04E-13)	-	-	-
	FEP	1.14E-13(1.49E-13)	t(25)=4.1	0.002*	[-0.0008 0.0048]
Right HES	**HC**	-1.30E-13(2.07E-13)	t(47)=-4.2	0.001*	[-0.001 0.003]
	CHR	-2.99E-14(2.28E-13)	-	-	-
	FEP	3.59E-15(2.12E-13)	-	-	-
Left ST	**HC**	-7.15E-14(1.67E-13)	t(47)=-3.0	0.004*	[0.0001 0.0079]
	CHR	-2.93E-14(1.68E-13)	t(109)= -1.9	0.027	[0.017 0.037]
	FEP	6.67E-14(1.36E-13)	t(25)= 2.7	0.005*	[0.0006 0.0094]
Right ST	**HC**	-1.22E-13(2.43E-13)	t(47)=-3.4	0.001*	[-0.001 0.003]
	CHP	-3.81E-14(2.18E-13)	-	-	-
	FEP	7.05E-15(2.09E-13)	-	-	-

Upper panel: Main condition effects of M100 amplitude across groups. Lower panel: M100 condition effect within the group. Abbreviations: HES: Heschl's Gyrus; ST: Superior Temporal Cortex; HC: Healthy Controls; CHR: Clinical High-risk Psychosis; FEP: First-episode Psychosis; SD: Standard Deviation; CI-range: Confidence Interval Range. * survive after false discovery rate (FDR) correction.

Table 4.4 Condition effect of M100 amplitude within CHR subgroups at the virtual-channel level

		Sensory attenuation Mean（SD)	t-value	*p*	CI-range
Left HES	HC	-3.8E-14(1.7E-13)	-	-	-
	CHR-SPI	-4.2E-14(1.9E-13)	-	>0.05	-
	CHR-CAM	-6.8E-14(1.8E-13)	t(29)= -2.2	0.025	[0.153 0.0357]
	CHR-both	-2.3E-14(2.2E-13)	-	>0.05	
Right HES	HC	-1.3E-13(2.1E-13)	t(47)= -4.2	0.001*	[-0.001 0.003]
	CHR-SPI	-2.0E-14(2.2E-13)	-	>0.05	-
	CHR-CAM	-6.2E-14(2.1E-13)	-	>0.05	-
	CHR-both	-2.1E-14(2.4E-13)	-	>0.05	
Left ST	HC	-7.2E-14(1.7E-13)	t(47)= -3.0	0.004*	[0.0001 0.0079]
	CHR-SPI	-5.3E-14(1.6E-13)	t(29)= -2.3	0.048	[0.0348 0.0612]
	CHR-CAM	-6.3E-14(1.5E-13)	t(29)= -2.3	0.017	[0.0009 0.025]
	CHR-both	5.2E-15(1.7E-13)	-	>0.05	
Right ST	HC	-1.2E-13(2.4E-13)	t(47)= -3.4	0.001*	[-0.001 0.003]
	CHR-SPI	-3.4E-14(1.9E-13)	-	>0.05	-
	CHR-CAM	-7.0E-14(2.3E-13)	t(29)= -1.7	0.048	[0.0348 0.0612]
	CHR-both	-2.1E-14(2.3E-13)	-	>0.05	

Notes: Main condition effects of M100 amplitude across groups. Lower panel: M100 condition effect within groups. Abbreviations: HES: Heschl's Gyrus; ST: Superior Temporal Cortex; HC: Healthy Controls; CHR: Clinical High-risk Psychosis; FEP: First-episode Psychosis; SD: Standard Deviation; CI-range: Confidence Interval Range. * survive after false discovery rate (FDR) correction.

Table 4.5 Condition effect of M100 amplitude in CHR-persistent and CHR-nonpersistent at the virtual-channel level

		Sensory attenuation Mean(SD)	t-value	*p*	CI-range
Left HES	HC	-3.8E-14(1.8E-13)	-	>0.05	-
	CHR-nonpersistent	-8.5E-15(1.8E-13)	-	>0.05	-
	CHR-persistent	-1.8E-14(2.3E-13)	-	>0.05	-
Right HES	HC	-1.3E-13(2.1E-13)	t(47)=-4.2	0.001*	[-0.001 0.003]
	CHR-nonpersistent	-3.9E-14(2.5E-13)	-	>0.05	-
	CHR-persistent	-3.2E-14(2.3E-13)	-	>0.05	-
Left ST	HC	-7.2E-14(1.7E-13)	t(47)=-3.0	0.004*	[0.0001 0.0079]
	CHR-nonpersistent	-2.4E-14(1.4E-13)	-	>0.05	-
	CHR-persistent	-2.3E-14(1.4E-13)	-	>0.05	-
Right ST	HC	-1.2E-13(2.4E-13)	t(47)=-3.4	0.001*	[-0.001 0.003]
	CHR-nonpersistent	-2.7E-14(2.4E-13)	-	>0.05	-
	CHR-persistent	-4.9E-14(2.4E-13)	-	>0.05	-

Notes: The condition effect is tested within an interesting time window between 90 ms and 150 ms. The condition effect is disappeared in either CHR-persistent or CHR-nonpersistent group at 12 months. Abbreviations: HES: Heschl's Gyrus; ST: Superior Temporal Cortex; HC: Healthy Controls; CHR: Clinical High-risk Psychosis; FEP: First-episode Psychosis; SD: Standard Deviation; CI-range: Confidence Interval Range. * survive after false discovery rate (FDR) correction.

4.3.2.2.2 **M100 sensory attenuation difference across groups**

There was a group effect in the left HES and ST (corrected $p < 0.05$, two-tailed) and in the right HES/ST (uncorrected $p < 0.05$, two-tailed). The post-hoc test suggested a significant sensory attenuation difference between HC- and CHR- participants in the right HES and right ST (uncorrected $p < 0.05$, two-tailed). In addition, both CHR and FEP groups showed a significant reduction of sensory attenuation in the left HES and the left ST compared to HC (corrected $p < 0.05$, two-tailed) (Table 4.6).

Regarding CHR subgroups, the result suggested that the sensory attenuation effect was impaired in the CHR-both group (uncorrected $p < 0.05$, two-tailed). Furthermore, according to different clinical state at 12 months in CHR-participants, the CHR-persistent group displayed impaired sensory attenuation effect in the right HES (uncorrected $p < 0.05$, one-tailed), and there was a trend of deficits in right ST(Figure 4.3).

Table 4.6 Group effects of auditory sensory attenuation at the source level

		F/t-value	*p*-value	CI-range
Group effect of sensory attenuation (HC versus CHR versus FEP)				
Left HES		F(182)= 6.6	0.003*	[-0.0004 0.0064]
Right HES		F(182)= 4.0	0.014*	[0.0067 0.0213]
Left ST		F(182)= 6.5	0.004*	[0.0001 0.0079]
Right ST		F(182)= 3.1	0.037	[0.0253 0.0487]
Post-hoc test of sensory attenuation				
HC vs CHR	**Left HES**	-	-	-
	Right HES	t(156)=-2.6	0.012	[0.0053 0.0187]
	Left ST	-	-	-
	Right ST	t(156)=-2.1	0.034	[0.022 0.046]
HC vs FEP	**Left HES**	t(72)=-3.8	0.004*	[0.0001 0.0079]
	Right HES	t(72)=-2.3	0.024*	[0.0145 0.0335]
	Left ST	t(72)=-3.7	0.004*	[0.0001 0.0079]
	Right ST	t(72)=-2.0	0.042	[0.0296 0.0544]
CHR vs FEP	**Left HES**	t(134)=-3.3	0.002*	[-0.008 0.0048]
	Right HES	-	-	-
	Left ST	t(134)=-2.9	0.004*	[0.0001 0.0079]
	Right ST	-	-	-

Notes: The upper table displays the group effect of sensory attenuation in the left and right HES, ST with non-parametric permutation tests, followed by post-hoc test of sensory attenuation between groups. The degree of freedom is shown in the bracket of t-value (or F-value). The *p*-value with black asterisk indicates the survival of multiple corrections with a false discovery rate (FDR) correction method across four nodes. The significant statistical *p*-value is 0.05. Abbreviations: HES: Heschl's Gyrus; ST: Superior Temporal Cortex; HC: Healthy Controls; CHR: Clinical High-risk Psychosis; FEP: First-episode Psychosis. CI-range: Confidence Interval Range. * survive after FDR correction.

Figure 4.3 Sensory attenuation of CHR-persistent and CHR-nonpersistent group at 12 months at the virtual-channel level

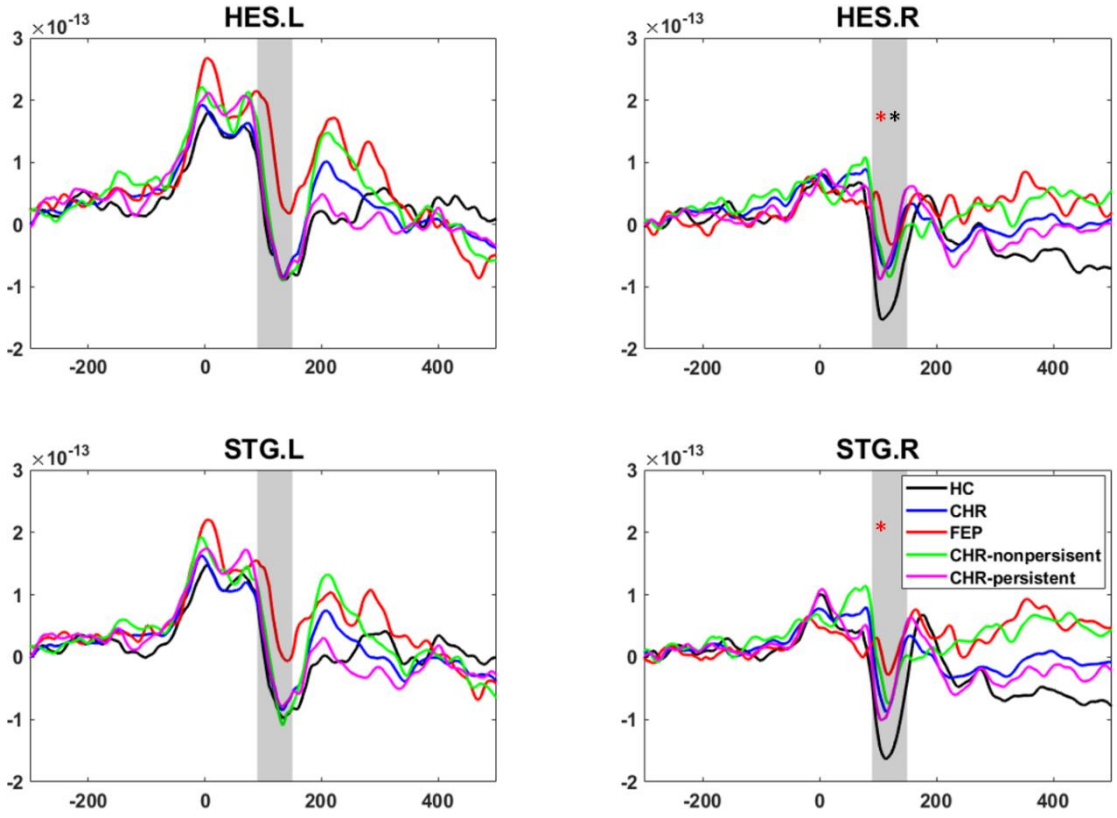

This figure plots sensory attenuation waves in 4 ROIs per group (HC: black, CHR: blue, FEP: red; CHR-nonpersistent: green; CHR-persistent: magenta). The interested time window of M100 is highlighted with the grey shadow (between 90 and 150 ms). Non-parametric permutation tests find no strong group difference across five groups. In addition, the differences between HC and participants with different clinical outcome of CHR are examined, separately. The red asterisk indicates the group difference between HC and CHR-nonpersistent, and the black asterisk marks the difference between HC and CHR-persistent. The statistically significant *p*-value is 0.05 (uncorrected, one-tailed). Abbreviations: HES: Heschl's Gyrus; ST: Superior Temporal Cortex; HC: Healthy Controls; CHR: Clinical High-risk Psychosis; FEP: First-episode Psychosis; ROI: Region of Interest.

4.3.2.2.3 **M100 amplitude differences in the passive and active condition**

Group effects for the M100 amplitude in the active and passive conditions were investigated (corrected $p < 0.05$, two-tailed). There was a significant group difference in the M100 amplitude in the passive condition in the left HES and left ST (corrected $p < 0.05$, two-tailed). The post-hoc analysis revealed that the difference has resulted from the reduction of the M100 amplitude for the contrast between HC vs FEP groups (corrected $p < 0.05$,two-tailed), as well as between FEP vs CHR groups (corrected $p < 0.05$,two-tailed, Table 4.7). There were no significant M100 amplitude difference in the active condition ($p > 0.05$, two-tailed).

4.3.1 Correlations

4.3.1.1 Correlations between sensory attenuation, psychopathology and cognition

Correlations between sensory attenuation in the auditory cortex, psychopathology, and CAARMS-ratings were examined (Table 4.8). There was a significant correlation between GAF and sensory attenuation effects in the left HES across CHR- and FEP-groups. Furthermore, ratings on the unusual thought content and disorganized speech subscales of the CAARMS were significantly correlated with sensory attenuation in left HES (Figure 4.4).

Table 4.7 Group effects of M100 at the source level

		F/t-value	p-value	CI-range
Group effect of M100 amplitude (HC versus CHR versus FEP)				
Left HES		F(182)=5.0	0.009*	[0.0032 0.0148]
Right HES		-	-	
Left ST		F(182)=7.4	0.001*	[-0.001 0.003]
Right ST		-	-	
Passive M100 across three groups				
Left HES		F(182)=8.2	0.002*	[-0.0008 0.0048]
Right HES		-	-	-
Left ST		F(182)=9.5	0.001*	[-0.001 0.003]
Right ST		-	-	-
Post-hoc test of Passive M100 amplitude				
HC VS FEP	**Left HES**	t(73) = 3.8	0.009*	[0.0007 0.011]
	Right HES	-	-	-
	Left ST	t(73) = 4.1	0.009*	[0.0007 0.011]
	Right ST	-	-	-
CHR VS FEP	**Left HES**	t(135) = 3.8	0.009*	[0.0007 0.011]
	Right HES	-	-	-
	Left ST	t(135) = 3.9	0.009*	[0.0007 0.011]
	Right ST	-	-	-

Notes: M100 amplitudes are tested across three groups and between groups. The degree of freedom is shown in the bracket of t-value(F-value). The *p*-value with black asterisk indicates the survival of multiple corrections with a false discovery rate (FDR) correction method across four nodes. Abbreviations: HES: Heschl's gyrus;

ST: Superior Temporal Cortex; HC: Healthy Controls; CHR: Clinical High-risk Psychosis; FEP: First-episode Psychosis.CI-range: Confidence Interval Range. * survive after FDR correction.

Table 4.8 Correlations between sensory attenuation, clinical variables, and cognition across groups

items	CHR and FEP			
	SAP Left HES	SAP Right HES	SAP Left ST	SAP Right ST
GAF_baseline	*r*=-0.29 *p*=0.0011*		*r*=-0.18 *p*=0.046	
Total CAARMS severity	*r*=0.27 *p*=0.0023*	-	*r*=0.20 *p*=0.024	-
Total SPI-A severity	*r*=0.20 *p*=0.022	-	*r*=0.17 *p*=0.051	-
CAARMS-subitems				
UTC_global	*r*=0.29 *p*=0.00069*	-	*r*=0.23 *p*=0.009	-
NBI_global	*r*=0.17 *p*=0.048	-	*r*=0.18 *p*=0.051	-
PA_global	*r*=0.19 *p*=0.027	-	-	-
DS_global	*r*=0.29 *p*=0.00071*	-	*r*=0.26 *p*=0.0023	-

Notes: Spearman rank correlations ($p < 0.05$). *FDR corrected. Abbreviations: GAF: Global Assessment of Functioning; CAARMS: Comprehensive Assessment of At-Risk Mental States; SPI-A: Schizophrenia Proneness Instrument, Adult Version; UTC_global: Global Score of Unusual Thought Content; NBI_global: global score of the non-bizarre idea; PA_global: global score of perceptual abnormality; DS_global: Global Score of Disorganized Speech; CHR: Clinical High-risk Psychosis; FEP: First-episode Psychosis. HES: Heschl's Gyrus; ST: Superior Temporal Cortex.

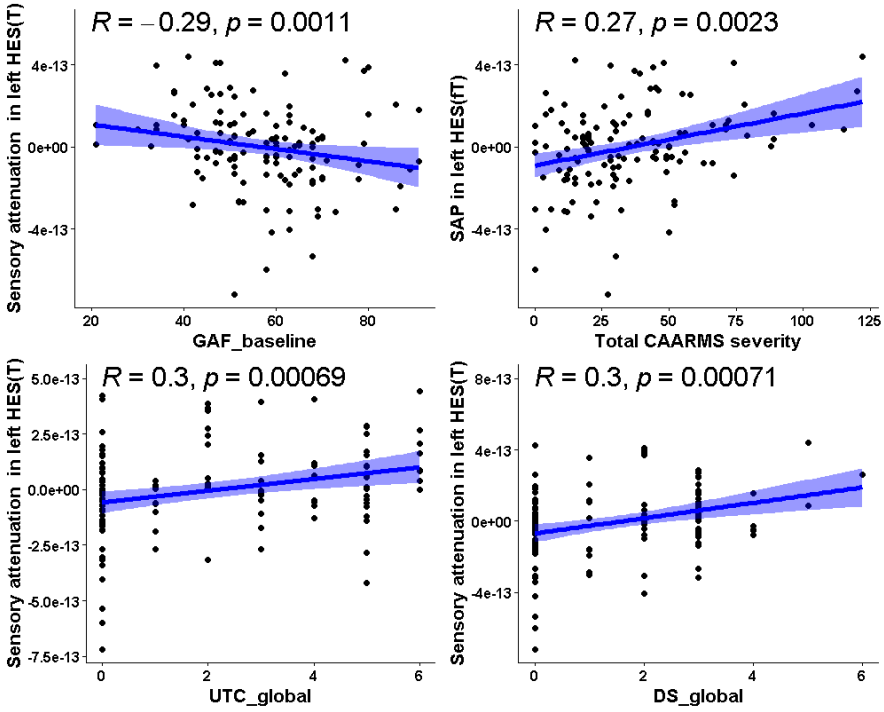

Figure 4.4 Correlation between sensory attenuation in left HES and clinical features across CHR- and FEP-participants

Abbreviations: HES: Heschl's Gyrus; UTC_global: Global Score of Unusual Thought Content; DS_global: Global Score of Disorganized Speech. GAF: Global Assessment of Functioning; *R*: correlation coefficient; $p < 0.05$.

4.4 Discussion

This study examined whether deficits in auditory M100 sensory attenuation are present in emerging psychosis. Also, we explored the association between impaired sensory attenuation and clinical as well as cognitive variables. The results indicated that auditory sensory attenuation was impaired in both CHR and FEP groups. Moreover, auditory sensory attenuation deficits were linked to the severity of CAARMS symptoms, GAF-ratings, and cognitive functions.

Consistent with previous studies (Baess, Widmann, Roye, Schröger, & Jacobsen, 2009), we observed sensory attenuation of the M100 within a 40 Hz ASSR paradigm at both sensor and source level that was particularly prominent over the right hemisphere. This finding is in line with previous evidence that simple tones are preferentially processed in the right hemisphere (Zatorre, Bouffard, Ahad, & Belin, 2002; Zatorre, Evans, Meyer, & Gjedde, 1992).

The FEP-group was featured by reduced M100 sensory attenuation in the bilateral HES and ST compared to the HC-group. In addition, FEP-patients were characterized by impaired M100 suppression in the left HES and ST relative to CHR-participants. The finding of reduced sensory attenuation in FEP-patients is consistent with previous studies that employed paradigms involving speech stimuli (Ford & Mathalon, 2004; Perez et al., 2012).

In combination with source reconstruction, the MEG-approach in the current study identified the impairment of M100 sensory attenuation was present in the bilateral auditory cortex in FEP. Intriguingly, the M100 amplitude in the left HES and ST in FEP-individuals during self-generated conditions was significantly enhanced compared to passive listening conditions. The increased contralateral auditory activity during self-generated sounds have been reported in previous fMRI studies in HC-participants (Reznik, Henkin, Schadel, & Mukamel, 2014; Reznik, Ossmy, & Mukamel, 2015). The increased contralateral auditory cortex activity in FEP-participants was modulated by the motor-related cortex (Reznik et al., 2015) to increase perceptual sensitivity (Reznik et al., 2014) in FEP-participants. However, this needs further exploration in future studies.

Importantly, we observed deficits in M100 sensory attenuation in CHR-participants. Previous results revealed a trend-level impairment in CHR that was intermediate between HC and ScZ (Perez et al., 2012; Whitford et al., 2018). In line with our current findings, the impairment in N100 sensory attenuation was significantly different between HC and CHR with a relatively larger sample size(Mathalon et al., 2019). However, with a MEG-approach, our current finding showed that sensory attenuation deficits involved the right auditory cortex, while the sensory attenuation in the left HES and ST were intact and intermediate between HC and FEP. Dysfunctions in sensory attenuation in the right auditory cortex are supported by structural MRI-data that have highlighted reduced grey matter in CHR-participants (Fusar-Poli et al., 2011). In combination with the alteration of sensory attenuation in genetically vulnerable individuals of ScZ(Ford et al., 2013) and schizotypy subjects (Oestreich et al., 2015, 2016), it is therefore likely that dysfunction of N100/M100 suppression is a marker for psychosis vulnerability.

Consistent with previous finding (Simon et al., 2006), current findings suggested that CHR-participants who met both BS and UHR criteria were linked to greater CAARMS symptom and more severe global functioning outcome than participants meeting UHR criteria alone. Furthermore, CHR with both UHR and BS threshold displayed impaired sensory attenuation rather than in CHR met BS or UHR. BS criteria is often used as a complementary approach

to identify individuals of high risk to develop psychosis. Simultaneously, the meta-analysis concluded that individuals who met both UHR and BS criteria have a higher risk to develop psychosis than UHR criteria along (Fusar-Poli, Cappucciati, Bonoldi, et al., 2016). It is therefore suggested that the BS criteria improves the sensitivity to detect individuals with the risk to develop psychosis. Moreover, the follow-ups results indicated that approximately 45% of CHR met the UHR criteria at 12 months, possibly because the sample was from the community. The individuals still met the CHR criteria at 12 months displayed impaired sensory attenuation at baseline, while the CHR-nonpersistent individuals were interact at baseline, indicating the different clinical outcome could potentially contribute to the alteration of auditory sensory attenuation.

We also examined whether sensory attenuation deficits in CHR- and FEP-groups could involve more basic impairments in the M100. The reduced M100 amplitude in the passive condition in FEP participants was consistent with previous data that have shown reduced M100 responses in the auditory cortex in FEP (Del Re et al., 2015) and ScZ-patients (for a review see(Rosburg, Boutros, & Ford, 2008)), possibly due to impaired attention in FEP(Ren, Fribance, Coffman, & Salisbury, 2021). Interestingly, the M100 amplitude in the active condition was interact in FEP. The account that can be taken was that attention-related reduction of M100 amplitude in active condition was possibly compensated by increased prediction error due to the inability to suppress M100 amplitude in FEP. Furthermore, although the sensory attenuation in the right auditory cortex was impaired in CHR, the M100 amplitude in the bilateral auditory cortex in the active and passive conditions were intact in CHR individuals. Therefore, no strong evidence in the current Chapter revealed that the basic M100 impairment could account for impaired sensory attenuation, while it remains further demonstration in the future study.

In addition, our results suggested that auditory M100 attenuation in the left HES and ST was negatively associated with GAF-ratings, indicating that more pronounced impairments in sensory attenuation were correlated with poorer functioning. Moreover, the impaired sensory attenuation showed a significant relationship with unusual thought content and disorganized speech symptoms across CHR- and FEP-participants. Although such correlation between M100 suppression and clinical symptoms is not found in precious studies (Ford et al., 2007; Ford, Mathalon, Whitfield, Faustman, & Roth, 2002), our finding is consistent with previous results in the literature (Mathalon et al., 2019; Perez et al., 2012), in support of the notion that sensory attenuation helps to illustrate clinical psychotic symptoms(Feinberg & Guazzelli, 1999),

In summary, the current findings implicate that sensory attenuation is impaired in both CHR- and FEP-participants, which cannot be interpreted by the basic M100 malfunction in the active and passive condition. Furthermore, sensory attenuation of the M100-response correlated with the severity of subthreshold attenuated psychotic symptoms and general functioning, highlighting the potential relevance of dysfunctional sensory attenuation to account for core features of emerging psychosis.

Chapter 5 Effective connectivity during sensory attenuation in clinical high-risk participants and first-episode psychosis: A Dynamic Causal Modelling approach

5.1 Introduction

Brain is organized into functionally separated areas that dynamically cooperate during processing sensory and cognitive functions. The interaction between brain areas arises from anatomical and functional connections (Friston, 2011; Peterson & Fling, 2018). The disrupted interaction can give rise to clinical symptoms, such as auditory hallucinations and delusions in ScZ (Friston, 1999; Friston & Frith, 1995). One potential neuropsychological mechanism for auditory hallucinations/delusions is the failure to predict the sensory consequence of actions, resulting in an inability to distinguish between internal- and external-generated sensations. Successfully distinguishing between internal- and external-induced sensations leads to sensory attenuation. One neurophysiological index of sensory attenuation is the auditory N/M100 (see Chapter 3).

The generation of auditory sensory attenuation is resulted from precise interaction among the sensory system with motor network in the normal brain. Specifically, frontal motor-related areas have been proposed to underlie the generation of the efference copy signal (Christensen et al., 2007; Haggard & Whitford, 2004), while the thalamus may act as a hub to propagate efference copy signals to higher-order cortical areas (Sherman, 2016). In addition, the cerebellum plays a key role in comparing predicted and forthcoming signals (Blakemore & A. Sirigu, 2003). The parietal cortex may contribute towards sensory attenuation (Blakemore & A. Sirigu, 2003) through its role in combing sensory and motor information (Anderson, Glibert, & Burkholder, 2002).

According to the predictive coding account (Friston & Kiebel, 2009), the sensorimotor network of auditory sensory attenuation integrates into a hierarchical modulation pattern where the top-down information transmits the prediction signal and the bottom-up conveys the prediction error(Ford & Mathalon, 2019). Of note, DCM is one of the effective connectivity approaches, designed to explore causal interaction between brain areas (Friston et al., 2003) by testing numerous competing models with different types of connections (forward, backward and lateral). Notably, DCM was employed to examine neural mechanism underlying perceptual and cognitive functions in psychiatric disorder(Heinzle &

Stephan, 2018). Studies by using fMRI and EEG demonstrated an imbalance of top-down and bottom-up communication in ScZ individuals (Dima et al., 2010a; Tso et al., 2020), supporting the notion of dysconnectivity in ScZ (Friston, 2002). Specially, DCM of evoked response has been widely used to explore auditory MMN and visual N100 response (Dima et al., 2012a; Dima et al., 2009) in ScZ-patients. For instance, the study employed DCM to discuss the aberrant connectivity in ScZ during an auditory oddball MMN paradigm. ScZ patients displayed abnormal top-down connectivity from the right inferior frontal cortex to the right ST, and a decreased intrinsic inhibitory self-connectivity within the right ST(Dima et al., 2012a).

Moreover, the alteration of effective connectivity has been investigated in different stages of psychosis. DCM provides new insights in the development of psychotic symptoms and effective disconnection at the network level in the subjects of risk to develop psychosis(Schmidt & Borgwardt, 2013). CHR individuals revealed greater modulation of connectivity from the ventral striatum to the midbrain than HC, and the connection strength in CHR-participants was associated with the severity of psychotic symptoms(Winton-Brown et al., 2017). One more DCM study suggested similar intrinsic connection impairment within the right inferior frontal cortex in psychotic patients and their unaffected relatives during auditory MMN (Ranlund et al., 2016), indicating the abnormality of connection emerged at the risk state of psychosis.

DCM method has been applied to investigate the hierarchical interaction of top-down prediction and bottom-up sensory input related to sensory prediction in healthy controls, particularly in the visual (Summerfield et al., 2006) and auditory cortices (Dürschmid et al., 2016; Garrido et al., 2008). In Chapter 3, we employed DCM to investigate hierarchical interaction of sensory attenuation network among thalamo-cortical circuit in the normal brain, indicating that successful generation of auditory sensory attenuation resulted in enhanced top-down control and subsequently reduced bottom-up prediction error. Importantly, it has been suggested that aberrant top-down prediction and bottom-up sensory input potentially contributed to the illusory perception in psychosis(Rao & Ballard, 1999). Moreover, supporting evidence from ScZ found that the impaired auditory N100 sensory attenuation has resulted from disrupted communication between frontal and temporal cortices during voluntary-initiated auditory stimuli (Ford et al., 2002), particularly in the gamma oscillations(Ford et al., 2005).

However, hierarchical interactions in a sensory attenuation network across different stages of psychosis illness has not been explored so far. Therefore, in our current Chapter, we employed DCM to explore sensory attenuation networks during emerging psychosis. I hypothesized that FEP-patients would display impaired top-down and bottom-up interactions within the sensory attenuation network, while such dysfunction in CHR was assumed to be intermediate between HC and FEP.

5.2 Methods

5.2.1 Participants

Forty-eight HC, 110 CHR-participants, and 26 FEP-participants were included in this study. The detailed recruitment process and demographic information were described in Chapter 2 and Chapter 4.

5.2.2 Data collection and pre-processing

MEG data were collected and processed by following Chapter 4.

5.2.3 DCM analysis

ROIs for DCM analysis consisted of the left and right thalamus (left: [-10.85, -17.56, 7.98], right: [13, -17.55, 8.09]), HES (left: [-41.99, -18.88, 9.98], right: [45.86, -17.15, 10.41]), right IPL ([46.46, -46.29, 49.54]), and right IFG ([50.2, 14.98, 21.41])(Figure 5.1). Apart from the ROIs in Chapter 3, right IFG was additionally included in model structures as evidence suggested the role of IFG in sensory prediction (Garrido et al., 2008), as well as the malfunction of the IFG in psychosis and first-degree unaffected relatives (Ranlund et al., 2016). Because the operculum part of the IFG is related to auditory processing (Opitz, Rinne, Mecklinger, Von Cramon, & Schröger, 2002) and was activated in our study, it was chosen as our interested frontal regions.

MEG data of ROIs were pre-processed and extracted based on the central coordinates of the AAL atlas template (Xia et al., 2013). After baseline correction and averaging across trials, the ROIs were converted to the SPM merged format.

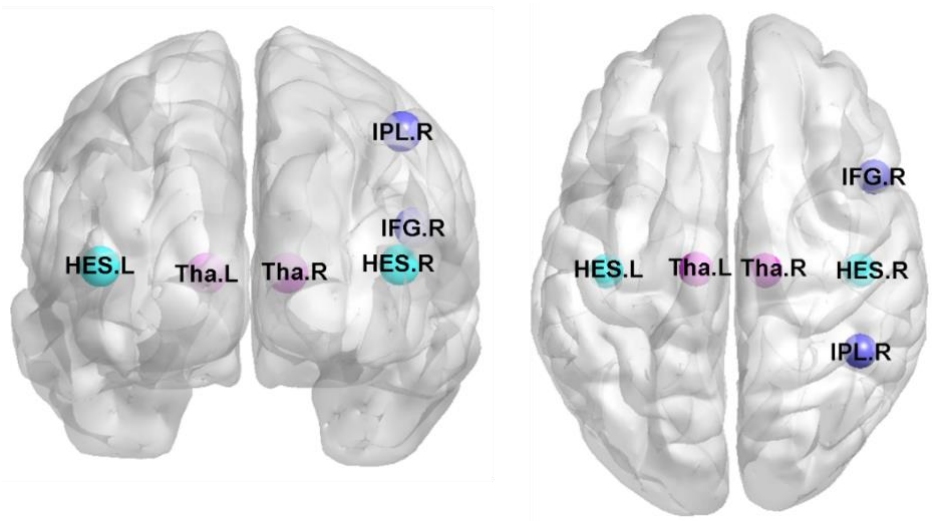

Figure 5.1 Nodes include in DCM analysis at the coronal and axial direction

Abbreviations: Tha: Thalamus; HES: Heschl's Gyrus; IPL: Inferior Parietal Lobe; IFG: Inferior Frontal Cortex; L: Left; R: Right.

Finally, ROIs were utilized to specify DCM models into three families for all participants. To test the contribution of the right IFG, Family A was characterized by switching off the connection between IFG and other ROIs in order to investigate whether IFG was involved in generating sensory attenuation. Compared to Family A, the unique feature of Family B was the hierarchical relationship between IPL and IFG, while the relationship between IPL and IFG in Family C was lateral. In particular, each family was designed with three sub-families, characterized by the forward, backward, and bidirectional modulation connection between ROIs. Within each sub-family, the modulatory connection patterns varied in combination with self-modulation and lateral modulation (4 models for each sub-family) (Figure 5.2). Also, we built up a null DCM model within only intrinsic connections for Family A, Family B, and Family C, separately. In total, 39 models were constructed for all participants.

DCM-analysis of evoked responses uses excitatory and inhibitory neuronal subpopulations in a neural mass model that was applied to auditory ERF responses between -100 ms and 200 ms. Source-space data were entered into the DCM analysis and local-field potentials (LFP, use to model real or virtual electrode data) were used to model ERF data without spatial reconstruction. Given that we were interested in the changes in connection strengths during sensory attenuation relative to a baseline condition (auditory input without sensory attenuation), between-condition effects were set to 0 (baseline) and 1. DCM was performed based on Statistical Parametric Mapping 12 (SPM 12,v7487) (https://www.fil.ion.ucl.ac.uk/spm/).

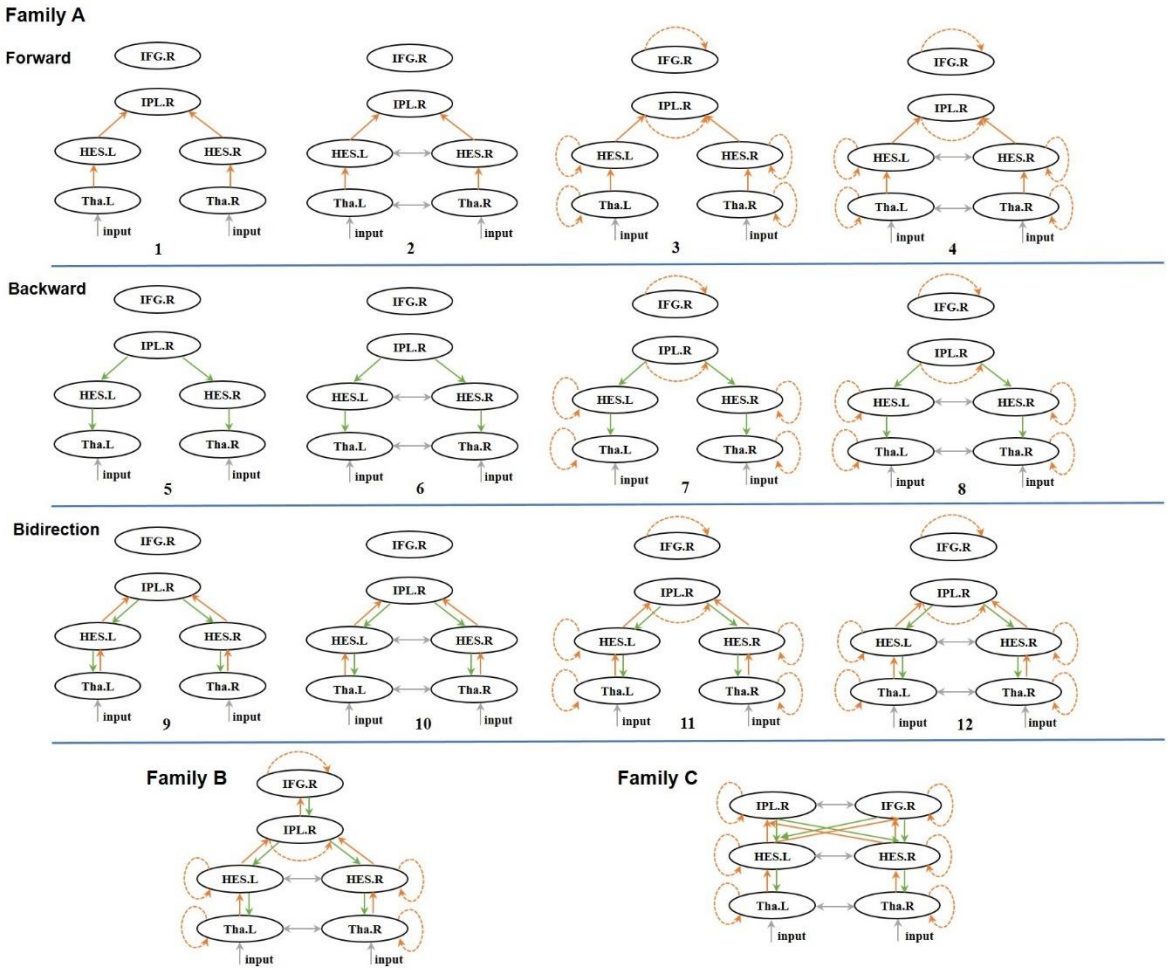

Figure 5.2 DCM-model structures

This figure shows the model structure of Family A. Each family is split into three sub-families, referring to forward, backward and bidirectional family. Each sub-family are varied within or without self- and lateral-modulatory connections. The orange lines represent forward modulatory connections, and the green lines show backward modulatory connections. Besides, the grey dotted lines show the lateral modulatory connections, and the yellow dotted lines represent the self-modulated connections. The distinctive features of Family B and Family C are the causal interaction between IFG and IPL. The IFG occupy a higher hierarchical position than IPL in family B, while the relationship between IFG and IPL is lateral in Family C. Tha: Thalamus; HES: Heschl's Gyrus; IPL: Inferior Parietal Lobe; IFG: Inferior Frontal Cortex; L: Left; R: Right.

5.2.4 Statistics

5.2.4.1 Model structure: Bayesian modelling selection (BMS)

As DCM is a framework for constructing models to estimate the parameters of effective connectivity, the first step is a Bayesian model inversion to detect the optimal posterior parameters that balance the accuracy (the precision of predicted data to the observed data) and the complexity of each model for every single participant. The quantification of model performance was the free energy approximation to the model evidence: the probability of

the observed data given the model (integrating over all possible parameter values). Finally, the posterior probability and exceedance probability were computed at the group level. The exceedance probability denotes the probability that this model is more likely than any other model in a given dataset.

Regarding the model structure comparisons, random-effects Bayesian model selection (RFX-BMS) was employed to detect the winning DCM-model across three groups and three model families to examine: 1) whether IFG is important in generating sensory attenuation and to explore the hierarchical relationship between IFG and IPL; 2) to investigate the modulatory connection contributing towards sensory attenuation. The reason to choose RFX-BMS is that the winning model was assumed to vary across individual subjects. Furthermore, RFX-BMS across all participants first determined the winning family, then fixed-effects BMS(FFX-BMS) was applied to examine models from the winning family to test the optimal model within each group, assuming that the winning model was identical.

Our first performance of RFX-BMS results (Supplementary Figure 2) supported the involvement of IFG in generating sensory attenuation across all participants. Although the exceedance probability of the winning Family C (0.54) was not better than Family B (0.46), the overall model evidence in Family C was larger than in Family B. The distinctive difference between Family B and Family C was the relationship between IPL and IFG, namely whether the relationship was lateral or hierarchical. Although the model structure in Family C was more complex than in Family B, model evidence in our dataset preferred Family C after trading off between the accuracy and complexity of the models. Hence, the following analysis was based on Family C.

5.2.4.2 **Connectivity parameter estimation: parametric empirical bayes (PEB)**

The posterior parameter from Bayesian model reversion can be estimated directly by a t-test or ANOVA. However, the potential impact of covariance on the connection strength is not estimated in classic statistics. Currently, the PEB framework is proposed to estimate parameter difference at the group-level (between-subject), aiming to quantify the commonalities and differences across groups (Friston, Litvak, et al., 2016). The PEB scheme is distinctive in several aspects in conducting group-level inference (between-subject) in SPM 12. One of the benefits of PEB is to increase the robustness of the DCM connection to a random (uncertain) effect. Specifically, PEB takes account of both expected values and

covariance of parameters. Moreover, the PEB framework is efficient, particularly when estimating a large number of models (for further details see (Zeidman et al., 2019).

In brief, PEB assumes that all participants have identical model structures, but with different connection strength. The posterior parameters (including posterior expectation and covariance) estimate from the first level (Bayesian model inversion) are collated and modelled by using a general linear model (GLM) to compute averaged group-level parameters. Meanwhile, the unexplained covariance or uncertain random effect of parameters are captured by a covariance component model. Specifically, the average group-level parameters are weighted by estimated precision of individual connection (from Bayesian model inversion), which are then used as empirical priors to estimate a full-model to obtain all free parameters of interest. Having calculated all free parameters, Bayesian model reduction (BMR) automatically searches over all reduced models, and iteratively discards connection parameters by switching off the connection that cannot ascribe to the model evidence. BMR procedure stops when disregarding parameters reduces model evidence, aiming to find the optimal reduced models. Finally, Bayesian model averaging (BMA) is applied to average the posterior parameter over 256 models from the final iteration of BMR, weighted by the posterior model probability across models.

Apart from the interest in modulatory connection, we were interested in examining whether the deficits in sensory attenuation also arose from the dysconnectivity at the level of intrinsic connection corresponding to early auditory ERFs generation in the passive condition. We conducted a similar PEB procedure for intrinsic connection (matrix A).

Of note, the GLM matrix was assigned to -1, 0, 1 to investigate between-participants differences. Given the imbalance of sample size across groups, the GLM matrix was designed with mean-centred regressors to set the first regressor to explain the group mean value of connection strength. As the design matrix in GLM is rank deficient, we designed the GLM matrix twice to examine between-group differences. Namely, one specific hypothesis was that there was a linear group effect in connection strength. Accordingly, the GLM matrix was designed with two regressors: 1) the overall mean; 2) the difference between HC and FEP. Secondly, commonalities and between-group differences (without linear effect) with three regressors were explored: 1) the overall mean across all participants; 2) the difference between HC and CHR and 3) the difference between CHR- and FEP-groups.

The random effect at the between-subject level was set to the default value with 1/16 of prior variance.

Finally, we identified the candidate-modulatory connections that could distinguish between groups during sensory attenuation from the PEB procedures. Furthermore, the predictive validity of the candidate connections was performed by the approach of leave-one-out cross-validation to test the effect size of candidate connections based on whether they can significantly classify a subject into a specific group(for a detailed description of the procedure see (Zeidman et al., 2019)).

5.3 Results

5.3.1 Model structures

The results from RFX-BMS suggested that the IFG contributed towards the sensory attenuation. Furthermore, the exceedance probability in Family C (0.52) was slightly better than in Family B (0.48) (Supplementary Figure 2). Hence, all the following analyses were based upon Family C. The winning model across all participants was model 12 with an exceedance probability of 100%, which compromised bidirectional, lateral, and self-modulation connections (Figure 5.3). Within each group, the winning model within Family C for HC- and CHR-groups was model 12. In contrast, FEP-participants preferred model 8 from the backward modulation family without feedforward-modulatory connections (Figure 5.4). Additionally, the observed and predicted ERFs from the winning model across all the subjects were plotted (Figure 5.5).

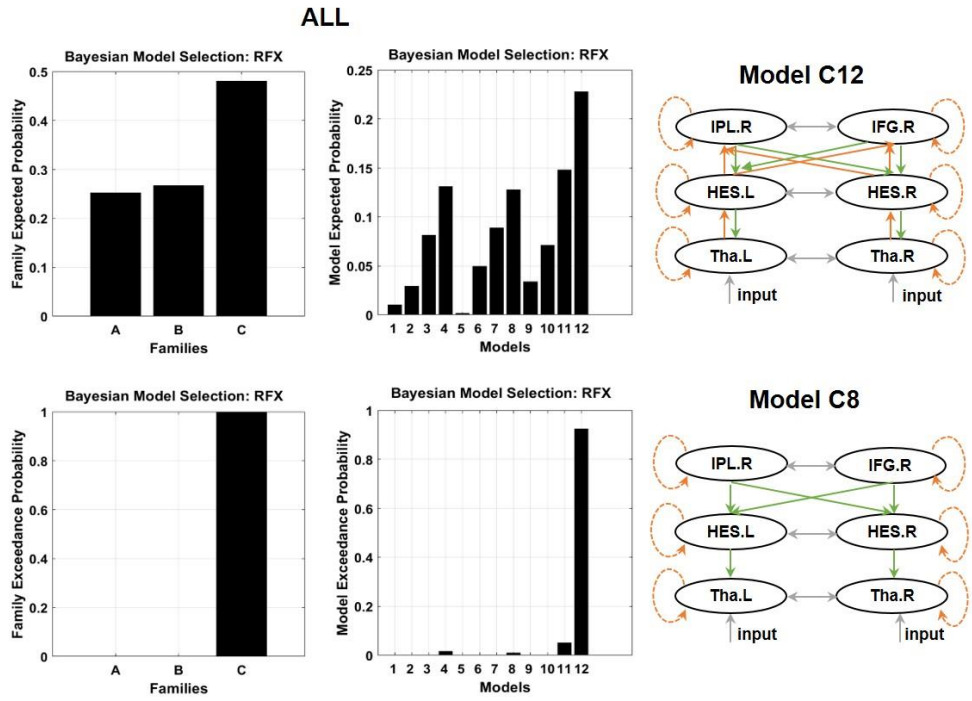

Figure 5.3 BMS results of DCM-models across and within groups

This panel displays the results of the RFX-BMS across all participants among models in Family C (12 models without null model). Family C is further split into three subfamilies according to forward, backward, bi-direction modulatory connections. Panel A displays the expected and exceedance posterior probability at the family- and model- level for all participants separately. The winning model 12 across all the constructed models is presented on the right side with almost 100% posterior probability. RFX: Random Effect. Tha: Thalamus; HES: Heschl's Gyrus; IPL: Inferior Parietal Lobe; IFG: Inferior Frontal Cortex; L: left; R: Right.

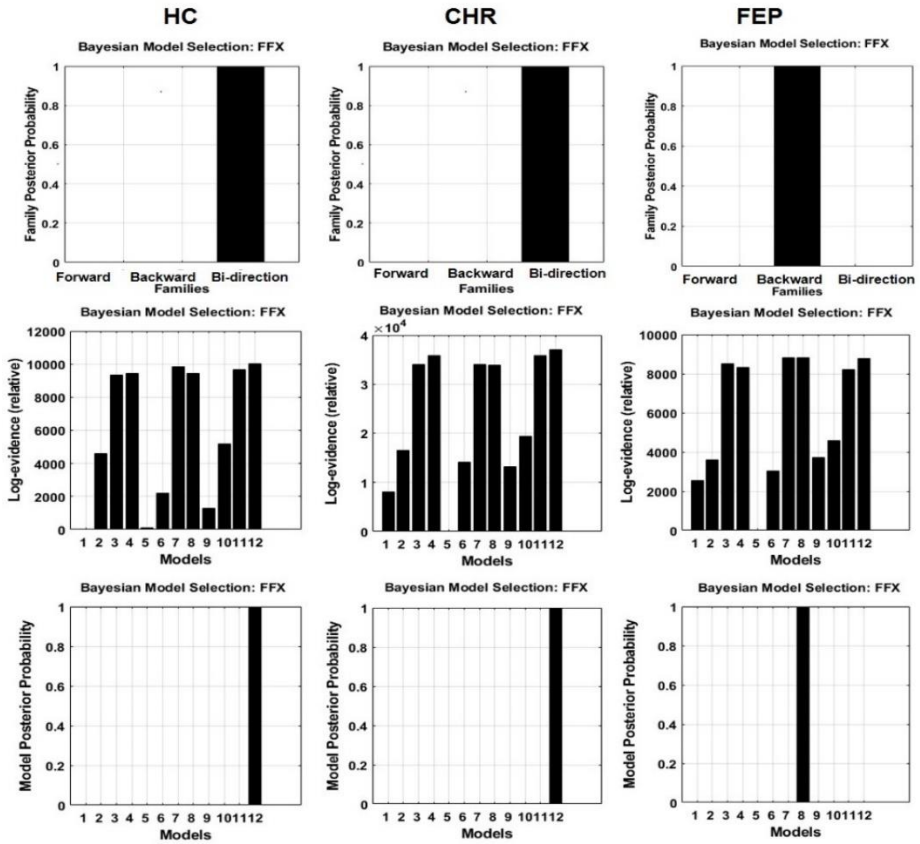

Figure 5.4 BMS results of DCM-models across and within groups

This panel displays the FFX-BMS results of winning family and model within each group in each column. Both HC and CHR group prefer the family with bi-directional modulatory connection, and the winning model is model 12. In contrast, FEP-patients prefer the family that incorporated backward modulatory connections. The structure of winning model 8 in the FEP group is presented in panel A. FFX: Fixed Effect; HC: Healthy Controls; CHR: Clinical High-risk Psychosis; FEP: First-episode Psychosis.

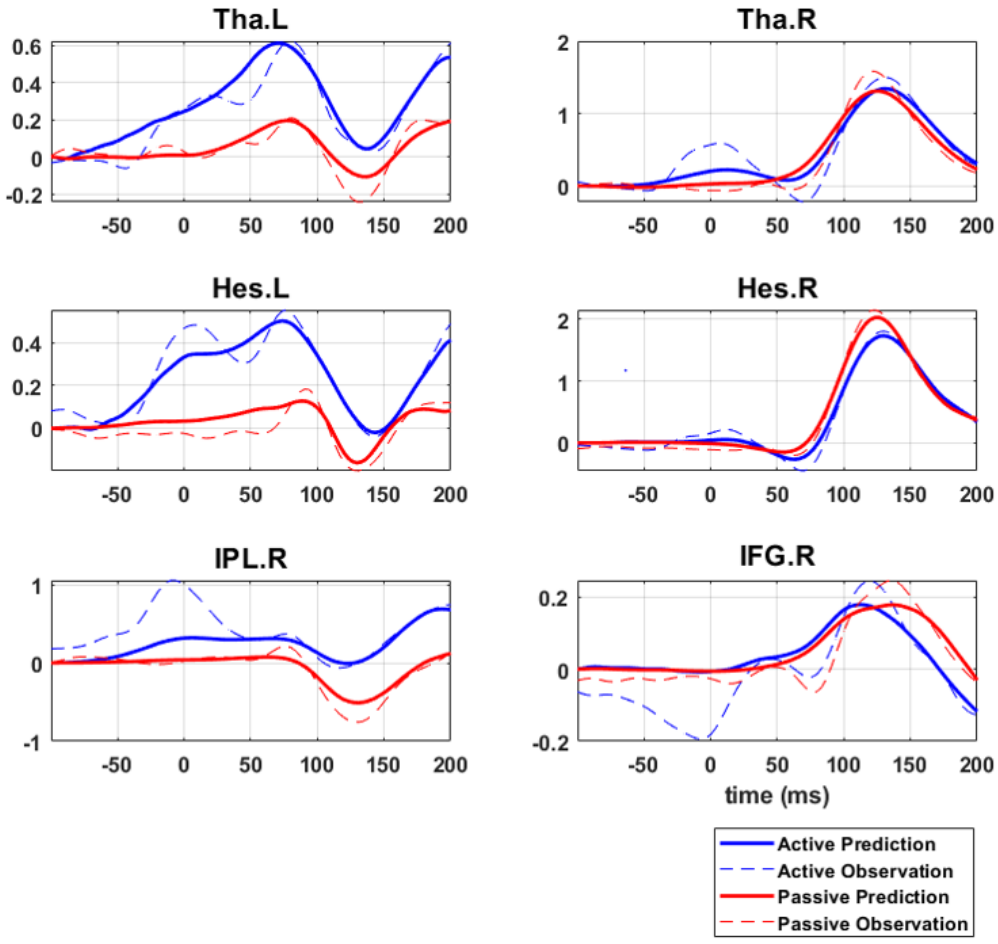

Figure 5.5 Predicted and observed ERFs of winning model 12 across all groups

The grand-average ERFs of predicted and observed evoked-potential response within the winning model 12 (Family C) are present in 6 nodes. The solid and dotted lines represent the predicted and observed ERFs in the active (red line) and passive condition (blue line). The x-axis is the time (ms), and the y-axis is the ERFs amplitude. Tha: Thalamus; HES: Heschl's Gyrus; IPL: Inferior Parietal Lobe; IFG: Inferior Frontal Cortex; L: left; R: Right.

5.3.2 Connection parameter comparison between groups with PEB

The PEB procedure estimated the parameter difference of modulatory connection across groups within a GLM matrix. The averaged group-level GLM parameters for every modulatory connection (Figure 5.6, left panel), and the connections corresponding to sensory attenuation for all participants were calculated (Figure 5.6, middle panel).

GLM with a linear effect of the group revealed that, compared to the HC group, there was a linearly increased connection strength from CHR- to FEP-patients, characterized by an increased connection strength from the right HES to the right IPL and right IFG, which differed between HC and FEP with 95% posterior probability. In addition, the GLM analysis without the group's linear effect showed elevated effective connectivity strength between right HES to right IPL in CHR-participants compared to the HC group. Moreover, the CHR-group displayed reduced connection strength from the right IPL to the left HES compared to FEP-patients (Figure 5.6). Moreover, the leave-one-out cross-validation approach revealed that this connection's effect size could significantly predict group membership (r= 0.30, p =0.00002) (Figure 5.7).

We also estimated the intrinsic connection (matrix A) strength related to auditory ERFs in the passive condition. The averaged group connection strengths indicated a reduced input from the HES to the high-order cortex in the IPL and the IFG. In contrast, the top-down controls from the IPL and the IFG to the auditory cortex were increased for all participants. Furthermore, there was a significant reduction between the HES and the IPL for both CHR- and FEP-groups compared to HC. Moreover, The FEP-group was also characterized by impaired lateral connections (Figure 5.8).

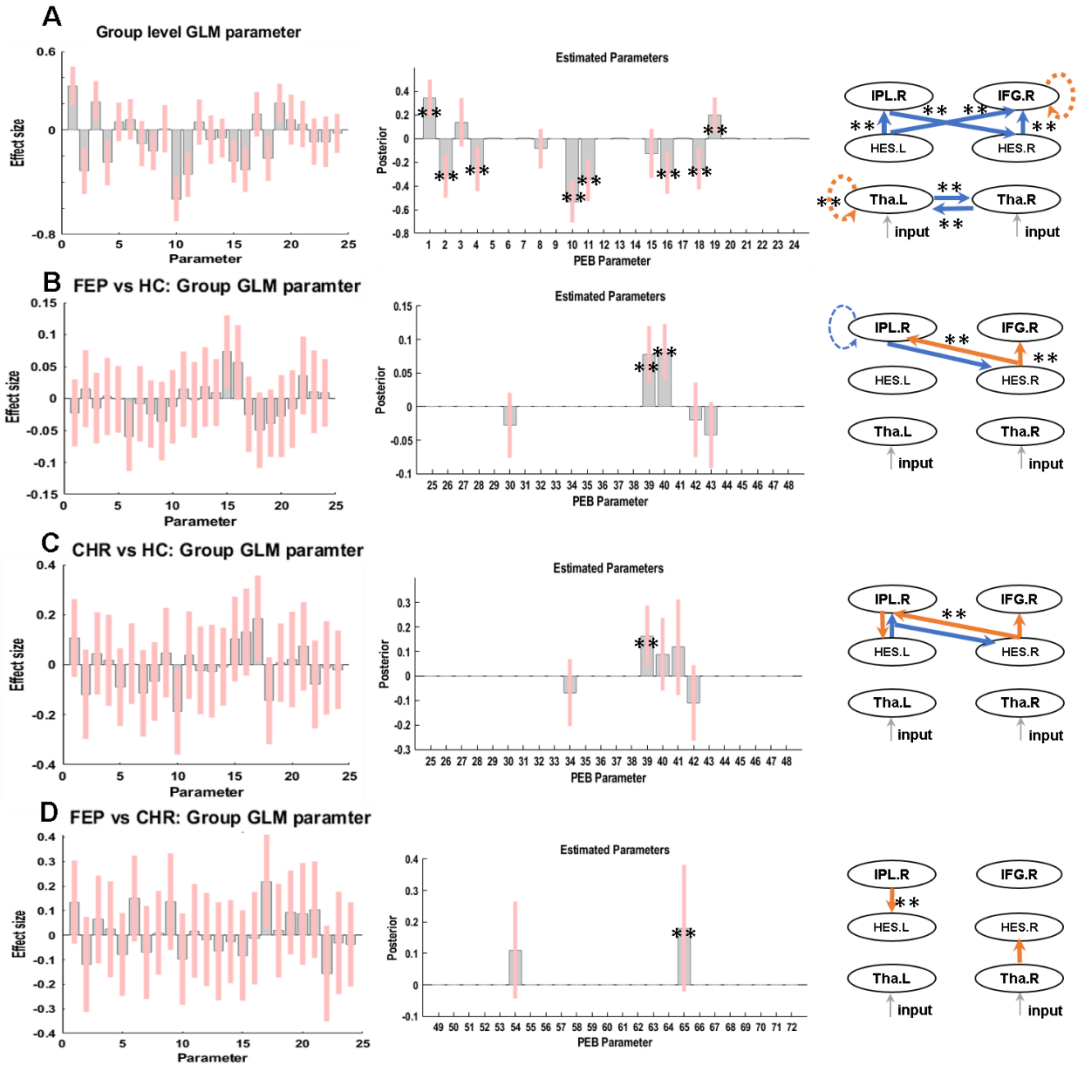

Figure 5.6 Group-level GLM parameters and BMA of parameters

The left plot in panel A depicts the parameters of group-level Bayesian GLM across all participants. The parameter for every connection (22 modulatory connections in total) was plotted with an averaged value and 95% Bayesian confidence intervals of the connection strength (unit: Hz). The middle column in panel A displays the Bayesian model average (BMA) of connection parameters relating to sensory attenuation, which is averaged the group parameters over 256 reduced models. Decreased connection strengths (blue arrow) and increased connection strengths (orange arrow) are displayed in the right model structure. Asterisks indicate a connection with more than 95% posterior probability (one asterisk: 95%; two asterisks: 99%). Panel B, C, and Panel D displayed PEB estimation of differences of modulatory connections between groups (Panel B: FEP vs HC; Panel C: CHR vs HC; Panel D: FEP vs CHR) during sensory attenuation. The negative value indicates decreased connection (blue arrow) and the positive value indicates increased connection (orange arrow) in the right model structure. Of note, panel B is the result of the GLM matrix with a linear effect of the group, and the results in Panel C and Panel D are the findings of the GLM matrix without the linear effect of the group. The left column in panel B, C, D shows the averaged group parameters within the GLM matrix. The middle panel exhibits effective connections that contributed to group differences. Asterisks indicate connections with more than 95% posterior probability that contributes to group differences (one asterisk: 95%, two asterisks: 99%). In Panel B and C, the connection in CHR- or FEP-group is compared to HC (baseline), while in Panel D, the connection in the FEP-groups is compared to CHR-participants (baseline).GLM: General Linear Model;

PEB: Parametric Empirical Bayesian; HC: Healthy Controls; CHR: Clinical High-risk Psychosis; FEP: First-episode Psychosis.

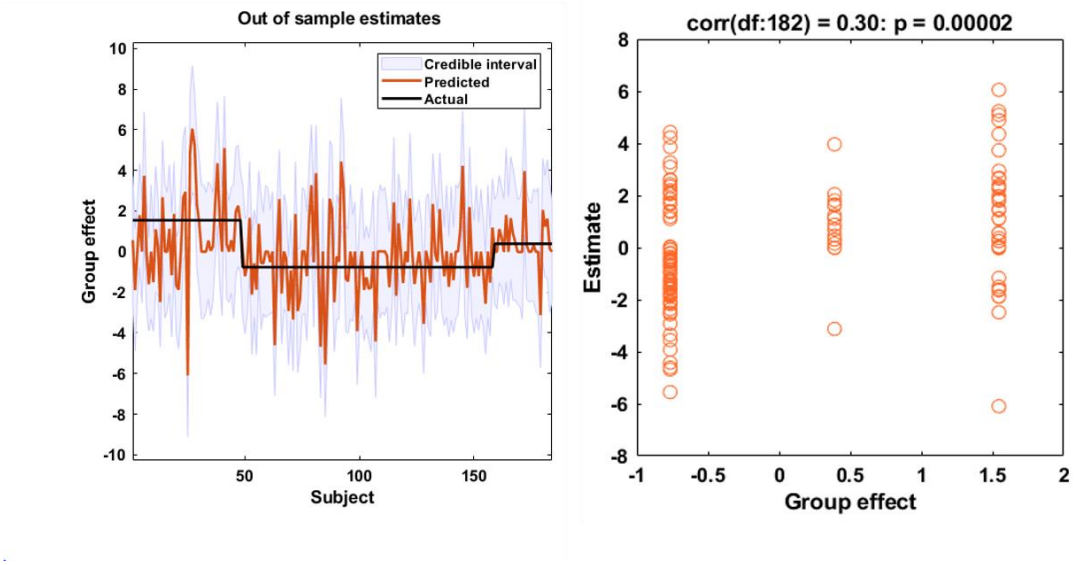

Figure 5.7 Leave-one-out cross-validation results

The left panel displays the out-of-sample estimation (mean-centre) of effective connectivity from the right IPL to the left HES for each participant (red line) with a 95% credible(confidence) interval (grey shadowed area). The right panel shows the correlation between the actual subject effect and the expected subject effect (r=0.30, *p*= 0.00002).

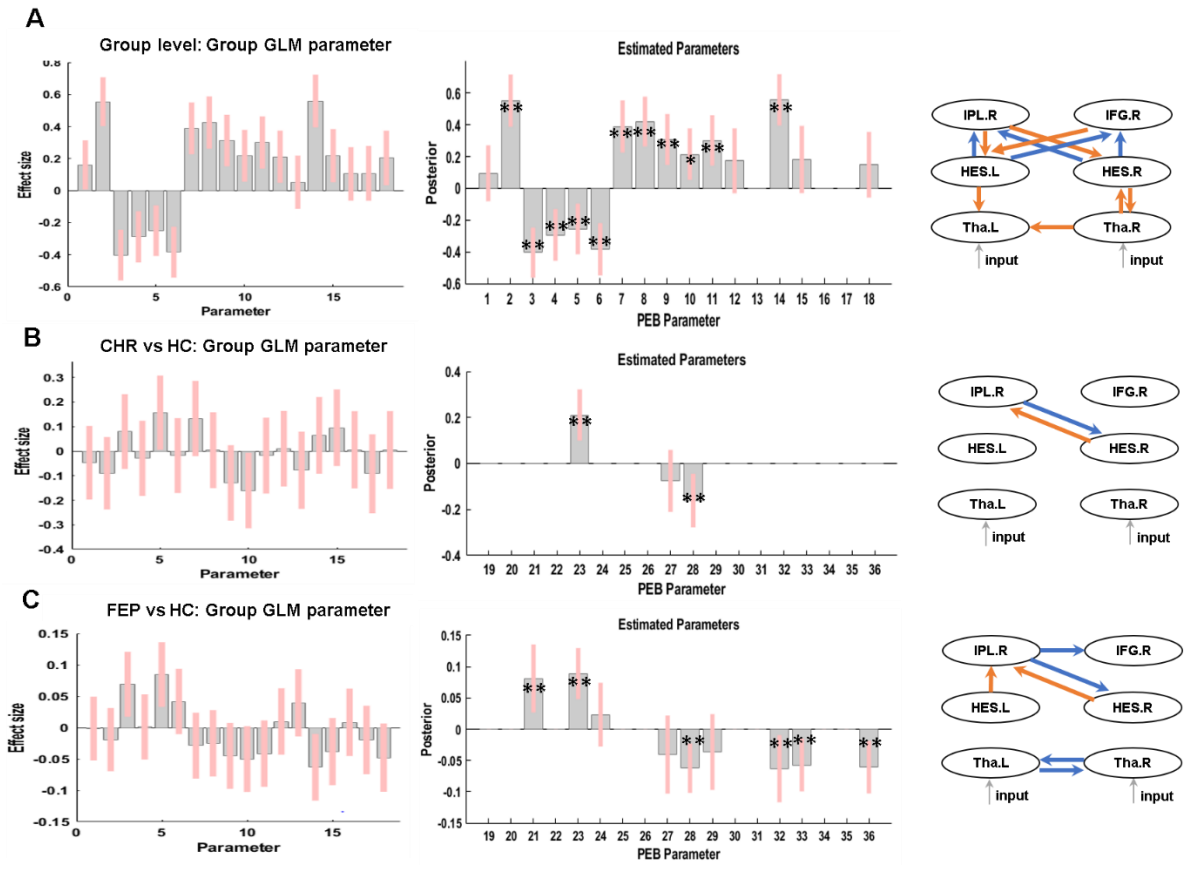

Figure 5.8 Group-level GLM parameters of intrinsic connections and BMA of parameters in the passive condition

The left column in panel A displays averaged group-level GLM connections across all the participants. The middle column of panel A shows the intrinsic connection that differed from zero, indicating the connection in generating auditory ERFs. The intrinsic connections with more than 95% posterior probability are marked with the asterisks and further exhibited in the right model structure (one asterisk: 95%; two asterisks: 99%). Panel B and panel C display the difference of intrinsic connection between groups during generating auditory ERFs (Panel B: CHR vs HC; Panel C: FEP vs HC). The left pictures in Panel B and Panel C display the overall connection strength for both groups. The middle panel displays the estimation of intrinsic connection that differed between groups. The connections with the asterisk have more than 95% posterior probability that differed between two groups (one asterisk: 95%; twoasterisks:99%). The connections are displayed on the right model structure with the blue arrows (decreased connection strength) and orange arrows (increased connection strength) in FEP (Panel B) or CHR (Panel C) compared to the HC group during generating auditory ERFs.

5.4 Discussion

In the current Chapter, I employed DCM to explore the features of hierarchical interactions during generating sensory attenuation in emerging psychosis. The RFX-BMS results revealed effective connectivity patterns across three groups and indicated that FEP-patients displayed modulatory connections with a lack of top-down modulation during sensory attenuation. CHR- and FEP-participants shared an impaired bottom-up connection from the HES to the IPL. Furthermore, the distinctive feature between CHR- and FEP-groups was the top-down connection from the IPL to the auditory cortex. In particular, the effect size of the connection from the right IPL to the left HES was robust enough to distinguish between groups.

After a balance between accuracy and complexity of the models, RFX-BMS results supported the involvement of the IFG in sensory attenuation networks across groups. The bi-directional modulation connections among thalamus, HES, IPL, and IFG, as well as the self-modulation and lateral modulation, have the highest exceedance probability (100%) to explain sensory attenuation in both HC and CHR groups. This is in line with current theories that highlighted the contribution of both top-down control and bottom-up information flow in the generation of sensory attenuation (Friston & S. Kiebel, 2009). Interestingly, the winning family and model in FEP-patients did not include top-down mediated effective connectivity, which is consistent with findings from the DCM studies in ScZ using auditory mismatch negativity (MMN) paradigms (Dima, S. Frangou, L. Burge, S. Braeutigam, & A. James, 2012b) and during the perception of illusory stimuli (Dima et al., 2010a).

Moreover, the BMR-analysis process revealed that effective connections were associated with sensory attenuation mostly involved reduced bottom-up connections from the auditory

cortex to the IPL and IFG during sensory attenuation for all subjects. We found a linearly increased bottom-up connection strength from the right HES to the right IPL and the right IFG in CHR and FEP groups compared to HC. Importantly, this connection strength differed between HC and FEP with 99% posterior probability, as well as between HC and CHR with 95% posterior probability. This increased connection pattern was in line with existing functional coupling studies that abnormalities in CHR were intermediate between HC and FEP(Crossley et al., 2009). In light of the predictive coding account that bottom-up information flow transmits a prediction error to update the higher level that in turn predicts the forthcoming sensory consequence (Friston & S. Kiebel, 2009), this enhanced bottom-up connection strength is suggestive of an increased prediction error when predicting the consequence of voluntary action.

However, reduced top-down modulation from the high-order cortex to the right auditory cortex in CHR and FEP was not strong enough to differ from HC. Interestingly, the enhanced top-down modulation from the right IPL to the left auditory cortex was robustly increased in FEP than in CHR with 99% posterior probability. The enhanced connection between the high-order cortex (frontal cortex) and the auditory cortex has been reported in normal brain functioning during self-initiated speech (Ford et al., 2005), while this pattern was disrupted in chronic ScZ with the feature of reduction (Ford et al., 2002). Interestingly, they noticed that ScZ patients with auditory hallucinations displayed increased connection strength than those without auditory hallucinations (Ford et al., 2002), indicating the association between enhanced top-down modulation and clinical symptoms. Furthermore, the top-down prediction was calibrated by the bottom-up input (Friston & S. Kiebel, 2009) during voluntary action, possibly through mediating the parietal cortex(Della-Maggiore, Malfait, Ostry, & Paus, 2004; Savoie, Thénault, Whittingstall, & Bernier, 2018). Therefore, this increased connection was possibly due to enhanced motor command adjustment when responding to increased bottom-up input. Furthermore, the increased connection strength was large enough to classify the new subject into HC, CHR, or FEP, confirmed by the leave-one-out cross-validation approach.

Finally, the analysis of intrinsic connections at the group-level revealed an interaction among the Tha, HES, IPL, and IFG. The top-down connections from the higher-order areas in the IPL and IFG to the auditory cortex and Tha were increased in the passive condition, in line with the notion of top-down control in sensory processing (for a review see(Gilbert & Sigman, 2007)). Specifically, reduced bottom-up connections and increased top-down

connections were involved in the generating early auditory ERF components. Moreover, we observed reduced connections from the auditory cortex to the high-order cortex in the IPL and the IFG. One possible explanation for this finding is the auditory adaptation theory which posits that repeated auditory stimuli alter the neural plasticity within auditory areas, resulting in the reduced intrinsic connection between sources (Garrido et al., 2009). Regarding alterations of effective connectivity in clinical groups, both CHR- and FEP-participants exhibited changes in intrinsic connection patterns compared to HC. Specifically, these changes involved increased bottom-up connections from the auditory cortex to IFG and/ or IPL, while top-down control over the auditory cortex was reduced. As we observed impaired M100 in the passive condition in FEP in Chapter 4, the impaired interaction between the auditory cortex and high-order cortex from IPL and IFG possibly contributed to the abnormal generation of auditory M100 in FEP in Chapter 4.

In summary, this is the first DCM study to investigate the sensory attenuation network in CHR- and FEP-groups. BMS results of DCM found an aberrant modulation structure in FEP-patients when compared to HC and CHR groups, while the PEB procedure provided evidence for impaired top-down and bottom-up interactions in FEP-patients. Furthermore, aberrant bottom-up neural interactions in CHR-participants was intermediate between HC and FEP, suggesting common but progressive impairment in emerging psychosis. Overall, our current results indicated abnormal neural substrates of sensory attenuation in CHR and FEP, indicating the emergence of abnormal neural interaction in the early stage of psychosis.

Chapter 6 General discussion

6.1 Overview

ScZ is a debilitating psychiatric condition that it is associated with profound cognitive deficits (Heinrichs & Zakzanis, 1998) as well as early sensory information processing impairments (Javitt, 2009a). Furthermore, research suggests that such deficits are detectable before illness onset in childhood and adolescents (Gur et al., 2014).

Recent approaches have highlighted the importance of internally generated predictions for sensory and higher cognitive processes (Picard & Friston, 2014) that involve a continuous updating of an internal model against which incoming sensory information is compared. Event-Related Potential/Field (ERP/ERF) components, such as the auditory M/N100, are potentially informative to explore such predictive processes, for example, in the context of sensory attenuation(Aliu et al., 2009; Cao, Veniero, Thut, & Gross, 2017), the suppression of the evoked M/N100 response to self-initiated sounds. Sensory attenuation has been consistently observed in healthy individuals (Aliu et al., 2009; Cao et al., 2017). However, despite existing models attempting to explain this phenomenon, the actual underlying neural networks and their interactions are still largely unknown.

Moreover, impairments in sensory attenuation, as evidenced by impaired auditory N100 suppression, have been observed in psychosis-spectrum disorders including, schizotypy(Oestreich et al., 2015, 2016), schizoaffective disorder (Ford et al., 2013), and in chronic-ScZ (Ford & Mathalon, 2004; Ford et al., 2001) as well as in first-degree relatives of ScZ(Ford et al., 2013). However, it is currently unclear whether they also exist prior to the onset of the disorder, in the at-risk state (CHR). Because the failure of sensory attenuation could theoretically underly psychotic symptoms such as auditory hallucinations and illusions, as suggested by Feinberg and Guazzelli (1999) and (Ford & D. H. Mathalon, 2005), studying this phenomenon in CHR participants could provide a sensitive marker for the detection of those individuals at the highest risk for the development of a psychotic disorder.

Accordingly, the main goal was to study sensory attenuation in the CHR population. As a first step, in order to gain more insights into the underlying mechanism of potential impairments, the precise network and interactions between network nodes underlying sensory attenuation were investigated in HC (Chapter 3), using a DCM-approach. Using a comparable framework, I then explored the deficits of M100 sensory attenuation in emerging

psychosis as well as the underlying neurocognitive and clinical correlates. These investigations are reported in Chapter 4. Finally, in Chapter 5, I reported on the results of DCM applied to the data from the two main clinical groups (CHR and FEP individuals) to investigate more precisely potential impairments in effective connectivity underlying the observed aberrant sensory attenuation.

6.2 Key findings and their implications

6.2.1 The sensory attenuation in HC

Auditory sensory attenuation has been widely explored in both human and animal studies with neurophysiological techniques (Aliu et al., 2009; Rummell et al., 2016). By employing MEG, we observed M100 sensory attenuation over temporal-parietal sensors in HC, which we could localize to a network of temporal, parietal, and subcortical areas, including the thalamus. The effect was most pronounced in right HES and ST, in line with evidence suggesting the dominance of the right hemisphere in simple tone processing and the left hemisphere in speech-related tone processing(Zatorre et al., 2002; Zatorre et al., 1992). The finding of sensory attenuation effects being strongest in the primary (HES) and secondary auditory cortex (ST) also replicates previous EEG/MEG studies(Cao, Thut, et al., 2017; Heinks-Maldonado et al., 2006; Martikainen et al., 2005a). Moreover, our current findings suggest that reduced neural activity during self-initiated action is not limited to early auditory-processing areas but is detectable in a much wider network of brain areas, including the parietal cortex (IPL and precuneus), the thalamus, and the rolandic operculum during auditory perception. This indicates that motor-related signals could influence many sites in the brain during auditory processing and change its early responses to incoming signals.

One important finding of our study is that the sensory attenuation effect is present in the parietal cortex, including the IPL and the precuneus, at early latencies (i.e., prior to the onset of SAP effects in the primary auditory cortex). Sensory attenuation in parietal areas has been reported in the visual domain(Benazet et al., 2016), as well as in the auditory domain (precuneus) during voluntary actions(Cao, Veniero, et al., 2017). The IPL plays an important role in the integration of auditory‐motor information (Alain, He, & Grady, 2008; Hickok, Okada, & Serences, 2009; Pa & Hickok, 2008) through interactions with the cerebellum (Pollok et al., 2008) and in the prediction of motor outcomes (Blakemore & A. Sirigu, 2003). Accordingly, it is plausible that the IPL integrates auditory and motor responses in the

current task. However, more work is necessary to precisely elucidate the role of the IPL in sensory attenuation.

Another important finding is the involvement of the thalamus in sensory attenuation. There is evidence of suppression of midbrain areas during vocal production in bats (Suga & Schlegel, 1972; Suga & Shimozawa, 1974). Importantly, such altered response has been noticed in humans at the subcortical level during auditory processing (Mukerji, Windsor, & Lee, 2010), although during self-initiated speech (Curio et al., 2000) a change in thalamic activity was not seen. However, reduced thalamus activity has been reported during self-produced tactile stimulation via fMRI (Blakemore et al., 2001), although it is unclear what the timing of this effect is due to fMRI-recording's low temporal resolution (i.e., it could also reflect activity following the early M100 response). More specifically, the traditional role of the thalamus during auditory processing was seen as limited to the function of a relay centre for external sensory inputs(Alitto & Usrey, 2003), but there is now general consensus about its important role also in higher-level processing (Sherman & Guillery, 2006). For example, the thalamus can provide stimulus-specific information to the cortex by thalamus-cortical circuitry that goes beyond simple relaying the bottom-up signal. In particular, the afferent sensory information to the thalamus can be modulated by motor cortex activity(Lee, Carvell, & Simons, 2008; Zagha, Casale, Sachdev, McGinley, & McCormick, 2013), and then the output from the thalamus serves as an efference copy to the cortical area(Sherman, 2016), possibly by corticocortical communication(Zagha et al., 2013) or by contacting the subcortical motor centres via branch axons(Sommer & Wurtz, 2008). Altogether, our current MEG findings reveal the involvement of the thalamus in sensory attenuation, but replication of this effect and determination of its exact role requires more investigation.

The fact that sensory attenuation is a multi-level network response is important with respect to the evaluation of its proposed underlying mechanisms. For example, according to the empirical framework of efference copy, the reduced brain activity during self-initiated conditions should be primarily observed in the sensory cortex (Von Holst, 1954; von Holst & Mittelstaedt, 1950). In other words, an outflow of an actual copy (efference copy) of motor command was expected to directly target the sensory cortex to predict the consequence of voluntary action (von Holst & Mittelstaedt, 1950). We found some evidence for this in our regression models, showing strong predictive relationships between early PoCG/PreCG activity and later reduction of the auditory cortex M100 response (SAP effect). There is also evidence from rats supporting the direct projection from the motor cortex to the auditory

cortex (Budinger & Scheich, 2009; Nelson et al., 2013). However, whether such direct pathways also exist in humans is currently unknown(Morillon, Hackett, Kajikawa, & Schroeder, 2015). An important question, therefore, is how to explain the suppressed activity in brain areas other than the primary auditory cortex. Theoretically, the corollary discharge model is similar to the efference copy theory in that the efferent copy was proposed to be generated in motor-related areas, but distinct in its prediction of the efference copy signal targeting a network of areas involved in higher- and lower- order processing of sensory information(Crapse & Sommer, 2008a, 2008b). Such areas could include both thalamus and IPL. Therefore, the corollary discharge framework would better predict our network findings.

In summary, our current findings provide electrophysiological evidence that self-initiated sounds attenuate neural activity in a wide network of brain areas, with initial predictive processes of the motor action influencing responses in multiple brain areas before it expresses itself in the attenuation of the M100 amplitude in primary auditory cortex.

6.2.2 The sensory attenuation in CHR and FEP

In Chapter 4, we reported sensory attenuation effects over the bilateral auditory-parietal areas in HC at the sensor level, while this effect was absent in CHR- and FEP-groups over the left hemisphere. In line with sensor-level results, sensory attenuation was shown in the bilateral HES and ST in HC at the source level. Consistent with previous ScZ findings utilizing a speech-related experimental paradigm(Ford & Mathalon, 2004), we could show sensory dysfunctions in FEP during auditory tone stimuli, particularly involving bilateral HES and ST. Interestingly, aberrant sensory attenuation in CHR-participants was limited to the right auditory cortex. In line with our current finding, the work from Mathalon et al. (2019) identified impairments of sensory attenuation in CHR, although they did not capture this effect with a smaller sample size(Perez et al., 2012; Whitford et al., 2018).

The deficits found in CHR and FEP provide evidence that impairments of sensory attenuation are also present in the at-risk state, in individuals who potentially develop a psychotic disorder. Furthermore, these deficits could not be explained by impairments in the auditory M100 component itself and thus reflect a true impairment in attenuation of the M100 as a result of higher-prediction accuracy of sound onset in the self-initiated condition. The general consensus is that generation of sensory attenuation entails successful motor-sensory integration, with the cancellation of auditory M100 during voluntary action relying

on the precision of top-down prediction signals(Sperry, 1950b; von Holst & Mittelstaedt, 1950). Our cognitive data indicated specific deficits in processing speed and attention and motor speed in CHR and FEP participants. lt is therefore conceivable that the deficits of sensory attenuation are reflective of disrupted sensorimotor integration in CHR and FEP. Interestingly, in contrast to the impaired sensory attenuation, the FEP group showed an increased M100 amplitude in the left auditory cortex. In line with these results, increased left-lateralized auditory N100 activity during the active condition was also found in an EEG study, including ScZ patients (Ford et al., 2007). Such increased auditory activity was further shown to be modulated by motor-cortex movement-related signals, presumably in order to maintain the sensitivity to self-initiated tone (Reznik et al., 2014; Reznik et al., 2015). According to the predictive coding framework (Friston & S. Kiebel, 2009), this enhanced auditory cortex is thought to be the consequence of the misperception of self-generated tones. Moreover, the left auditory cortex impairments have been reported to correlate with auditory hallucinations in ScZ (for a review see((Allen, Larøi, McGuire, & Aleman, 2008)) and with formal thought disorder (Feinberg & Guazzelli, 1999) and thus represents a potential treatment target of rTMS (for a review see (Slotema, Blom, van Lutterveld, Hoek, & Sommer, 2014)). In support of this, sensory attenuation in the left auditory cortex was closely linked to clinical symptoms in CHRs, indicating the clinical relevance of left-lateralized sensory attenuation impairments.

Moreover, the sensory attenuation effect in the left auditory cortex could discriminate between CHR and FEP individuals, suggesting a progressive alteration of sensory attenuation from initial right impairments to bilateral auditory cortex impairments over the subsequent stages of psychosis development. Supporting evidence from structural anatomy revealed progressive alteration of reduced grey matter in the left HES and ST during the transition to psychosis(Kasai et al., 2003). The extent of deficits of sensory attenuation in the CHR-group was comparable to FEP in the right auditory cortex, indicating that sensory attenuation in the right auditory cortex could be an index of risk state of psychosis, in line with a meta-analytical finding of reduced grey matter in the right ST in CHR (Fusar-Poli, Radua, McGuire, & Borgwardt, 2011).

Finally, hemispheric impairment in the auditory cortex remains controversial even in ScZ(Corballis & Häberling, 2017; Mitchell & Crow, 2005), as various factors could contribute to the reported inconsistency of such findings. In contrast, our current findings provide clinically meaningful evidence for a progression from only right-sided impairments

in the at-risk state to bilateral impairments after the onset of FEP. It is thus of importance to recognize the distinct role of the bilateral auditory cortex during the development of psychosis, for example, for potential prevention. Such lateralization effects could potentially also be used as a marker for detecting those individuals that are at the highest risk for psychosis development.

6.2.3 Effective connectivity during sensory attention in the development of psychosis

One of our main goals was to investigate effective connectivity during sensory attenuation in both CHR- and FEP-groups. First of all, we identified the networks underlying sensory attenuation in HC, which we subsequently applied to the CHR- and FEP-groups to investigate aberrant neural interaction that contributed to their impaired sensory attenuation effect. As far as we know, this is the first DCM study to probe the neural substrate explaining sensory attenuation in both healthy individuals and in clinical samples.

Our modelling approach showed a winning family that included bilateral thalamus and HES, as well as the right IPL. Furthermore, the winning model indicated that auditory sensory attenuation in the right HES was shaped by both descending and ascending modulatory influences from the subcortical thalamus and high-order cortex IPL in HC individuals. So far, limited evidence exists for the contribution of the thalamus in sensory attenuation(Adams et al., 2013). As the thalamus has been implemented as a crucial structure driving abnormal brain activity and behaviour/symptomatology in ScZ(Pratt et al., 2017), one of the strengths of our model is that it explores the potential role of the thalamus in sensory attenuation. DCM results showed an initially enhanced connectivity from the right thalamus to the right HES, followed by a reduction of information transmission from the auditory cortex to the high-order IPL area. The reduced communication between the auditory cortex and the high-order cortex could indicate the reduction of prediction error. Furthermore, we identified increased top-down modulation from the IPL to the lower-level sensory cortex, particularly in the right hemisphere. Conceptually, this could represent the feedback connectivity that serves to predict the sensory consequences of voluntary action(Friston & S. Kiebel, 2009). Accordingly, our winning DCM model in HC individuals supports a hierarchical interaction pattern underlying sensory attenuation generation.

For the DCM-analysis of the CHR- and FEP-data, we expanded the model structure with IFG as existing evidence from auditory MMN-impairments has indicated a role of the IFG

in impaired top-down predictions in ScZ (Dima et al., 2012b; Michie, Malmierca, Harms, & Todd, 2016). The DCM-modelling supported the role of IFG in sensory attenuation networks across all groups. Moreover, in agreement with the model structure in Chapter 3, the winning family and model showed reciprocal modulatory connections in combination with self-modulation, and lateral connections were crucial for sensory attenuation. However, it is important to highlight that the features of the winning family and model in the FEP-group were different from HC- and CHR-groups. Specifically, the FEP-group was characterized by lacking feedback control. This is in line with previous MMN-DCM studies in ScZ(Dima et al., 2012b) and during the perception of illusory stimuli (Dima, D. E. Dietrich, W. Dillo, & H. M. Emrich, 2010b), indicating deficits of high-order cognitive function in psychosis (Zakzanis & Hansen, 1998).

Furthermore, the bottom-up connections, particularly the connection from right HES to right IPL, was enhanced in CHR and FEP individuals, with the strongest increase found in the FEP group. As mentioned earlier, as the connection strength from right HES to right IPL declined in HC, the increased connection strength in CHR and FEP implies enhanced prediction error input, which could thus explain the failure of sensory attenuation in the CHR and FEP. This intermediate connection strength of CHR in between HC and FEP is in agreement with existing effective connectivity studies in CHR during working memory (Crossley et al., 2009; Schmidt et al., 2013) and resting-state (Andreou et al., 2015; Wang et al., 2016), and shows that the impairment might precede the onset of psychosis.

The impaired sensory attenuation in CHR (Chapter 4), particularly in the right auditory cortex, was expected to result from an imbalance between feedforward and backward communication, particularly the high-level modulation. In contrast to our expectation, however, there was only a trend toward decreased top-down modulation from the right IPL to the right HES in CHR and FEP. Nonetheless, it provides cues of potential impairment of top-down modulation in the right hemisphere during sensory attenuation in emerging psychosis.

In contrast to reduced top-down modulation in the right auditory cortex, the connection strength from the right IPL to the left auditory cortex connection was weakly increased in CHR, compared to HCs. Importantly, this aspect allowed us to distinguish between CHR and FEP individuals. This enhanced connection strength presumably accounts for the overactivated left auditory cortex during the self-initiated condition in FEP, compared to

CHR, and might indicate a compensatory mechanism (Su et al., 2015; Wang et al., 2016)to adjust motor command(Della-Maggiore et al., 2004; Savoie et al., 2018). In contrast, reduced frontotemporal coupling in chronic ScZ during talking compared to listening was found in the left hemisphere (Ford, Mathalon, Whitfield, Faustman, & Roth, 2002). As they observed that ScZ patients with auditory hallucinations displayed stronger connection strength than those without, this could indicate a relationship with symptom severity. Similarly, such hyper-connectivity patterns have been reported in FEP or early illness of ScZ (Crossley et al., 2009; Yoon et al., 2015). In addition, this increased top-down connection is robust enough to significantly categorize CHR, FEP, HC individuals by our leave-one-out cross-validation. Notably, in line with our sensory attenuation findings that it was in the left auditory cortex discriminating between CHR and FEP, the increased top-down modulation from the right IPL to the left auditory cortex instead of the right auditory cortex again highlighted the different role of the bilateral auditory cortices in developing psychosis. It will be important to explore this alteration in follow-up data to elucidate whether the left auditory cortex is a biomarker of onset of psychosis.

Our current DCM results provide evidence of bottom-up deficits during sensory processing that is comparable in CHRs and FEP patients, but increase in strength from CHR to FEP status, whereas top-down modulation impairments are more likely related to psychosis, as it was only impaired in FEP patients. Existing studies of functional coupling in CHR mainly focused on higher-order cognitive function. For example, several lines of evidence have shown aberrant functional coupling in CHR and FEP, including frontal, temporal, parietal, cerebellum areas, and the thalamus(Andreou et al., 2015; Collin et al., 2018; Du et al., 2018; Schmidt et al., 2013; Shim et al., 2010; Wang et al., 2016). However, limited evidence is available showing disrupted neural interaction during early sensory processing. According to current neurophysiological models that ScZ is associated with both top-down and bottom-up dysfunction, the bottom-up deficits in sensory processing could subsequently drive the disruption of high-order processing(Javitt, 2009b). It is thus important to investigate the underlying deficit of functional coupling during early sensory processing, particularly in light of understanding of abnormalities in high-order processing areas. Comparable work from our project also revealed deficits of functional coupling during visual processing in CHR(Gajwani et al., 2020), although no significant impairment was detected in auditory MMN (Mikanmaa, 2020).

6.2.4 The sensory attenuation in CHR subgroups

Given that the CHR-phenotype involves distinct clinical criteria and outcomes (Fusar-Poli, 2017; Fusar-Poli, Cappucciati, Borgwardt, et al., 2016; Schultze-Lutter et al., 2015a), it is important to address the heterogeneity of CHR. Hence, CHR-participants in our study were initially divided into three sub-groups: 1) SPI-A only criteria (BS); 2) CAARMS only criteria (CHR-CAM, or UHR); 3) SPI-A/CAARMS combined (see supplementary materials for Chapter 4). Notably, 96% (3/80) of our UHR participants met the criteria of APS. Although we did not capture any significant group differences of sensory attenuation across three sub-groups, each sub-group displayed a unique feature. More specifically, CHR-both and BS groups displayed an absence of sensory attenuation in the auditory regions, while the sensory attenuation was present in the UHR group. Furthermore, among the three subgroups, only the CHR-both group displayed impairment of sensory attenuation in comparison to HC participants. This is in support of the notion that meeting both UHR and BS threshold criteria is linked to greater clinical symptom severity than meeting UHR or BS threshold criteria alone (Simon et al., 2006). Also, meeting both criteria have been shown to improve the prediction of clinical outcomes of CHR individuals, both in the short term(Ruhrmann et al., 2010) and over longer periods (Schultze-Lutter, Klosterkötter, & Ruhrmann, 2014). Therefore, our current results provide neuroimaging evidence that those individuals meeting UHR and BS criteria display robust neural abnormalities, whereas this was not so clear for the BS or UHR only groups.

Interestingly, the SAP effect was absent in the BS group instead of in the UHR group. Our current findings seem contradictory to the clinical definition of BS and UHR that BS has been featured as an earlier phase of prodromal psychosis than UHR, constituting a continuum psychosis (Fusar-Poli et al., 2013). Some evidence exists suggesting no difference in cognitive function between BS and UHR(Simon et al., 2006), as well as similar long-term outcomes of BS and UHR groups(Schultze-Lutter et al., 2015a). Hence, it appears that the trajectory of clinical symptoms and cognitive functioning, as well as of clinical outcomes, do not fully align with each other. However, neuroimaging studies supporting such subgroup differences are scarce. In fact, in line with our finding previous work has addressed the aberrant neural substrates of BS, involving reduced grey matter in temporal-limbic areas and disrupted functional coupling (for a review see (Schultze-Lutter et al., 2016)), indicative of abnormalities of brain function in psychosis stemming from the earlier phase of psychosis (BS). Furthermore, one more work by employing auditory oddball task showed spatial distribution difference of reduced P300 amplitude in BS (particular

COPPER) and APS/BLIPS, indicating potential different neural substrates of BS and APS(Frommann et al., 2008). Overall, our current findings provided some links between BS- and UHR-criteria in CHR patients that might be associated with different states of disturbed information processing(Schultze-Lutter et al., 2016).

Moreover, heterogeneity of CHR individuals also appears to be related to heterogeneity in the long-term outcomes (Cross, Scott, Hermens, & Hickie, 2018; Fusar-Poli, Cappucciati, Borgwardt, et al., 2016; Suvisaari et al., 2018). As mentioned in the introduction, the transition rate to psychosis is about 20% within 24 months follow-up period, at least according to the latest data (Fusar-Poli et al., 2013). Therefore, the majority of individuals with CHR are not likely to develop frank psychosis, and approximately one-third of CHR-positive psychosis can be expected to be remitted at the end of the study period(Michel, Ruhrmann, Schimmelmann, Klosterkötter, & Schultze-Lutter, 2018). Currently, major efforts are undertaken to try to predict conversion to psychosis, for example by trying to classify convertors among non-converters(Addington et al., 2011; Michel et al., 2018; Tang et al., 2019; Woods et al., 2014).

So far, limited neuroimaging studies exist investigating potential neural differences between CHR-individuals that are later in remission and those who show the persistence of CHR symptoms. As follow-ups in our project were available at 12 months for most CHR participants, we explored separating them into CHR-persistent and CHR-nonpersistent at 12 months according to CAARMS assessment (see supplementary materials for Chapter 4). Of note, we utilized the word persistent instead of non-remission as our follow-up time is not long enough to conclude CHR's final status. It turned out that 44.5 % (54.5% remission) of CHR-participants at 12 months still met the criteria of UHR, higher than the rate from the meta-analysis that reported around 35 % remission at 2-year follow-up(Simon et al., 2013). This might be due to the fact that current persistent criteria were dependent only on symptoms rather than both symptom and functional remission. Notably, in contrast to existing findings that captured differences in auditory MMN and P300 between CHR remitters and non-remitters(Kim, Lee, Yoon, Lee, & Kwon, 2018; Tang et al., 2019), our one-year follow-up data did not show differences in sensory attenuation between CHR-persistent and CHR-nonpersistent in comparison to HC at baseline, in line with auditory MMN findings in our project(Mikanmaa, 2020). However, the visual gamma in our project did capture the significance of these two groups(Gajwani et al., 2020). This is possibly due to different experiment tasks and still relatively short follow-up period. Accordingly, it

remains to be seen whether or not sensory attenuation could be regarded as a potential biomarker for predicting future psychosis risk.

6.2.5 Clinical features in CHR and correlation with sensory attenuation

Demographic information, cognitive functioning, and clinical characteristics of all participants were presented in Chapter 2 and Chapter 4. Overall, age and sex were matched across three groups as existing evidence has suggested that age and sex potentially has an impact on the prevalence and clinical symptoms of CHR (Amminger et al., 2006; Bendfeldt et al., 2015; Romans & Seeman, 2006). In line with existing findings(Bora et al., 2014; Fusar-Poli et al., 2015), CHR- and FEP-participants displayed lower GAF scores than HC individuals although general functioning in the current sample was somewhat higher than in previous CHR-cohorts (Fusar-Poli et al., 2015). One possible explanation for this finding is that the participants in the current project were largely recruited from the community (Fusar-Poli, Schultze-Lutter, Cappucciati, et al., 2016; Fusar‐Poli, 2017). Related to this finding, circumscribed impairments in cognition were observed in our data, mainly involving motor speed, processing speed and attention when compared to previous findings(Carrión et al., 2011; Fusar-Poli, Deste, et al., 2012).

According to different CHR criteria, the CHR-both group had significantly lower GAF scores and more severe clinical symptoms than either the BS or UHR subgroup. This is in line with previous findings that a combined BS and UHR approach is associated with stronger impairments (Simon et al., 2006). Interestingly, despite BS being identified as an earlier stage than UHR(Fusar-Poli et al., 2013), we did not find differences in either GAF score or clinical symptoms between BS and UHR groups. Furthermore, considering that previous evidence suggested a similar clinical outcome of CHR for BS and UHR subgroups(Schultze-Lutter et al., 2015b), identifying BS as a fairly sensitive marker of psychosis risk is validated. Nonetheless, more evidence from our longitudinal study in the future will be needed to confirm this.

Given currently limited available follow-up data, we only investigated CHR status at 12 months, aiming to illustrate differences in baseline clinical and neural features that predict future CHR status. Our current results support reported findings that CHR non-converters (Addington et al., 2011; Lee et al., 2014) remained at a lower level of functioning at 12 months in contrast to HC individuals by showing reduced GAF scores in both CHR-

persistent and CHR-nonpersistent groups. Furthermore, in agreement with the study from Lee et al. (2014), impaired functioning is indeed more prominent in the CHR-persistent group than the non-persistent group, possibly due to more severe symptomatology already present in the CHR-persistent group at baseline. Furthermore, both CHR-persistent and CHR non-persistent groups displayed impaired cognitive function compared to HC individuals. However, in contrast to previous findings (Lee et al., 2014), the cognitive function difference was not significant between CHR-persistent and CHR-nonpersistent group in our results. Overall, our findings suggested that the clinical symptoms and functioning were more impaired at baseline in the CHR-persistent group, while a long-term investigation is necessary for both CHR-persistent and CHR-non persistent groups to clarify their final status.

Moreover, I also investigated correlations between clinical features and sensory attenuation. The sensory attenuation effect in the left hemisphere was negatively associated with GAF scores in the CHR-group, indicating the lower GAF scores were linked to less sensory attenuation effect. Furthermore, the less sensory attenuation was related to more severe CAARMS symptoms, particularly in unusual thought content and disorganized speech, in line with previous EEG findings (Mathalon et al., 2019; Perez et al., 2012). The correlation, to some extent, supports the theory that the deficits of sensory attenuation potentially contributed towards clinical symptoms (Feinberg & Guazzelli, 1999), due to failure to distinguish self- and external- generated thoughts. In addition, the sensory attenuation in the right auditory cortex was independent of clinical symptoms, which could indicate that this is a more trait-like impairment in CHR.

6.2.6 Early evoked M100 responses

In order to test whether the sensory attenuation effect resulted from the aberrant early auditory information processing deficits, we investigated the M100 amplitude activity in the active and passive conditions. In contrast to previous findings (Del Re et al., 2015), the current study did not support the M100 impairments in either the passive or active condition in CHR. In contrast, we did observe a reduced auditory M100 in the FEP group in the passive condition, particularly in the left auditory cortex, in line with previous findings in FEP-patients(Del Re et al., 2015) and a study including ScZ-patients (Rosburg et al., 2008). This reduced M100 amplitude in FEP/ScZ represents the dysfunction of early auditory information processing. Conversely, the M100 amplitude in the active condition in the left auditory cortex was significantly increased instead of suppressed than in the passive

condition in FEP, indicative of the failure of suppressing self-initiated tone. As the M100 per se in the active condition was already impaired, the deficit of sensory attenuation in the left auditory cortex cannot be fully explained by the impaired auditory M100 in the passive condition.

Furthermore, we also estimated the aberrant intrinsic connection patterns underpinning passively listening to auditory tones. The bottom-up connection from the HES to the high-order cortex was reduced, while top-down modulation from the high-order cortex to HES was increased in averaged connection strength across all subjects. However, this modulation pattern was impaired in both CHR and FEP group, who displayed reduced top-down regulation from the IPL to the auditory cortex and enhanced bottom-up connection from the auditory cortex to IPL during generating auditory M100, mainly in the right hemisphere. Interestingly, we did not capture any M100 amplitude difference in the right auditory cortex in either CHR or FEP. A reasonable explanation could be that ScZ is regarded as a disconnection disease that region-specific abnormalities are secondary to functional integration in ScZ (Friston, 2002; Friston & Frith, 1995). Therefore, it is plausible to assume that the connection abnormalities might subserve or precede the local activity changes. Additionally, FEP-participants exhibited more impairment between brain communication than CHR. Particularly, the augmented bottom-up connection from the left HES to right possibly accounted for impaired auditory M100 in the left auditory cortex in FEP. This enhanced bottom-up connection is reflective of the inability to attenuate sensory precision in ScZ(Friston, Brown, Siemerkus, & Stephan, 2016). In other words, they cannot recall prior beliefs (prediction) to predict the sensation, thus everything is surprising (statistical term), resulting in increased input (sensory prediction errors) to the high-order cortex. In summary, the DCM results revealed disrupted neural interaction during auditory M100 generation in emerging psychosis. Importantly, this malfunction of neural interaction possibly existed before the alteration of local auditory activity. this needs confirmation in the longtidicual data who converted to FEP.

6.3 Limitations and future directions

Current thesis explored the sensory attenuation by employing the action-auditory paradigm with the technology of MEG. One potential concern of the experimental paradigm is that we did not include the motor-only condition to rule out the potential motor contamination on auditory sensory attenuation, while the existing paradigm disclosed the truth that motor activity has a subtle impact on auditory sensory attenuation(Horváth, 2014; Martikainen, K.-

i. Kaneko, & R. Hari, 2005b). Furthermore, given the sensory attenuation could be resulted from various implicit factors, such as attention, temporal prediction, existing evidence confirmed the role of the prediction component in sensory attenuation after controlling those potential contributors(Klaffehn, Baess, Kunde, & Pfister, 2019; Martikainen et al., 2005b).

MEG was applied to investigate the auditory M100 sensory attenuation. Indeed, MEG has better spatial resolution than EEG, while MEG is more sensitive to orthogonal signals, namely the main signal from gyri(Ahlfors, Han, Belliveau, & Hämäläinen, 2010). Therefore, the biomagnetic signal detected by MEG is reflective of a part of brain activity. One consideration of our sensory attenuation results is the ability of MEG to detect deep sources, such as the subcortical thalamus. However, converging evidence suggested the capability of MEG to capture deep source activity(Attal & Schwartz, 2013; Recasens, Gross, & Uhlhaas, 2018b).

In addition, we employed DCM to initially explore the underlying neural interaction mechanisms of sensory attenuation, while due to the constrained DCM for ERP analysis that the driving input in two conditions should be identical, frontal motor-related areas were not involved in our DCM models. The involvement of motor-related areas in sensory prediction has been primarily explored by DCM(Ritterband-Rosenbaum, Nielsen, & Christensen, 2014), therefore, future analysis to explore the role of motor activity in the sensory attenuation network will be necessary, possibly with DCM or granger causal modelling approach by modelling the interaction of neural oscillations.

In the current thesis, our CHR was community-based outreach in comparison to existing CHR centres that subjects were from clinical help-seeking centres. This possibly accounts for relatively good clinical functioning (GAF) and neurocognitive function (constrained impairment) in our study. One concern is that community-based enrolment possibly dilutes the effectiveness to detect CHR(Fusar-Poli, Schultze-Lutter, & Addington, 2016), while our current data provided strong evidence of impaired global functioning, social function, cognitive function, and even brain function in community-based CHR. Given existing evidence revealed different features between these inclusion sources(Kelleher et al., 2012; Mills, Fusar‐Poli, Morgan, Azis, & McGuire, 2017; Schultze-Lutter, Michel, Ruhrmann, & Schimmelmann, 2018), our community-based enrolment helps to draw a full perspective picture for CHR from the general population.

Given the criteria to enrol CHR remain under discussion, the heterogeneous criteria of CHR potentially contributed to different CHR features and outcomes (Fusar-Poli, Cappucciati, et al., 2016). Our CHR samples were included by combining both BS and positive symptoms of UHR strategies, facilitating to depict a continuous map of prodromal psychosis. One strength of our project is the relatively homogeneous clinical symptoms in UHR, because we only estimated the positive symptoms of CAARMS in UHR, and 96% of UHR participants me the APS sub-criteria. However, one consideration is that we did not estimate the negative symptoms in our CHR samples if they potentially exhibited negative symptoms. Raising attention has been paid to negative symptoms in CHR because it is linked to poor social functioning(Meyer et al., 2014; Schlosser et al., 2015), as well as poor community-based functioning outcome(Strauss, Pelletier-Baldelli, Visser, Walker, & Mittal, 2020).

Moreover, due to limited available longitudinal data in CHR at the analysis time, we only explored the clinical outcome at 12 months. Given a one-year follow-up is not long enough to estimate the final clinical outcomes, further investigation at 24 months and 36 months will help to eventually trace the CHR status. Furthermore, considering small numbers of CHR convertors at the analysis time, future work should also be conducted to explore the distinctive features between CHR converters and non-converters.

6.4 Conclusions

The features of sensory attenuation in the normal brain laid a foundation for exploring the abnormalities in emerging psychosis. Firstly, my current thesis indicates that the sensory attenuation is distributed beyond the auditory cortex, involving in cortical-subcortical areas in the normal brain. Importantly, the successful generation of sensory attenuation relies upon both feedforward and feedback modulation across the sensory attenuation network in HC. Furthermore, our analysis confirmed the dysfunction of sensory attenuation in FEP and provided evidence for the vulnerability of auditory M100 sensory attenuation in CHR, which was related to clinical psychotic symptoms and cognitive functioning. However, this thesis cannot strongly support the hypothesis that the heterogeneity of CHR-samples influence sensory attenuation features at baseline. Furthermore, the current thesis implies that the deficits in sensory attenuation result from imprecise interaction between top-down and bottom-up modulation in emerging psychosis. In summary, our findings suggested that the auditory sensory attenuation could be a candidate biomarker to early detect psychosis.

Appendices

Appendix 1

Supplementary materials for Chapter 4

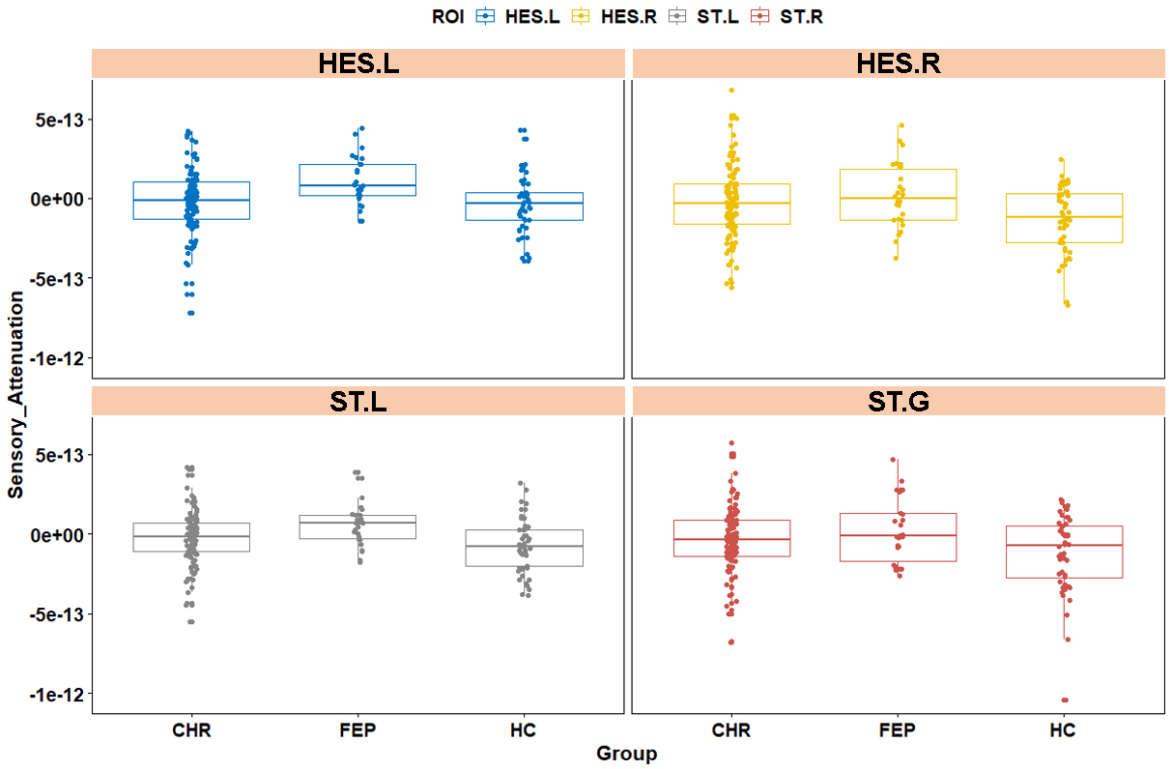

Supplementary Figure 1 The distribution and boxplot of sensory attenuation in 4 ROIs at the virtual-channel level

The sensory attenuation is extracted based on the mean value of an interesting time window of M100 between 90 and 150 ms from individual subjects. The line in the boxplot displays the median value of the sensory attenuation effect within each group. ROIs: Region of Interest. HC: Healthy Controls; CHR: Clinical High-risk Psychosis; FEP: First-episode Psychosis; HES: Heschl's Gyrus; ST: Superior Temporal Cortex; L: left; R: Right.

Supplementary Table 1 Cognitive variables in subgroups of CHR and HC

BACS	CHR-SPI	CHR-CAM	CHR-both	HC	F value	*p*	Post-hoc
Working Memory mean(SD)	-0.7(1.8)	-0.03(1.3)	-0.03(1.6)	0(1)	-	>0.05[a]	
Motor Speed mean(SD)	-0.6(1.2)	-0.4(0.8)	-0.6(1.0)	0(1)	-	<0.05*[a]	HC> CHR-SPI HC> CHR-CAM HC> CHR-both
Verbal Memory mean(SD)	-0.5(1.5)	-0.13(1.3)	-0.36(1.3)	0(1)	1.5	>0.05	
Verbal Fluency mean(SD)	-0.17(1.6)	0.13(0.9)	-0.014(1.5)	0(1)	0.3	>0.05	
Executive Function mean(SD)	-0.40(2.5)	-0.35(1.6)	-0.08(1.3)	0(1)	-	<0.05*[a]	HC> CHR-SPI HC> CHR-CAM HC> CHR-both
Processing Speed &attention mean(SD)	-5.02(0.8)	-4.9(1.0)	-4.6(1.0)	0(1)	0.6	>0.05	
BACS Composite score mean(SD)	-0.8(2.3)	-0.3(1.1)	-0.3(1.5)	0(1)	-	>0.05[a]	

Notes: Abbreviations: SD: Standard Deviation; HC: Healthy Controls; CHR: Clinical High-risk Psychosis; CHR-CAM: CHR subjects who only met the criteria of the Comprehensive Assessment of At-Risk Mental States(CAARMS); CHR-SPI: CHR subjects who only met the criteria of Schizophrenia Proneness Instrument, Adult Version(SPI-A); CHR-both: CHR subjects who met the criteria of both SPI-A and CAARMS. FEP: First-episode Psychosis; ScZ; Schizophrenia; BACS: Brief Assessment of Cognition n Schizophrenia.* $p<0.05$, [a] non-parametric permutation statistics.

Supplementary Table 2 Cognitive variables in CHR-persistent and CHR non-persistent at 12 months

BACS	CHR-non persistent	CHR-persistent	HC	F value	*p*	Post-hoc
Working Memory mean(SD)	-0.2(1.5)	-0.1(1.6)	0(1)	-	>0.05[a]	
Motor Speed mean(SD)	-0.6(0.8)	-0.6(1.1)	0(1)	3.8	<0.05	HC> CHR-nonpersistent
Verbal Memory mean(SD)	-0.21(1.26)	-0.5(1.4)	0(1)	1.2	>0.05	
Verbal Fluency mean(SD)	0.24(1.31)	-0.2(1.3)	0(1)	1.1	>0.05	
Executive Function mean(SD)	0.0001(1.3)	-0.4(1.4)	0(1)	1.2	>0.05	
Processing Speed &attention mean(SD)	-5.0(1.0)	-4.6(1.0)	0(1)	228.4	<0.05*	HC> CHR-nonpersistent HC> CHR-persistent
BACS Composite score mean(SD)	-0.3(1.4)	-0.4(1.5)	0(1)		>0.05[a]	

Notes: Abbreviations: y: year; SD: Standard Deviation; HC: Healthy Controls; CHR: Clinical High-risk Psychosis; FEP: First-episode Psychosis; ScZ; Schizophrenia; BACS: Brief Assessment of Cognition in Schizophrenia. * p<0.05, [a] non-parametric permutation statistics.

Supplementary Table 3 The correlation between sensory attenuation and cognitive functions in HC

	HC			
	SAP Left HES	SAP Right HES	SAP Left ST	SAP Right ST
GAF_baseline	-	-	-	-
Total CAARMS severity	NaN	NaN	NaN	NaN
Total SPI-A severity	NaN	NaN	NaN	NaN
CAARMS-subitems				
UTC_global	NaN	NaN	NaN	NaN
NBI_global	NaN	NaN	NaN	NaN
PA_global	NaN	NaN	NaN	NaN
DS_global	NaN	NaN	NaN	NaN
BACS				
Working memory	-	-	-	-
Motor speed	-	-	-	-
Verbal Memory	-	-	-	-
Verbal fluency	-	-	-	-
Executive function	-	-	-	-
Processing speed & attention	-	-	-	-
BACS composite score	-	-	-	-

Notes: There is no significant correlation between sensory attenuation and cognitive variables in HC (Spearman rank correlation, uncorrected p < 0.05).Abbreviations: GAF: Global Assessment of Functioning; CAARMS: Comprehensive Assessment of At-Risk Mental States; SPI-A: Schizophrenia Proneness Instrument, Adult Version; UTC_global: Global Score of Unusual Thought Content; NBI_global: Global Score of a Non-bizarre Idea; PA_global: Global Score of Perceptual Abnormality; DS_global: Global Score of Disorganized Speech; BACS: Brief Assessment of Cognition in Schizophrenia; CHR: Clinical High-risk Psychosis; FEP: First-episode Psychosis; HES: Heschl's Gyrus; ST: Superior Temporal Cortex; NaN: Not a number.

Supplementary Table 4 The correlation between sensory attenuation and cognitive functions in CHR and FEP

Group / Items	CHR				FEP			
	Left HES	Right HES	Left ST	Right ST	Left HES	Right HES	Left ST	Right ST
GAF_baseline	*r*=-0.21 *p*=0.024	-	-	-	-	-	-	-
Total CAARMS severity	-	-	-	-	-	-	-	-
SPI-A Severity	*r*=0.19 *p*=0.039	-	-	-	-	-	-	-
CAARMS-subitems								
UTC_global	*r*=0.25 *p*=0.009	-	*r*=0.21 *p*=0.025	-	-	-	-	-
NBI_global	-	-	-	-	*r=0.57* *p*=0.027	-	-	-
PA_global	-	-	-	-	-	-	-	-
DS_global	r=0.22 *p*=0.020	-	r=0.22 *p*=0.018	-	-	-	-	-
BACS								
Working Memory	*r*=-0.23 *p*=0.015	*r*=-0.31 *p*=0.0011*	*r*=-0.22 *p*=0.023	*r*=-0.26 *p*=0.0055	-	-	-	-
Motor Speed	-	-	-	-	-	-	-	-
Verbal Memory	-	-	-	-	-	-	-	-
Verbal Fluency	-	-	*r*=-0.21 *p*=0.028	-	-	-	-	-
Executive Function	*r*=-0.19 *p*=0.043	-	-	-	-	-	-	-
Processing Speed &attention	-	-	-	-	-	-	-	-
BACS composite score	r=-0.19 p=0.046	-	*r*=-0.21 *p*=0.026	-	-	-	-	-

Notes: The association between sensory attenuation and cognitive variables in CHR and FEP (Spearman rank correlation, uncorrected p <0.05).Abbreviations: GAF: Global Assessment of Functioning; CAARMS: Comprehensive Assessment of At-Risk Mental States; SPI-A: Schizophrenia Proneness Instrument, Adult Version; UTC_global: Global Score of Unusual Thought Content; NBI_global: Global Score of a Non-bizarre Idea; PA_global: Global Score of Perceptual Abnormality; DS_global: Global Score of Disorganized Speech; BACS: Brief Assessment of Cognition in Schizophrenia; CHR: Clinical High-risk Psychosis; FEP: First-Episode Psychosis; HES: Heschl's Gyrus; ST: Superior Temporal Cortex; NaN: Not a number.

Supplementary Material for Chapter 5

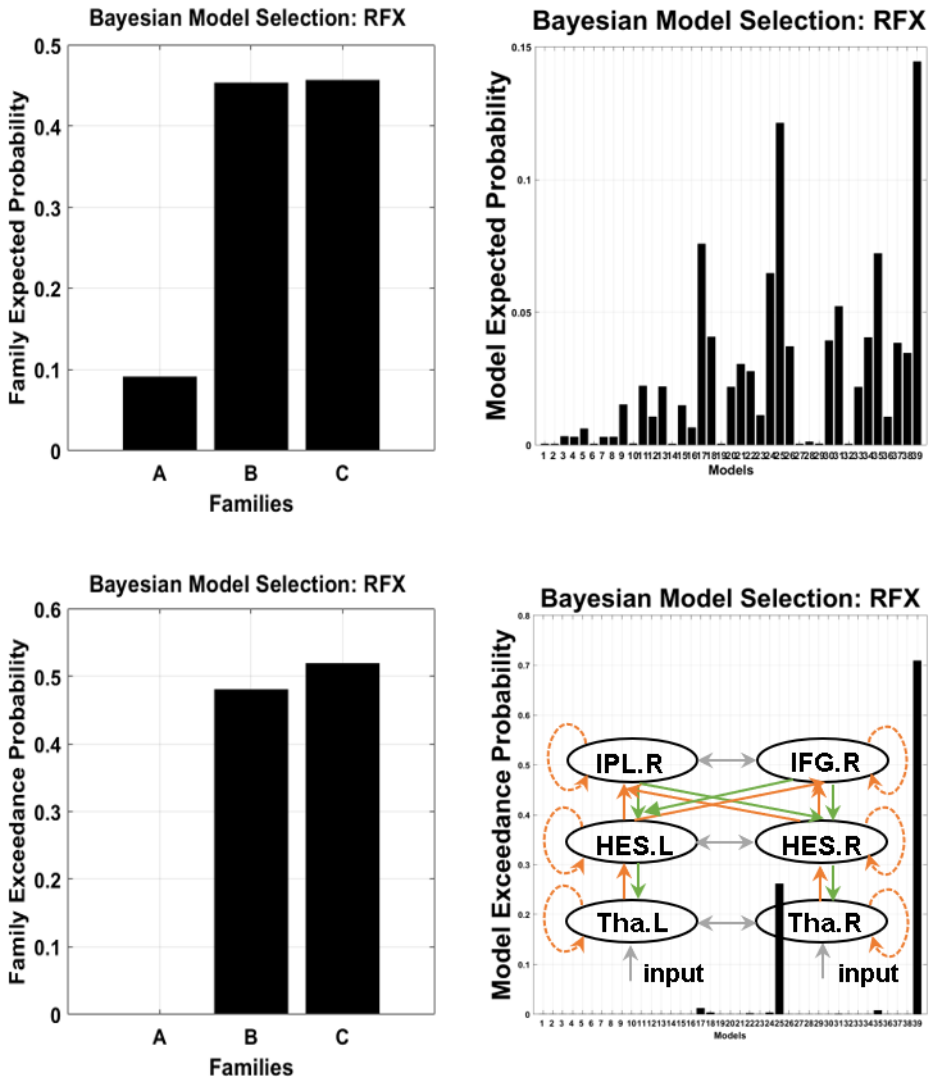

Supplementary Figure 2 RFX-BMS of DCM across all the subjects

The panel displays the results of RFX-BMS across all subjects in Family A, B, C (13 models in each family, 39 models in all). The upper panel displays the expected probability at the family- and model-level. The bottom panel displays exceedance probability at the family- and model-level. The exceedance probability for Family B is 0.46 and from Family C is 0.54.

Appendix 2

YouR-Study Assessment Checklist

At-Risk Group

Participant ID: _____

Visit 1: Date: _____
_____ At-risk Consent
_____ At-Risk Information sheet
_____ Demographics (including substance use, family history and risk asset.)
_____ Positive scale, CAARMS
_____ COGDIS/COPER, SPI-A

Visit 2: Date: _____
_____ Debrief

Visit 3: Date: _____
_____ COGDIS/COPER, SPI-A (Opt)
_____ Positive scale, CAARMS (Opt)
_____ M.I.N.I
_____ Scale for Premorbid Adjustment
_____ Social role scale
_____ Functional role scale

Visit 4: Date: _____
_____ Brief Assessment of Cognition in Schizophrenia Battery (BACS)
_____ Neuropsychological Testing Battery
_____ Edinburgh Handedness Inventory
_____ National Adult Reading Test
_____ Beliefs About Paranoia Scale (BAPS)
_____ Brief Core Schema Scale (BCSS)
_____ Psychosis Attachment Measure (PAM-SR)
_____ Adverse Childhood Experience Scale (ACES)
_____ The Rust Inventory of Schizotypal Cognitions (RISC)

Visit 5: Date: _____
_____ MEG
_____ MRI
_____ Blood sample (opt)
_____ Urine sample (opt)
_____ Inventory of Interpersonal Problems
_____ Significant Others Scale
_____ International Positive and Negative Affect Schedule (I-PANAS-SF)
_____ Social Interaction Anxiety Scale
_____ Assessment of Musicality
_____ Assessment of Video Gaming
_____ The Autism Symptom Self-report for adolescents and adults (ASSERT)
_____ Early Symptomatic Syndromes Eliciting Neurodevelopmental Clinical Examinations (ESSENCE)
_____ Adult ADHD Self-Report Scale (ASRS)

Month 6: Date: _____
_____ Positive scale, CAARMS
_____ SCID I & II
_____ IIP
_____ SOS
_____ I-PANAS-SF
_____ Social role scale
_____ Functional role scale

Month 9: Date: _____
_____ Positive scale, CAARMS
_____ IIP
_____ SOS
_____ I-PANAS-SF

Month 12: Date: _____
_____ Positive Scale, CAARMS
_____ SCID I & II
_____ IIP
_____ SOS
_____ I-PANAS-SF
_____ Social role scale
_____ Functional role scale

Month 18: Date: _____
_____ Positive scale, CAARMS
_____ IIP
_____ SOS
_____ I-PANAS-SF

Month 24: Date: _____
_____ Positive Scale, CAARMS
_____ COGDIS/COPER, SPI-A
_____ SCID I & II
_____ IIP
_____ SOS
_____ I-PANAS-SF
_____ Social role scale
_____ Functional role scale
_____ FROGS

Month 30: Date: _____
_____ Positive scale, CAARMS
_____ IIP
_____ SOS
_____ I-PANAS-SF

Month 36: Date: _____
_____ Positive scale, CAARMS
_____ COGDIS/COPER, SPI-A
_____ IIP
_____ SOS
_____ I-PANAS-SF

YouR-Study Assessment Checklist

FEP Group

Participant ID: _____

Visit 1: Date: _____
_____ At-risk Information sheet
_____ At-risk Consent
_____ Demographics info (including substance use, family history and risk assessment)
_____ Positive scale, CAARMS
_____ COGDIS/COPER, SPI-A

Visit 2: Date: _____
_____ Debrief
_____ Potential referral to services

Visit 3: Date: _____
_____ SCID I & II
_____ PANSS
_____ Potential referral to services

Visit 4: Date: _____
_____ MEG
_____ MRI
_____ Blood sample (opt)
_____ Urine sample (opt)
_____ Assessment of musicality
_____ Assessment of video gaming

Month 3: Date: _____
_____ Brief Assessment of Cognition in Sz battery
_____ Neuropsychological battery
_____ PANSS
_____ Edinburgh Handedness Inventory
_____ National Adult Reading test

YouR-Study Assessment Checklist

Control Group

Participant ID: _____

Visit 1: Date: _____
_____ Control consent form
_____ Control information sheet
_____ Positive scale, CAARMS
_____ COGDIS/COPER, SPI-A
_____ M.I.N.I
_____ Premorbid Adjustment Scale
_____ Social role scale
_____ Functional role scale

Visit 2: Date: _____
_____ Brief Assessment of Cognition in Sz battery
_____ Neuropsychological testing battery
_____ Edinburgh Handedness Inventory
_____ National Adult Reading Test
_____ Beliefs about Paranoia Scale
_____ Brief Core Schema Scale (BCSS)
_____ Psychosis Attachment Measure
_____ Adverse Childhood Experience Scale (ACES)
_____ Rust Inventory of Schizotypal Cognitions (RISC)
_____ Inventory of Interpersonal Problems – 32 items (IIP)
_____ Significant Others Scale (SOS)
_____ The International Positive and Negative Affect Schedule – short form (I-PANAS-SF)
_____ Social Interaction Anxiety Scale

Visit 3: Date: _____
_____ MEG
_____ MRI
_____ Blood sample
_____ Urine sample
_____ Assessment of musicality
_____ Assessment of video gaming

Follow-up: Date:_____
_____ Psychophysical assessment
_____ MEG

Bibliography

Abbasi, O., & Gross, J. (2020). Beta – band oscillations play an essential role in motor – auditory interactions. *Human brain mapping, 41*(3), 656-665.

Abi-Dargham, A., Gil, R., Krystal, J., Baldwin, R. M., Seibyl, J. P., Bowers, M., . . . Laruelle, M. (1998). Increased striatal dopamine transmission in schizophrenia: confirmation in a second cohort. *American Journal of Psychiatry, 155*(6), 761-767.

Adams, R. A., Shipp, S., & Friston, K. J. (2013). Predictions not commands: active inference in the motor system. *Brain Structure and Function, 218*(3), 611-643.

Addington, & Barbato, M. (2012). The role of cognitive functioning in the outcome of those at clinical high risk for developing psychosis. *Epidemiology and psychiatric sciences, 21*(4), 335-342.

Addington, Cornblatt, B. A., Cadenhead, K. S., Cannon, T. D., McGlashan, T. H., Perkins, D. O., . . . Woods, S. W. (2011). At clinical high risk for psychosis: outcome for nonconverters. *American Journal of Psychiatry, 168*(8), 800-805.

Addington, Penn, D., Woods, S. W., Addington, D., & Perkins, D. O. (2008). Social functioning in individuals at clinical high risk for psychosis. *Schizophrenia research, 99*(1-3), 119-124.

Addington, Stowkowy, J., Liu, L., Cadenhead, K. S., Cannon, T. D., Cornblatt, B. A., . . . Tsuang, M. T. (2019). Clinical and functional characteristics of youth at clinical high-risk for psychosis who do not transition to psychosis. *Psychological Medicine, 49*(10), 1670-1677.

Agnew-Blais, J., & Seidman, L. J. (2013). Neurocognition in youth and young adults under age 30 at familial risk for schizophrenia: a quantitative and qualitative review. *Cognitive neuropsychiatry, 18*(1-2), 44-82.

Ahlfors, S. P., Han, J., Belliveau, J. W., & Hämäläinen, M. S. (2010). Sensitivity of MEG and EEG to source orientation. *Brain topography, 23*(3), 227-232.

Alain, C., He, Y., & Grady, C. (2008). The contribution of the inferior parietal lobe to auditory spatial working memory. *Journal of cognitive neuroscience, 20*(2), 285-295.

Alitto, H. J., & Usrey, W. M. (2003). Corticothalamic feedback and sensory processing. *Current opinion in neurobiology, 13*(4), 440-445.

Aliu, S. O., Houde, J. F., & Nagarajan, S. S. (2009). Motor-induced suppression of the auditory cortex. *Journal of cognitive neuroscience, 21*(4), 791-802.

Allen, P., Larøi, F., McGuire, P. K., & Aleman, A. (2008). The hallucinating brain: a review of structural and functional neuroimaging studies of hallucinations. *Neuroscience & Biobehavioral Reviews, 32*(1), 175-191.

Allen, P., Stephan, K. E., Mechelli, A., Day, F., Ward, N., Dalton, J., . . . McGuire, P. (2010). Cingulate activity and fronto-temporal connectivity in people with prodromal signs of psychosis. *Neuroimage, 49*(1), 947-955.

Amminger, G., Leicester, S., Yung, A., Phillips, L., Berger, G., Francey, S., . . . McGorry, P. (2006). Early-onset of symptoms predicts conversion to non-affective psychosis in ultra-high risk individuals. *Schizophrenia research, 84*(1), 67-76.

Anderson, D. M., Glibert, P. M., & Burkholder, J. M. (2002). Harmful algal blooms and eutrophication: nutrient sources, composition, and consequences. *Estuaries, 25*(4), 704-726.

Andreou, C., & Borgwardt, S. (2020). Structural and functional imaging markers for susceptibility to psychosis. *Molecular psychiatry*, 1-13.

Andreou, C., Leicht, G., Nolte, G., Polomac, N., Moritz, S., Karow, A., . . . Mulert, C. (2015). Resting-state theta-band connectivity and verbal memory in schizophrenia and in the high-risk state. *Schizophrenia research, 161*(2-3), 299-307.

Apps, M. A., & Tsakiris, M. (2014). The free-energy self: a predictive coding account of self-recognition. *Neuroscience & Biobehavioral Reviews, 41*, 85-97.

Association, A. P. (2013). Diagnostic and statistical manual of mental disorders. *BMC Med, 17*, 133-137.

Attal, Y., & Schwartz, D. (2013). Assessment of subcortical source localization using deep brain activity imaging model with minimum norm operators: a MEG study. *PloS one, 8*(3), e59856.

Auksztulewicz, R., & Friston, K. (2015). Attentional enhancement of auditory mismatch responses: a DCM/MEG study. *Cerebral cortex, 25*(11), 4273-4283.

Baess, P., Horváth, J., Jacobsen, T., & Schröger, E. (2011). Selective suppression of self – initiated sounds in an auditory stream: An ERP study. *Psychophysiology, 48*(9), 1276-1283.

Baess, P., Widmann, A., Roye, A., Schröger, E., & Jacobsen, T. (2009). Attenuated human auditory middle latency response and evoked 40 – Hz response to self – initiated sounds. *European Journal of Neuroscience, 29*(7), 1514-1521.

Bastiaansen, M. C., & Knösche, T. R. (2000). Tangential derivative mapping of axial MEG applied to event-related desynchronization research. *Clinical neurophysiology, 111*(7), 1300-1305.

Bellebaum, C., Daum, I., Koch, B., Schwarz, M., & Hoffmann, K.-P. (2005). The role of the human thalamus in processing corollary discharge. *Brain, 128*(5), 1139-1154.

Benazet, M., Thénault, F., Whittingstall, K., & Bernier, P.-M. (2016). Attenuation of visual reafferent signals in the parietal cortex during voluntary movement. *Journal of neurophysiology, 116*(4), 1831-1839.

Bendfeldt, K., Smieskova, R., Koutsouleris, N., Klöppel, S., Schmidt, A., Walter, A., . . . Taschler, B. (2015). Classifying individuals at high-risk for psychosis based on functional brain activity during working memory processing. *NeuroImage: Clinical, 9*, 555-563.

Besl, P. J., & McKay, N. D. (1992). *Method for registration of 3-D shapes*. Paper presented at the Sensor fusion IV: control paradigms and data structures.

Blakemore, Frith, C. D., & Wolpert, D. M. (2001). The cerebellum is involved in predicting the sensory consequences of action. *Neuroreport, 12*(9), 1879-1884.

Blakemore, & Sirigu. (2003). Action prediction in the cerebellum and in the parietal lobe. *Experimental Brain Research, 153*(2), 239-245.

Blakemore, & Sirigu, A. (2003). Action prediction in the cerebellum and in the parietal lobe. *Experimental Brain Research, 153*(2), 239-245.

Blakemore, Wolpert, & Frith. (1998a). Central cancellation of self-produced tickle sensation. *Nature neuroscience, 1*(7), 635-640.

Blakemore, Wolpert, D., & Frith, C. (2000). Why can't you tickle yourself? *Neuroreport, 11*(11), R11-R16.

Blakemore, Wolpert, D. M., & Frith, C. D. (1998b). Central cancellation of self-produced tickle sensation. *Nature neuroscience, 1*(7), 635-640.

Blakemore, Wolpert, D. M., & Frith, C. D. (1999). The cerebellum contributes to somatosensory cortical activity during self-produced tactile stimulation. *Neuroimage, 10*(4), 448-459.

Bleuler, E. (1950). Dementia praecox or the group of schizophrenias.

Boehme, R., Hauser, S., Gerling, G. J., Heilig, M., & Olausson, H. (2019). Distinction of self-produced touch and social touch at cortical and spinal cord levels. *Proceedings of the National Academy of Sciences, 116*(6), 2290-2299.

Boly, M., Garrido, M. I., Gosseries, O., Bruno, M.-A., Boveroux, P., Schnakers, C., . . . Friston, K. (2011). Preserved feedforward but impaired top-down processes in the vegetative state. *Science, 332*(6031), 858-862.

Bora, Lin, A., Wood, S., Yung, A., McGorry, P., & Pantelis, C. (2014). Cognitive deficits in youth with familial and clinical high risk to psychosis: a systematic review and meta – analysis. *Acta Psychiatrica Scandinavica, 130*(1), 1-15.

Bora, Yucel, M., & Pantelis, C. (2009). Theory of mind impairment in schizophrenia: meta-analysis. *Schizophrenia research, 109*(1-3), 1-9.

Bourque, F., van der Ven, E., & Malla, A. (2011). A meta-analysis of the risk for psychotic disorders among first-and second-generation immigrants. *Psychological medicine, 41*(5), 897-910.

Brekke, J. S., DeBonis, J. A., & Graham, J. W. (1994). A latent structure analysis of the positive and negative symptoms in schizophrenia. *Comprehensive Psychiatry, 35*(4), 252-259.

Brockhaus-Dumke, A., Schultze-Lutter, F., Mueller, R., Tendolkar, I., Bechdolf, A., Pukrop, R., . . . Ruhrmann, S. (2008). Sensory gating in schizophrenia: P50 and N100 gating in antipsychotic-free subjects at risk, first-episode, and chronic patients. *Biological psychiatry, 64*(5), 376-384.

Brown, Adams, R. A., Parees, I., Edwards, M., & Friston, K. (2013). Active inference, sensory attenuation and illusions. *Cognitive processing, 14*(4), 411-427.

Brown, & Derkits, E. J. (2009). Prenatal infection and schizophrenia: a review of epidemiologic and translational studies. *American Journal of Psychiatry, 167*(3), 261-280.

Brüne, M. (2005). "Theory of mind" in schizophrenia: a review of the literature. *Schizophrenia bulletin, 31*(1), 21-42.

Budinger, E., & Scheich, H. (2009). Anatomical connections suitable for the direct processing of neuronal information of different modalities via the rodent primary auditory cortex. *Hearing research, 258*(1-2), 16-27.

Burin, D., Battaglini, A., Pia, L., Falvo, G., Palombella, M., & Salatino, A. (2017). Comparing intensities and modalities within the sensory attenuation paradigm: Preliminary evidence. *Journal of advanced research, 8*(6), 649-653.

Cannon-Spoor, H. E., Potkin, S. G., & Wyatt, R. J. (1982). Measurement of premorbid adjustment in chronic schizophrenia. *Schizophrenia bulletin, 8*(3), 470-484.

Cantor-Graae, E., & Selten, J.-P. (2005). Schizophrenia and migration: a meta-analysis and review. *American Journal of Psychiatry, 162*(1), 12-24.

Cao, Chén, O. Y., Chung, Y., Forsyth, J. K., McEwen, S. C., Gee, D. G., . . . Cadenhead, K. S. (2018). Cerebello-thalamo-cortical hyperconnectivity as a state-independent functional neural signature for psychosis prediction and characterization. *Nature communications, 9*(1), 1-9.

Cao, Thut, G., & Gross, J. (2017). The role of brain oscillations in predicting self-generated sounds. *Neuroimage, 147*, 895-903.

Cao, Veniero, D., Thut, G., & Gross, J. (2017). Role of the cerebellum in adaptation to delayed action effects. *Current Biology, 27*(16), 2442-2451. e2443.

Carlsson, A. (1959). The occurrence, distribution and physiological role of catecholamines in the nervous system. *Pharmacological reviews, 11*(2), 490-493.

Carlsson, A., Lindqvist, M., & Magnusson, T. (1957). 3, 4-Dihydroxyphenylalanine and 5-hydroxytryptophan as reserpine antagonists. *Nature, 180*(4596), 1200.

Carrión, R. E., Goldberg, T. E., McLaughlin, D., Auther, A. M., Correll, C. U., & Cornblatt, B. A. (2011). Impact of neurocognition on social and role functioning in individuals at clinical high risk for psychosis. *American Journal of Psychiatry, 168*(8), 806-813.

Carrión, R. E., McLaughlin, D., Goldberg, T. E., Auther, A. M., Olsen, R. H., Olvet, D. M., . . . Cornblatt, B. A. (2013). Prediction of functional outcome in individuals at clinical high risk for psychosis. *JAMA psychiatry, 70*(11), 1133-1142.

Christensen, M. S., Lundbye-Jensen, J., Geertsen, S. S., Petersen, T. H., Paulson, O. B., & Nielsen, J. B. (2007). Premotor cortex modulates somatosensory cortex during voluntary movements without proprioceptive feedback. *Nature neuroscience, 10*(4), 417-419.

Chronicle, E. P., & Glover, J. (2003). A ticklish question: does magnetic stimulation of the primary motor cortex give rise to an 'efference copy'? *Cortex, 39*(1), 105-110.

Cloutier, M., Aigbogun, M. S., Guerin, A., Nitulescu, R., Ramanakumar, A. V., Kamat, S. A., . . . Henderson, C. (2016). The economic burden of schizophrenia in the United States in 2013. *The Journal of clinical psychiatry, 77*(6), 764-771.

Collin, G., Seidman, L. J., Keshavan, M. S., Stone, W. S., Qi, Z., Zhang, T., . . . Niznikiewicz, M. A. (2018). Functional connectome organization predicts conversion to psychosis in clinical high-risk youth from the SHARP program. *Molecular psychiatry*, 1-10.

Corballis, M. C., & Häberling, I. S. (2017). The many sides of hemispheric asymmetry: A selective review and outlook. *Journal of the International Neuropsychological Society: JINS, 23*(9-10), 710.

Cornblatt, Auther, A. M., Niendam, T., Smith, C. W., Zinberg, J., Bearden, C. E., & Cannon, T. D. (2007). Preliminary findings for two new measures of social and role functioning in the prodromal phase of schizophrenia. *Schizophrenia bulletin, 33*(3), 688-702.

Cornblatt, Obuchowski, M., Roberts, S., Pollack, S., & Erlenmeyer–Kimling, L. (1999). Cognitive and behavioral precursors of schizophrenia. *Development and psychopathology, 11*(3), 487-508.

Cornwell, B. R., Carver, F. W., Coppola, R., Johnson, L., Alvarez, R., & Grillon, C. (2008). Evoked amygdala responses to negative faces revealed by adaptive MEG beamformers. *Brain research, 1244*, 103-112.

Crapse, T. B., & Sommer, M. A. (2008a). Corollary discharge across the animal kingdom. *Nature Reviews Neuroscience, 9*(8), 587-600.

Crapse, T. B., & Sommer, M. A. (2008b). Corollary discharge circuits in the primate brain. *Current opinion in neurobiology, 18*(6), 552-557.

Creutzfeldt, O., Ojemann, G., & Lettich, E. (1989). Neuronal activity in the human lateral temporal lobe. II. Responses to the subjects own voice. *Experimental Brain Research, 77*(3), 476-489.

Cross, Crow, T., & Owen, F. (1981). 3 H-flupenthixol binding in post-mortem brains of schizophrenics: Evidence for a selective increase in dopamine D2 receptors. *Psychopharmacology, 74*(2), 122-124.

Cross, Scott, J. L., Hermens, D. F., & Hickie, I. B. (2018). Variability in clinical outcomes for youths treated for subthreshold severe mental disorders at an early intervention service. *Psychiatric Services, 69*(5), 555-561.

Crossley, N. A., Mechelli, A., Fusar – Poli, P., Broome, M. R., Matthiasson, P., Johns, L. C., . . . McGuire, P. K. (2009). Superior temporal lobe dysfunction and frontotemporal dysconnectivity in subjects at risk of psychosis and in first – episode psychosis. *Human brain mapping, 30*(12), 4129-4137.

Cuesta, M. J., & Peralta, V. (1995). Cognitive disorders in the positive, negative, and disorganization syndromes of schizophrenia. *Psychiatry research, 58*(3), 227-235.

Curio, G., Neuloh, G., Numminen, J., Jousmäki, V., & Hari, R. (2000). Speaking modifies voice – evoked activity in the human auditory cortex. *Human brain mapping, 9*(4), 183-191.

D'Souza, D. C., Cho, H.-S., Perry, E. B., & Krystal, J. H. (2004). Cannabinoid'model'psychosis, dopamine-cannabinoid interactions and implications. *Marijuana and madness: psychiatry and neurobiology*, 142.

Daprati, E., Franck, N., Georgieff, N., Proust, J., Pacherie, E., Dalery, J., & Jeannerod, M. (1997). Looking for the agent: an investigation into consciousness of action and self-consciousness in schizophrenic patients. *Cognition, 65*(1), 71-86.

Dauvermann, M. R., Whalley, H. C., Romaniuk, L., Valton, V., Owens, D. G., Johnstone, E. C., . . . Moorhead, T. W. (2013). The application of nonlinear dynamic causal modelling for fMRI in subjects at high genetic risk of schizophrenia. *Neuroimage, 73*, 16-29.

David, O., Kiebel, S. J., Harrison, L. M., Mattout, J., Kilner, J. M., & Friston, K. J. (2006). Dynamic causal modeling of evoked responses in EEG and MEG. *Neuroimage, 30*(4), 1255-1272.

Davis, K. L., Kahn, R. S., Ko, G., & Davidson, M. (1991). Dopamine in schizophrenia: a review and reconceptualization. *The American journal of psychiatry*.

Del Re, E. C., Spencer, K. M., Oribe, N., Mesholam-Gately, R. I., Goldstein, J., Shenton, M. E., . . . Niznikiewicz, M. A. (2015). Clinical high risk and first episode schizophrenia: auditory event-related potentials. *Psychiatry Research: Neuroimaging, 231*(2), 126-133.

Della-Maggiore, V., Malfait, N., Ostry, D. J., & Paus, T. (2004). Stimulation of the posterior parietal cortex interferes with arm trajectory adjustments during the learning of new dynamics. *Journal of Neuroscience, 24*(44), 9971-9976.

Diez, A., Ranlund, S., Pinotsis, D., Calafato, S., Shaikh, M., Hall, M. H., . . . Bramon, E. (2017). Abnormal frontoparietal synaptic gain mediating the P300 in patients with psychotic disorder and their unaffected relatives. *Hum Brain Mapp, 38*(6), 3262-3276. doi:10.1002/hbm.23588

Dima, Dietrich, Dillo, & Emrich. (2010a). Impaired top-down processes in schizophrenia: a DCM study of ERPs. *NeuroImage, 52*(3), 824-832. doi:10.1016/j.neuroimage.2009.12.086

Dima, Dietrich, D. E., Dillo, W., & Emrich, H. M. (2010b). Impaired top-down processes in schizophrenia: A DCM study of ERPs. *Neuroimage, 52*(3), 824-832.

Dima, Frangou, Burge, Braeutigam, & James. (2012a). Abnormal intrinsic and extrinsic connectivity within the magnetic mismatch negativity brain network in schizophrenia: a preliminary study. *Schizophrenia Research, 135*(1-3), 23-27.

Dima, Frangou, S., Burge, L., Braeutigam, S., & James, A. (2012b). Abnormal intrinsic and extrinsic connectivity within the magnetic mismatch negativity brain network in schizophrenia: a preliminary study. *Schizophrenia research, 135*(1-3), 23-27.

Dima, Roiser, Dietrich, D. E., Bonnemann, C., Lanfermann, H., Emrich, H. M., & Dillo, W. (2009). Understanding why patients with schizophrenia do not perceive the hollow-mask illusion using dynamic causal modelling. *NeuroImage, 46*(4), 1180-1186. doi:10.1016/j.neuroimage.2009.03.033

Du, Y., Fryer, S. L., Fu, Z., Lin, D., Sui, J., Chen, J., . . . Loewy, R. L. (2018). Dynamic functional connectivity impairments in early schizophrenia and clinical high-risk for psychosis. *Neuroimage, 180*, 632-645.

Dürschmid, S., Edwards, E., Reichert, C., Dewar, C., Hinrichs, H., Heinze, H.-J., . . . Knight, R. T. (2016). Hierarchy of prediction errors for auditory events in human temporal and frontal cortex. *Proceedings of the National Academy of Sciences, 113*(24), 6755-6760.

Dzafic, I., Larsen, K. M., Darke, H., Pertile, H., Carter, O., Sundram, S., & Garrido, M. I. (2021). Stronger Top-Down and Weaker Bottom-Up Frontotemporal Connections During Sensory Learning Are Associated With Severity of Psychotic Phenomena. *Schizophr Bull*. doi:10.1093/schbul/sbaa188

Eastwood, S. L., Burnet, P. W., & Harrison, P. J. (1997). GluR2 glutamate receptor subunit flip and flop isoforms are decreased in the hippocampal formation in schizophrenia: A reverse transcriptase-polymerase chain reaction (RT–PCR) study. *Molecular brain research, 44*(1), 92-98.

Eastwood, S. L., McDonald, B., Burnet, P. W., Beckwith, J. P., Kerwin, R. W., & Harrison, P. J. (1995). Decreased expression of mRNAs encoding non-NMDA glutamate receptors GluRl and GluR2 in medial temporal lobe neurons in schizophrenia. *Molecular brain research, 29*(2), 211-223.

Edwards, J., Pattison, P. E., Jackson, H. J., & Wales, R. J. (2001). Facial affect and affective prosody recognition in first-episode schizophrenia. *Schizophrenia research, 48*(2-3), 235-253.

Egerton, A., Chaddock, C. A., Winton-Brown, T. T., Bloomfield, M. A., Bhattacharyya, S., Allen, P., . . . Howes, O. D. (2013). Presynaptic striatal dopamine dysfunction in people at ultra-high risk for psychosis: findings in a second cohort. *Biological psychiatry, 74*(2), 106-112.

Eliades, S. J., & Wang, X. (2003). Sensory-motor interaction in the primate auditory cortex during self-initiated vocalizations. *Journal of neurophysiology, 89*(4), 2194-2207.

Ellaway, P., Prochazka, A., Chan, M., & Gauthier, M. (2004). The sense of movement elicited by transcranial magnetic stimulation in humans is due to sensory feedback. *The Journal of physiology, 556*(2), 651-660.

Elvevag, B., & Goldberg, T. E. (2000). Cognitive impairment in schizophrenia is the core of the disorder. *Critical Reviews™ in Neurobiology, 14*(1).

Erickson, M. A., Ruffle, A., & Gold, J. M. (2016). A meta-analysis of mismatch negativity in schizophrenia: from clinical risk to disease specificity and progression. *Biological psychiatry, 79*(12), 980-987.

Feinberg, I. (1978). Efference copy and corollary discharge: implications for thinking and its disorders. *Schizophrenia bulletin, 4*(4), 636.

Feinberg, I., & Guazzelli, M. (1999). Schizophrenia–a disorder of the corollary discharge systems that integrate the motor systems of thought with the sensory systems of consciousness. *The British Journal of Psychiatry, 174*(3), 196-204.

First, Spitzer, R. L., Gibbon, M., & Williams, J. B. (1995). Structured clinical interview for DSM-IV axis I disorders-patient edition (SCID-I/P, Version 2.0). *New York: Biometrics Research Department, New York State Psychiatric Institute, 722*.

First, Williams, J., Karg, R., & Spitzer, R. (2015). Structured clinical interview for DSM-5—Research version (SCID-5 for DSM-5, research version; SCID-5-RV). *Arlington, VA: American Psychiatric Association*, 1-94.

Fogelson, N., Litvak, V., Peled, A., Fernandez-del-Olmo, M., & Friston, K. (2014). The functional anatomy of schizophrenia: A dynamic causal modeling study of predictive coding. *Schizophr Res, 158*(1-3), 204-212. doi:10.1016/j.schres.2014.06.011

Folsom, D. P., Hawthorne, W., Lindamer, L., Gilmer, T., Bailey, A., Golshan, S., . . . Jeste, D. V. (2005). Prevalence and risk factors for homelessness and utilization of mental health services among 10,340 patients with serious mental illness in a large public mental health system. *American Journal of Psychiatry, 162*(2), 370-376.

Ford, Gray, Faustman, Heinks, & Mathalon. (2005). Reduced gamma-band coherence to distorted feedback during speech when what you say is not what you hear. *International Journal of Psychophysiology, 57*(2), 143-150.

Ford, Gray, M., Faustman, W. O., Roach, B. J., & Mathalon, D. H. (2007). Dissecting corollary discharge dysfunction in schizophrenia. *Psychophysiology, 44*(4), 522-529.

Ford, & Mathalon. (2005). Corollary discharge dysfunction in schizophrenia: can it explain auditory hallucinations? *International Journal of Psychophysiology, 58*(2-3), 179-189.

Ford, & Mathalon. (2019). Efference copy, corollary discharge, predictive coding, and psychosis. *Biological Psychiatry: Cognitive Neuroscience and Neuroimaging, 4*(9), 764-767.

Ford, Mathalon, Whitfield, S., Faustman, W. O., & Roth, W. T. (2002). Reduced communication between frontal and temporal lobes during talking in schizophrenia. *Biological psychiatry, 51*(6), 485-492.

Ford, & Mathalon, D. H. (2004). Electrophysiological evidence of corollary discharge dysfunction in schizophrenia during talking and thinking. *Journal of psychiatric research, 38*(1), 37-46.

Ford, & Mathalon, D. H. (2005). Corollary discharge dysfunction in schizophrenia: can it explain auditory hallucinations? *International Journal of Psychophysiology, 58*(2-3), 179-189.

Ford, Mathalon, D. H., Heinks, T., Kalba, S., Faustman, W. O., & Roth, W. T. (2001). Neurophysiological evidence of corollary discharge dysfunction in schizophrenia. *American Journal of Psychiatry, 158*(12), 2069-2071.

Ford, Mathalon, D. H., Roach, B. J., Keedy, S. K., Reilly, J. L., Gershon, E. S., & Sweeney, J. A. (2013). Neurophysiological evidence of corollary discharge

function during vocalization in psychotic patients and their nonpsychotic first-degree relatives. *Schizophrenia Bulletin, 39*(6), 1272-1280.
Ford, Palzes, Roach, & Mathalon. (2014). Did I do that? Abnormal predictive processes in schizophrenia when button pressing to deliver a tone. *Schizophrenia Bulletin, 40*(4), 804-812.
Franck, N., Farrer, C., Georgieff, N., Marie-Cardine, M., Daléry, J., d'Amato, T., & Jeannerod, M. (2001). Defective recognition of one's own actions in patients with schizophrenia. *American Journal of Psychiatry, 158*(3), 454-459.
Friston. (1999). Schizophrenia and the disconnection hypothesis. *Acta Psychiatrica Scandinavica, 99*, 68-79.
Friston. (2002). Dysfunctional connectivity in schizophrenia. *World Psychiatry, 1*(2), 66.
Friston. (2011). Functional and effective connectivity: a review. *Brain connectivity, 1*(1), 13-36.
Friston, Brown, H. R., Siemerkus, J., & Stephan, K. E. (2016). The dysconnection hypothesis (2016). *Schizophrenia research, 176*(2-3), 83-94.
Friston, & Frith, C. D. (1995). Schizophrenia: a disconnection syndrome. *Clin Neurosci, 3*(2), 89-97.
Friston, Harrison, L., & Penny, W. (2003). Dynamic causal modelling. *Neuroimage, 19*(4), 1273-1302.
Friston, & Kiebel. (2009). Predictive coding under the free-energy principle. *Philosophical Transactions of the Royal Society B: Biological Sciences, 364*(1521), 1211-1221.
Friston, & Kiebel, S. (2009). Predictive coding under the free-energy principle. *Philosophical Transactions of the Royal Society B: Biological Sciences, 364*(1521), 1211-1221.
Friston, Litvak, V., Oswal, A., Razi, A., Stephan, K. E., Van Wijk, B. C., . . . Zeidman, P. (2016). Bayesian model reduction and empirical Bayes for group (DCM) studies. *Neuroimage, 128*, 413-431.
Frommann, I., Brinkmeyer, J., Ruhrmann, S., Hack, E., Brockhaus-Dumke, A., Bechdolf, A., . . . Wagner, M. (2008). Auditory P300 in individuals clinically at risk for psychosis. *International Journal of Psychophysiology, 70*(3), 192-205.
Frommann, I., Pukrop, R., Brinkmeyer, J., Bechdolf, A., Ruhrmann, S., Berning, J., . . . Wölwer, W. (2011). Neuropsychological profiles in different at-risk states of psychosis: executive control impairment in the early—and additional memory dysfunction in the late—prodromal state. *Schizophrenia Bulletin, 37*(4), 861-873.
Fu, C. H., Vythelingum, G. N., Brammer, M. J., Williams, S. C., Amaro Jr, E., Andrew, C. M., . . . McGuire, P. K. (2005). An fMRI study of verbal self-monitoring: neural correlates of auditory verbal feedback. *Cereb Cortex, 16*(7), 969-977.
Fulham, W. R., Michie, P. T., Ward, P. B., Rasser, P. E., Todd, J., Johnston, P. J., . . . Schall, U. (2014). Mismatch negativity in recent-onset and chronic schizophrenia: a current source density analysis. *PLoS One, 9*(6), e100221.
Fusar-Poli, Borgwardt, Crescini, A., Deste, G., Kempton, M. J., Lawrie, S., . . . Sacchetti, E. (2011). Neuroanatomy of vulnerability to psychosis: a voxel-based meta-analysis. *Neuroscience & Biobehavioral Reviews, 35*(5), 1175-1185.
Fusar-Poli, P. (2017). The clinical high-risk state for psychosis (CHR-P), version II. In: Oxford University Press US.

Fusar-Poli, P., Bonoldi, I., Yung, A. R., Borgwardt, S., Kempton, M. J., Valmaggia, L., . . . McGuire, P. (2012). Predicting psychosis: meta-analysis of transition outcomes in individuals at high clinical risk. *Archives of general psychiatry, 69*(3), 220-229.

Fusar-Poli, P., Borgwardt, S., Bechdolf, A., Addington, J., Riecher-Rössler, A., Schultze-Lutter, F., . . . Seidman, L. J. (2013). The psychosis high-risk state: a comprehensive state-of-the-art review. *JAMA psychiatry, 70*(1), 107-120.

Fusar-Poli, P., Cappucciati, M., Bonoldi, I., Hui, L. C., Rutigliano, G., Stahl, D. R., . . . Lawrie, S. M. (2016). Prognosis of brief psychotic episodes: a meta-analysis. *JAMA psychiatry, 73*(3), 211-220.

Fusar-Poli, P., Cappucciati, M., Borgwardt, S., Woods, S. W., Addington, J., Nelson, B., . . . Riecher-Rössler, A. (2016). Heterogeneity of psychosis risk within individuals at clinical high risk: a meta-analytical stratification. *JAMA psychiatry, 73*(2), 113-120.

Fusar-Poli, P., Deste, G., Smieskova, R., Barlati, S., Yung, A. R., Howes, O., . . . Borgwardt, S. (2012). Cognitive functioning in prodromal psychosis: a meta-analysis. *Archives of general psychiatry, 69*(6), 562-571.

Fusar-Poli, P., Howes, O., Allen, P., Broome, M., Valli, I., Asselin, M., . . . McGuire, P. (2011). Abnormal prefrontal activation directly related to pre-synaptic striatal dopamine dysfunction in people at clinical high risk for psychosis. *Molecular psychiatry, 16*(1), 67.

Fusar-Poli, P., Howes, O. D., Allen, P., Broome, M., Valli, I., Asselin, M.-C., . . . McGuire, P. K. (2010). Abnormal frontostriatal interactions in people with prodromal signs of psychosis: a multimodal imaging study. *Archives of general psychiatry, 67*(7), 683-691.

Fusar-Poli, P., Radua, J., McGuire, P., & Borgwardt, S. (2011). Neuroanatomical maps of psychosis onset: voxel-wise meta-analysis of antipsychotic-naive VBM studies. *Schizophrenia bulletin, 38*(6), 1297-1307.

Fusar-Poli, P., Rocchetti, M., Sardella, A., Avila, A., Brandizzi, M., Caverzasi, E., . . . McGuire, P. (2015). Disorder, not just state of risk: meta-analysis of functioning and quality of life in people at high risk of psychosis. *The British Journal of Psychiatry, 207*(3), 198-206.

Fusar-Poli, P., Rutigliano, G., Stahl, D., Davies, C., Bonoldi, I., Reilly, T., & McGuire, P. (2017). Development and validation of a clinically based risk calculator for the transdiagnostic prediction of psychosis. *JAMA psychiatry, 74*(5), 493-500.

Fusar-Poli, P., Schultze-Lutter, F., & Addington, J. (2016). Intensive community outreach for those at ultra high risk of psychosis: dilution, not solution. *The Lancet Psychiatry, 3*(1), 18.

Fusar-Poli, P., Schultze-Lutter, F., Cappucciati, M., Rutigliano, G., Bonoldi, I., Stahl, D., . . . Perkins, D. O. (2016). The dark side of the moon: meta-analytical impact of recruitment strategies on risk enrichment in the clinical high risk state for psychosis. *Schizophrenia bulletin, 42*(3), 732-743.

Fusar – Poli, P. (2017). Why ultra high risk criteria for psychosis prediction do not work well outside clinical samples and what to do about it. *World Psychiatry, 16*(2), 212.

Gajwani, R., Gross, J., Gumley, A. I., Krishnadas, R., Lawrie, S., Schwannauer, M., . . . Uhlhaas, P. (2020). MEG-measured high-frequency oscillations in visual cortex indicate circuit dysfunctions in local and large scale networks during emerging psychosis. *JAMA psychiatry*.

Garrido, M. I., Friston, K. J., Kiebel, S. J., Stephan, K. E., Baldeweg, T., & Kilner, J. M. (2008). The functional anatomy of the MMN: a DCM study of the roving paradigm. *Neuroimage, 42*(2), 936-944.

Garrido, M. I., Kilner, J. M., Kiebel, S. J., Stephan, K. E., Baldeweg, T., & Friston, K. J. (2009). Repetition suppression and plasticity in the human brain. *Neuroimage, 48*(1), 269-279.

Geddes, J. R., & Lawrie, S. M. (1995). Obstetric complications and schizophrenia: a meta-analysis. *The British Journal of Psychiatry, 167*(6), 786-793.

Geddes, J. R., Verdoux, H., Takei, N., Lawrie, S. M., Bovet, P., Eagles, J. M., . . . O'Callaghan, E. (1999). Schizophrenia and complications of pregnancy and labor: an individual patient data meta-analysis. *Schizophrenia bulletin, 25*(3), 413-423.

Gejman, P. V., Sanders, A. R., & Kendler, K. S. (2011). Genetics of schizophrenia: new findings and challenges. *Annual review of genomics and human genetics, 12*, 121-144.

Gilbert, C. D., & Sigman, M. (2007). Brain states: top-down influences in sensory processing. *Neuron, 54*(5), 677-696.

Giraldo-Chica, M., & Woodward, N. D. (2017). Review of thalamocortical resting-state fMRI studies in schizophrenia. *Schizophr Res, 180*, 58-63. doi:10.1016/j.schres.2016.08.005

Giuliano, Li, H., I Mesholam-Gately, R., M Sorenson, S., A Woodberry, K., & J Seidman, L. (2012). Neurocognition in the psychosis risk syndrome: a quantitative and qualitative review. *Current pharmaceutical design, 18*(4), 399-415.

Goldman-Rakic, P. S., Castner, S. A., Svensson, T. H., Siever, L. J., & Williams, G. V. (2004). Targeting the dopamine D 1 receptor in schizophrenia: insights for cognitive dysfunction. *Psychopharmacology, 174*(1), 3-16.

Gonzalez-Heydrich, J., Enlow, M. B., D'Angelo, E., Seidman, L. J., Gumlak, S., Kim, A., . . . Graber, K. (2015). Early auditory processing evoked potentials (N100) show a continuum of blunting from clinical high risk to psychosis in a pediatric sample. *Schizophrenia research, 169*(1-3), 340-345.

Gore, F. M., Bloem, P. J., Patton, G. C., Ferguson, J., Joseph, V., Coffey, C., . . . Mathers, C. D. (2011). Global burden of disease in young people aged 10–24 years: a systematic analysis. *The Lancet, 377*(9783), 2093-2102.

Gray. (1991). The neuropsychology of schizophrenia. *Behavioral and Brain Sciences, 14*(1), 1-20.

Gur, R. C., Calkins, M. E., Satterthwaite, T. D., Ruparel, K., Bilker, W. B., Moore, T. M., . . . Gur, R. E. (2014). Neurocognitive Growth Charting in Psychosis Spectrum Youths. *Jama Psychiatry, 71*(4), 366-374. doi:10.1001/jamapsychiatry.2013.4190

Häfner, H., Maurer, K., Ruhrmann, S., Bechdolf, A., Klosterkötter, J., Wagner, M., . . . Gaebel, W. (2004). Early detection and secondary prevention of psychosis: facts and visions. *European archives of psychiatry and clinical neuroscience, 254*(2), 117-128.

Haggard, & Chambon, V. (2012). Sense of agency. *Current Biology, 22*(10), R390-R392.

Haggard, & Whitford. (2004). Supplementary motor area provides an efferent signal for sensory suppression. *Cognitive Brain Research, 19*(1), 52-58.

Hamilton, Williams, T. J., Ventura, J., Jasperse, L. J., Owens, E. M., Miller, G. A., . . . Yee, C. M. (2018). Clinical and Cognitive Significance of Auditory

Sensory Processing Deficits in Schizophrenia. *Am J Psychiatry, 175*(3), 275-283. doi:10.1176/appi.ajp.2017.16111203

Hare, E. (1956a). Family setting and the urban distribution of schizophrenia. *Journal of Mental Science, 102*(429), 753-760.

Hare, E. (1956b). Mental illness and social conditions in Bristol. *Journal of Mental Science, 102*(427), 349-357.

Harrison, P., McLaughlin, D., & Kerwin, R. (1991). Decreased hippocampal expression of a glutamate receptor gene in schizophrenia. *The Lancet, 337*(8739), 450-452.

Healy, D. J., Haroutunian, V., Powchik, P., Davidson, M., Davis, K. L., Watson, S. J., & Meador-Woodruff, J. H. (1998). AMPA receptor binding and subunit mRNA expression in prefrontal cortex and striatum of elderly schizophrenics. *Neuropsychopharmacology, 19*(4), 278-286.

Heinks-Maldonado, T. H., Mathalon, D. H., Houde, J. F., Gray, M., Faustman, W. O., & Ford, J. M. (2007). Relationship of imprecise corollary discharge in schizophrenia to auditory hallucinations. *Archives of General Psychiatry, 64*(3), 286-296.

Heinks-Maldonado, T. H., Nagarajan, S. S., & Houde, J. F. (2006). Magnetoencephalographic evidence for a precise forward model in speech production. *Neuroreport, 17*(13), 1375-1379.

Heinrichs, R. W., & Zakzanis, K. K. (1998). Neurocognitive deficit in schizophrenia: a quantitative review of the evidence. *Neuropsychology, 12*(3), 426.

Heinzle, J., & Stephan, K. E. (2018). Dynamic causal modeling and its application to psychiatric disorders. In *Computational Psychiatry* (pp. 117-144): Elsevier.

Hemsley, D. R., & Garety, P. A. (1986). The formation of maintenance of delusions: a Bayesian analysis. *The British Journal of Psychiatry, 149*(1), 51-56.

Hengartner, M. P., Heekeren, K., Dvorsky, D., Walitza, S., Rössler, W., & Theodoridou, A. (2017). Checking the predictive accuracy of basic symptoms against ultra high-risk criteria and testing of a multivariable prediction model: evidence from a prospective three-year observational study of persons at clinical high-risk for psychosis. *European Psychiatry, 45*, 27-35.

Hickok, G., Okada, K., & Serences, J. T. (2009). Area Spt in the human planum temporale supports sensory-motor integration for speech processing. *Journal of neurophysiology, 101*(5), 2725-2732.

Hollister, L. E., Krieger, G. E., Kringel, A., & Roberts, R. H. (1955). Treatment of chronic schizophrenic reactions with reserpine. *Annals of the New York Academy of Sciences, 61*(1), 92-100.

Hornix, B. E., Havekes, R., & Kas, M. J. (2018). Multisensory cortical processing and dysfunction across the neuropsychiatric spectrum. *Neuroscience & Biobehavioral Reviews*.

Horváth, J. (2014). The role of mechanical impact in action-related auditory attenuation. *Cognitive, Affective, & Behavioral Neuroscience, 14*(4), 1392-1406.

Horváth, J. (2015). Action-related auditory ERP attenuation: Paradigms and hypotheses. *Brain Research, 1626*, 54-65.

Howes, Bose, S. K., Turkheimer, F., Valli, I., Egerton, A., Valmaggia, L. R., . . . McGuire, P. (2011). Dopamine synthesis capacity before onset of

psychosis: a prospective [18F]-DOPA PET imaging study. *American Journal of Psychiatry, 168*(12), 1311-1317.

Howes, & Kapur, S. (2009). The dopamine hypothesis of schizophrenia: version III—the final common pathway. *Schizophrenia bulletin, 35*(3), 549-562.

Howes, McCutcheon, R., & Stone, J. (2015). Glutamate and dopamine in schizophrenia: An update for the 21st century. *Journal of Psychopharmacology, 29*(2), 97-115. doi:10.1177/0269881114563634

Hsieh, M. H., Shan, J.-C., Huang, W.-L., Cheng, W.-C., Chiu, M.-J., Jaw, F.-S., . . . Liu, C.-C. (2012). Auditory event-related potential of subjects with suspected pre-psychotic state and first – episode psychosis. *Schizophrenia research, 140*(1-3), 243-249.

Huber, G., & Gross, G. (1989). The concept of basic symptoms in schizophrenic and schizoaffective psychoses. *Recenti progressi in medicina, 80*(12), 646-652.

Hughes, G., Desantis, A., & Waszak, F. (2013). Mechanisms of intentional binding and sensory attenuation: The role of temporal prediction, temporal control, identity prediction, and motor prediction. *Psychological bulletin, 139*(1), 133-151.

Hughes, G., & Waszak, F. (2011). ERP correlates of action effect prediction and visual sensory attenuation in voluntary action. *Neuroimage, 56*(3), 1632-1640.

Ingraham, L. J., & Kety, S. S. (2000). Adoption studies of schizophrenia. *American Journal of Medical Genetics, 97*(1), 18-22.

Ising, H. K., Veling, W., Loewy, R. L., Rietveld, M. W., Rietdijk, J., Dragt, S., . . . Linszen, D. H. (2012). The validity of the 16-item version of the Prodromal Questionnaire (PQ-16) to screen for ultra high risk of developing psychosis in the general help-seeking population. *Schizophrenia bulletin, 38*(6), 1288-1296.

James, S. L., Abate, D., Abate, K. H., Abay, S. M., Abbafati, C., Abbasi, N., . . . Abdelalim, A. (2018). Global, regional, and national incidence, prevalence, and years lived with disability for 354 diseases and injuries for 195 countries and territories, 1990–2017: a systematic analysis for the Global Burden of Disease Study 2017. *The Lancet, 392*(10159), 1789-1858.

Jankelowitz, S., & Colebatch, J. (2002). Movement-related potentials associated with self-paced, cued and imagined arm movements. *Experimental Brain Research, 147*(1), 98-107.

Javitt, D. C. (2009a). Sensory processing in schizophrenia: neither simple nor intact. *Schizophrenia Bulletin, 35*(6), 1059-1064.

Javitt, D. C. (2009b). When doors of perception close: bottom-up models of disrupted cognition in schizophrenia. *Annual review of clinical psychology, 5*, 249-275.

Javitt, D. C., & Zukin, S. R. (1991). Recent advances in the phencyclidine model of schizophrenia. *The American journal of psychiatry*.

Jones, P., Murray, R., Rodgers, B., & Marmot, M. (1994). Child developmental risk factors for adult schizophrenia in the British 1946 birth cohort. *The Lancet, 344*(8934), 1398-1402.

Jordaan, G. P., Warwick, J. M., Nel, D. G., Hewlett, R., & Emsley, R. (2012). Alcohol-induced psychotic disorder: brain perfusion and psychopathology—before and after anti-psychotic treatment. *Metabolic brain disease, 27*(1), 67-77.

Kallmann, F. J. (1938). The genetics of schizophrenia.

Kallmann, F. J. (1946). The genetic theory of schizophrenia: An analysis of 691 schizophrenic twin index families. *American Journal of Psychiatry, 103*(3), 309-322.

Kantrowitz, J. T., & Javitt, D. C. (2010). N-methyl-d-aspartate (NMDA) receptor dysfunction or dysregulation: the final common pathway on the road to schizophrenia? *Brain research bulletin, 83*(3-4), 108-121.

Kasai, K., Shenton, M. E., Salisbury, D. F., Hirayasu, Y., Onitsuka, T., Spencer, M. H., . . . McCarley, R. W. (2003). Progressive decrease of left Heschl gyrus and planum temporale gray matter volume in first-episode schizophrenia: a longitudinal magnetic resonance imaging study. *Archives of general psychiatry, 60*(8), 766-775.

Kay, S. R., Fiszbein, A., & Opler, L. A. (1987). The positive and negative syndrome scale (PANSS) for schizophrenia. *Schizophrenia bulletin, 13*(2), 261-276.

Keefe, R. S., Goldberg, T. E., Harvey, P. D., Gold, J. M., Poe, M. P., & Coughenour, L. (2004). The Brief Assessment of Cognition in Schizophrenia: reliability, sensitivity, and comparison with a standard neurocognitive battery. *Schizophrenia research, 68*(2-3), 283-297.

Kelleher, I., Connor, D., Clarke, M. C., Devlin, N., Harley, M., & Cannon, M. (2012). Prevalence of psychotic symptoms in childhood and adolescence: a systematic review and meta-analysis of population-based studies.

Kelly, B. D., O'Callaghan, E., Waddington, J. L., Feeney, L., Browne, S., Scully, P. J., . . . Morgan, M. G. (2010). Schizophrenia and the city: A review of literature and prospective study of psychosis and urbanicity in Ireland. *Schizophrenia research, 116*(1), 75-89.

Kempton, M. J., Bonoldi, I., Valmaggia, L., McGuire, P., & Fusar-Poli, P. (2015). Speed of psychosis progression in people at ultra-high clinical risk: a complementary meta-analysis. *JAMA psychiatry, 72*(6), 622-623.

Kendler, K. S., & Diehl, S. R. (1993). The genetics of schizophrenia: a current, genetic-epidemiologic perspective. *Schizophrenia bulletin, 19*(2), 261-285.

Kiebel, S. J., Garrido, M. I., & Friston, K. J. (2007). Dynamic causal modelling of evoked responses: the role of intrinsic connections. *Neuroimage, 36*(2), 332-345.

Kilteni, K., & Ehrsson, H. H. (2017a). Body ownership determines the attenuation of self-generated tactile sensations. *Proceedings of the National Academy of Sciences, 114*(31), 8426-8431.

Kilteni, K., & Ehrsson, H. H. (2017b). Sensorimotor predictions and tool use: Hand-held tools attenuate self-touch. *Cognition, 165*, 1-9.

Kilteni, K., & Ehrsson, H. H. (2019). Functional connectivity between the cerebellum and somatosensory areas implements the attenuation of self-generated touch. *Journal of Neuroscience*.

Kim, M., Kim, S. N., Lee, S., Byun, M. S., Shin, K. S., Park, H. Y., . . . Kwon, J. S. (2014). Impaired mismatch negativity is associated with current functional status rather than genetic vulnerability to schizophrenia. *Psychiatry Research: Neuroimaging, 222*(1-2), 100-106.

Kim, M., Lee, T. H., Yoon, Y. B., Lee, T. Y., & Kwon, J. S. (2018). Predicting remission in subjects at clinical high risk for psychosis using mismatch negativity. *Schizophrenia bulletin, 44*(3), 575-583.

Klaffehn, A. L., Baess, P., Kunde, W., & Pfister, R. (2019). Sensory attenuation prevails when controlling for temporal predictability of self-and externally generated tones. *Neuropsychologia, 132*, 107145.

Klosterkötter, J., Hellmich, M., Steinmeyer, E. M., & Schultze-Lutter, F. (2001). Diagnosing schizophrenia in the initial prodromal phase. *Archives of General Psychiatry, 58*(2), 158-164.

Knolle, F., Schröger, E., Baess, P., & Kotz, S. A. (2012). The cerebellum generates motor-to-auditory predictions: ERP lesion evidence. *Journal of cognitive neuroscience, 24*(3), 698-706.

Knolle, F., Schröger, E., & Kotz, S. A. (2013). Cerebellar contribution to the prediction of self-initiated sounds. *Cortex, 49*(9), 2449-2461.

Koskinen, J., Löhönen, J., Koponen, H., Isohanni, M., & Miettunen, J. (2009). Rate of cannabis use disorders in clinical samples of patients with schizophrenia: a meta-analysis. *Schizophrenia bulletin, 36*(6), 1115-1130.

Krabbendam, L., & Van Os, J. (2005). Schizophrenia and urbanicity: a major environmental influence—conditional on genetic risk. *Schizophrenia bulletin, 31*(4), 795-799.

Kraepelin, E. (1971). *Dementia praecox and paraphrenia*: Krieger Publishing Company.

Laruelle, M. (1998). Imaging dopamine transmission in schizophrenia: a review and meta-analysis. *The Quarterly Journal of Nuclear Medicine and Molecular Imaging, 42*(3), 211.

Laruelle, M., Abi-Dargham, A., Gil, R., Kegeles, L., & Innis, R. (1999). Increased dopamine transmission in schizophrenia: relationship to illness phases. *Biological psychiatry, 46*(1), 56-72.

Lee, Carvell, G. E., & Simons, D. J. (2008). Motor modulation of afferent somatosensory circuits. *Nature neuroscience, 11*(12), 1430.

Lee, Kim, S. N., Correll, C. U., Byun, M. S., Kim, E., Jang, J. H., . . . Kwon, J. S. (2014). Symptomatic and functional remission of subjects at clinical high risk for psychosis: a 2-year naturalistic observational study. *Schizophrenia research, 156*(2-3), 266-271.

Lencz, T., Smith, C. W., Auther, A. M., Correll, C. U., & Cornblatt, B. A. (2003). The assessment of "prodromal schizophrenia": unresolved issues and future directions. *Schizophrenia bulletin, 29*(4), 717-728.

Li, H., Chan, R. C., McAlonan, G. M., & Gong, Q. Y. (2010). Facial emotion processing in schizophrenia: a meta-analysis of functional neuroimaging data. *Schizophr Bull, 36*(5), 1029-1039. doi:10.1093/schbul/sbn190

Liddle, P. F. (1987). The symptoms of chronic schizophrenia: a re-examination of the positive-negative dichotomy. *The British Journal of Psychiatry, 151*(2), 145-151.

Lieberman, J., Kane, J., & Alvir, J. (1987). Provocative tests with psychostimulant drugs in schizophrenia. *Psychopharmacology, 91*(4), 415-433.

Limanowski, J., Sarasso, P., & Blankenburg, F. (2018). Different responses of the right superior temporal sulcus to visual movement feedback during self–generated vs. externally generated hand movements. *European Journal of Neuroscience, 47*(4), 314-320.

Lindström, L. H., Gefvert, O., Hagberg, G., Lundberg, T., Bergström, M., Hartvig, P., & Långström, B. (1999). Increased dopamine synthesis rate in medial prefrontal cortex and striatum in schizophrenia indicated by L-(β-11C) DOPA and PET. *Biological psychiatry, 46*(5), 681-688.

Loewy, R., Fisher, M., Schlosser, D. A., Biagianti, B., Stuart, B., Mathalon, D. H., & Vinogradov, S. (2016). Intensive auditory cognitive training improves verbal memory in adolescents and young adults at clinical high risk for psychosis. *Schizophrenia bulletin, 42*(suppl_1), S118-S126.

Luby, E. D., Gottlieb, J. S., Cohen, B. D., Rosenbaum, G., & Domino, E. F. (1962). Model psychoses and schizophrenia. *American Journal of Psychiatry, 119*(1), 61-67.

Maher, B. A. (1974). Delusional thinking and perceptual disorder. *J Individ Psychol, 30*(1), 98-113. Retrieved from **https://www.ncbi.nlm.nih.gov/pubmed/4857199**

Mălîia, M.-D., Donos, C., Barborica, A., Popa, I., Ciurea, J., Cinatti, S., & Mîndruţă, I. (2018). Functional mapping and effective connectivity of the human operculum. *Cortex, 109*, 303-321.

March, D., Hatch, S. L., Morgan, C., Kirkbride, J. B., Bresnahan, M., Fearon, P., & Susser, E. (2008). Psychosis and place. *Epidemiologic reviews, 30*(1), 84-100.

Maris, E., & Oostenveld, R. (2007). Nonparametric statistical testing of EEG- and MEG-data. *J Neurosci Methods, 164*(1), 177-190. doi:10.1016/j.jneumeth.2007.03.024

Martikainen, Kaneko, & Hari. (2005a). Suppressed responses to self-triggered sounds in the human auditory cortex. *Cerebral cortex, 15*(3), 299-302.

Martikainen, Kaneko, K.-i., & Hari, R. (2005b). Suppressed responses to self-triggered sounds in the human auditory cortex. *Cerebral cortex, 15*(3), 299-302.

Marwaha, S., Johnson, S., Bebbington, P., Stafford, M., Angermeyer, M. C., Brugha, T., . . . Toumi, M. (2007). Rates and correlates of employment in people with schizophrenia in the UK, France and Germany. *The British Journal of Psychiatry, 191*(1), 30-37.

Mathalon, D. H., Roach, B. J., Ferri, J. M., Loewy, R. L., Stuart, B. K., Perez, V. B., . . . Ford, J. M. (2019). Deficient auditory predictive coding during vocalization in the psychosis risk syndrome and in early illness schizophrenia: the final expanded sample. *Psychological medicine, 49*(11), 1897-1904.

Mathers, D., & Ghodse, A. (1992). Cannabis and psychotic illness. *The British Journal of Psychiatry, 161*(5), 648-653.

McGlashan, T., Miller, T., Woods, S., Rosen, J., Hoffman, R., & Davidson, L. (2001). Structured interview for prodromal syndromes. *New Haven, CT: PRIME Research Clinic, Yale School of Medicine*.

Meador-Woodruff, J. H., & Healy, D. J. (2000). Glutamate receptor expression in schizophrenic brain. *Brain Research Reviews, 31*(2-3), 288-294.

Meijer, J., Simons, C. J., Quee, P. J., Verweij, K., & Investigators, G. (2012). Cognitive alterations in patients with non – affective psychotic disorder and their unaffected siblings and parents. *Acta Psychiatrica Scandinavica, 125*(1), 66-76.

Meyer, E. C., Carrión, R. E., Cornblatt, B. A., Addington, J., Cadenhead, K. S., Cannon, T. D., . . . Walker, E. F. (2014). The relationship of neurocognition and negative symptoms to social and role functioning over time in individuals at clinical high risk in the first phase of the North American Prodrome Longitudinal Study. *Schizophrenia bulletin, 40*(6), 1452-1461.

Miall, Weir, D. J., Wolpert, D. M., & Stein, J. (1993). Is the cerebellum a smith predictor? *Journal of motor behavior, 25*(3), 203-216.

Miall, & Wolpert, D. M. (1996). Forward models for physiological motor control. *Neural networks, 9*(8), 1265-1279.

Michel, C., Ruhrmann, S., Schimmelmann, B. G., Klosterkötter, J., & Schultze-Lutter, F. (2018). Course of clinical high-risk states for psychosis beyond

conversion. *European archives of psychiatry and clinical neuroscience, 268*(1), 39-48.
Michie, P. T., Malmierca, M. S., Harms, L., & Todd, J. (2016). The neurobiology of MMN and implications for schizophrenia. *Biological psychology, 116*, 90-97.
Mikanmaa, E. (2020). *Neuromagnetic mismatch negativity in individuals at clinical high risk state for psychosis*. University of Glasgow,
Miller, T. J., McGlashan, T. H., Woods, S. W., Stein, K., Driesen, N., Corcoran, C. M., . . . Davidson, L. (1999). Symptom assessment in schizophrenic prodromal states. *Psychiatric Quarterly, 70*(4), 273-287.
Mitchell, R. L., & Crow, T. J. (2005). Right hemisphere language functions and schizophrenia: the forgotten hemisphere? *Brain, 128*(5), 963-978.
Moore, T. M., Reise, S. P., Gur, R. E., Hakonarson, H., & Gur, R. C. (2015). Psychometric properties of the Penn Computerized Neurocognitive Battery. *Neuropsychology, 29*(2), 235.
Morillon, B., Hackett, T. A., Kajikawa, Y., & Schroeder, C. E. (2015). Predictive motor control of sensory dynamics in auditory active sensing. *Current opinion in neurobiology, 31*, 230-238.
Morrison, A. P., French, P., Stewart, S. L., Birchwood, M., Fowler, D., Gumley, A. I., . . . Murray, G. K. (2012). Early detection and intervention evaluation for people at risk of psychosis: multisite randomised controlled trial. *Bmj, 344*, e2233.
Mortensen, P. B., Nørgaard-Pedersen, B., Waltoft, B. L., Sørensen, T. L., Hougaard, D., Torrey, E. F., & Yolken, R. H. (2007). Toxoplasma gondii as a risk factor for early-onset schizophrenia: analysis of filter paper blood samples obtained at birth. *Biological psychiatry, 61*(5), 688-693.
Mukerji, S., Windsor, A. M., & Lee, D. J. (2010). Auditory brainstem circuits that mediate the middle ear muscle reflex. *Trends in amplification, 14*(3), 170-191.
Murray, R. M., & Lewis, S. W. (1987). Is schizophrenia a neurodevelopmental disorder? *British medical journal (Clinical research ed.), 295*(6600), 681.
Näätänen, R., & Kähkönen, S. (2009). Central auditory dysfunction in schizophrenia as revealed by the mismatch negativity (MMN) and its magnetic equivalent MMNm: a review. *International Journal of Neuropsychopharmacology, 12*(1), 125-135.
Nagamine, T., Toro, C., Balish, M., Deuschr, G., Wang, B., Sato, S., . . . Hallett, M. (1994). Cortical magnetic and electric fields associated with voluntary finger movements. *Brain topography, 6*(3), 175-183.
Naito, E. (2004). Sensing limb movements in the motor cortex: how humans sense limb movement. *The Neuroscientist, 10*(1), 73-82.
Nelson, Schneider, D. M., Takatoh, J., Sakurai, K., Wang, F., & Mooney, R. (2013). A circuit for motor cortical modulation of auditory cortical activity. *Journal of Neuroscience, 33*(36), 14342-14353.
Nemeroff, C. B. (2004). Neurobiological consequences of childhood trauma. *The Journal of clinical psychiatry*.
Nielsen, S., Toftdahl, N., Nordentoft, M., & Hjorthøj, C. (2017). Association between alcohol, cannabis, and other illicit substance abuse and risk of developing schizophrenia: a nationwide population based register study. *Psychological medicine, 47*(9), 1668-1677.
Ødegaard, Ø. (1973). Emigration and mental health. In *Uprooting and After...* (pp. 155-160): Springer.

Oestreich, Mifsud, N. G., Ford, J. M., Roach, B. J., Mathalon, D. H., & Whitford, T. J. (2015). Subnormal sensory attenuation to self-generated speech in schizotypy: electrophysiological evidence for a 'continuum of psychosis'. *International Journal of Psychophysiology, 97*(2), 131-138.

Oestreich, Mifsud, N. G., Ford, J. M., Roach, B. J., Mathalon, D. H., & Whitford, T. J. (2016). Cortical suppression to delayed self-initiated auditory stimuli in schizotypy: neurophysiological evidence for a continuum of psychosis. *Clinical EEG and neuroscience, 47*(1), 3-10.

Oldfield, R. C. (1971). The assessment and analysis of handedness: the Edinburgh inventory. *Neuropsychologia, 9*(1), 97-113.

Olney, J. W., & Farber, N. B. (1995). Glutamate receptor dysfunction and schizophrenia. *Arch Gen Psychiatry, 52*(12), 998-1007. doi:10.1001/archpsyc.1995.03950240016004

Oostenveld, R., Fries, P., Maris, E., & Schoffelen, J.-M. (2011). FieldTrip: open source software for advanced analysis of MEG, EEG, and invasive electrophysiological data. *Computational intelligence and neuroscience, 2011*, 1.

Opitz, B., Rinne, T., Mecklinger, A., Von Cramon, D. Y., & Schröger, E. (2002). Differential contribution of frontal and temporal cortices to auditory change detection: fMRI and ERP results. *Neuroimage, 15*(1), 167-174.

Oranje, B., Geyer, M. A., Bocker, K. B., Kenemans, J. L., & Verbaten, M. N. (2006). Prepulse inhibition and P50 suppression: commonalities and dissociations. *Psychiatry research, 143*(2), 147-158.

Owen, F., Crow, T., Poulter, M., Cross, A., Longden, A., & Riley, G. (1978). Increased dopamine-receptor sensitivity in schizophrenia. *The Lancet, 312*(8083), 223-226.

Pa, J., & Hickok, G. (2008). A parietal–temporal sensory–motor integration area for the human vocal tract: Evidence from an fMRI study of skilled musicians. *Neuropsychologia, 46*(1), 362-368.

Pedersen, M. G., Stevens, H., Pedersen, C. B., Nørgaard-Pedersen, B., & Mortensen, P. B. (2011). Toxoplasma infection and later development of schizophrenia in mothers. *American Journal of Psychiatry, 168*(8), 814-821.

Penfield, W., & Roberts, L. (2014). *Speech and brain mechanisms*: Princeton University Press.

Perez, V. B., Ford, J. M., Roach, B. J., Loewy, R. L., Stuart, B. K., Vinogradov, S., & Mathalon, D. H. (2011). Auditory cortex responsiveness during talking and listening: early illness schizophrenia and patients at clinical high-risk for psychosis. *Schizophrenia bulletin, 38*(6), 1216-1224.

Perez, V. B., Ford, J. M., Roach, B. J., Loewy, R. L., Stuart, B. K., Vinogradov, S., & Mathalon, D. H. (2012). Auditory cortex responsiveness during talking and listening: early illness schizophrenia and patients at clinical high-risk for psychosis. *Schizophrenia bulletin, 38*(6), 1216-1224.

Phillips, H. N., Blenkmann, A., Hughes, L. E., Bekinschtein, T. A., & Rowe, J. B. (2015). Hierarchical organization of frontotemporal networks for the prediction of stimuli across multiple dimensions. *Journal of Neuroscience, 35*(25), 9255-9264.

Picard, F., & Friston, K. (2014). Predictions, perception, and a sense of self. *Neurology, 83*(12), 1112-1118.

Piskulic, D., Barbato, M., Liu, L., & Addington, J. (2015). Pilot study of cognitive remediation therapy on cognition in young people at clinical high risk of psychosis. *Psychiatry research, 225*(1-2), 93-98.

Poels, E., Kegeles, L., Kantrowitz, J., Slifstein, M., Javitt, D., Lieberman, J., . . . Girgis, R. (2014). Imaging glutamate in schizophrenia: review of findings and implications for drug discovery. *Molecular psychiatry, 19*(1), 20.

Poletti, M., Tortorella, A., & Raballo, A. (2019). Impaired corollary discharge in psychosis and at risk states: integrating neurodevelopmental, phenomenological and clinical perspectives. *Biological Psychiatry: Cognitive Neuroscience and Neuroimaging*.

Pollok, B., Gross, J., Kamp, D., & Schnitzler, A. (2008). Evidence for anticipatory motor control within a cerebello-diencephalic-parietal network. *Journal of cognitive neuroscience, 20*(5), 828-840.

Poulet, & Hedwig, B. (2002). A corollary discharge maintains auditory sensitivity during sound production. *Nature, 418*(6900), 872-876.

Pratt, J., Dawson, N., Morris, B. J., Grent, T., Roux, F., & Uhlhaas, P. J. (2017). Thalamo-cortical communication, glutamatergic neurotransmission and neural oscillations: A unique window into the origins of ScZ? *Schizophrenia research, 180*, 4-12.

Pukrop, R., & Klosterkötter, J. (2010). Neurocognitive indicators of clinical high-risk states for psychosis: a critical review of the evidence. *Neurotoxicity research, 18*(3-4), 272-286.

Ranlund, S., Adams, R. A., Díez, Á., Constante, M., Dutt, A., Hall, M. H., . . . Schulze, K. (2016). Impaired prefrontal synaptic gain in people with psychosis and their relatives during the mismatch negativity. *Human brain mapping, 37*(1), 351-365.

Rao, R. P., & Ballard, D. H. (1999). Predictive coding in the visual cortex: a functional interpretation of some extra-classical receptive-field effects. *Nature neuroscience, 2*(1), 79-87.

Rapoport. (2005). The neurodevelopmental model of schizophrenia: update 2005. *Molecular psychiatry, 10*(5), 434.

Rapoport. (2012). Neurodevelopmental model of schizophrenia: update 2012. *Molecular psychiatry, 17*(12), 1228.

Read, J. (1997). Child abuse and psychosis: A literature review and implications for professional practice. *Professional Psychology: Research and Practice, 28*(5), 448.

Read, J., Perry, B. D., Moskowitz, A., & Connolly, J. (2001). The contribution of early traumatic events to schizophrenia in some patients: a traumagenic neurodevelopmental model. *Psychiatry: Interpersonal and Biological Processes, 64*(4), 319-345.

Read, J., van Os, J., Morrison, A. P., & Ross, C. A. (2005). Childhood trauma, psychosis and schizophrenia: a literature review with theoretical and clinical implications. *Acta Psychiatrica Scandinavica, 112*(5), 330-350.

Recasens, M., Gross, J., & Uhlhaas, P. J. (2018a). Low-frequency oscillatory correlates of auditory predictive processing in cortical-subcortical networks: A MEG-Study. *Scientific reports, 8*(1), 14007.

Recasens, M., Gross, J., & Uhlhaas, P. J. (2018b). Low-frequency oscillatory correlates of auditory predictive processing in cortical-subcortical networks: A MEG-Study. *Scientific reports, 8*(1), 1-12.

Ren, X., Fribance, S. N., Coffman, B. A., & Salisbury, D. F. (2021). Deficits in attentional modulation of auditory N100 in first – episode schizophrenia. *European Journal of Neuroscience*.

Reznik, D., Henkin, Y., Schadel, N., & Mukamel, R. (2014). Lateralized enhancement of auditory cortex activity and increased sensitivity to self-generated sounds. *Nature communications, 5*(1), 1-11.

Reznik, D., Ossmy, O., & Mukamel, R. (2015). Enhanced auditory evoked activity to self-generated sounds is mediated by primary and supplementary motor cortices. *Journal of Neuroscience, 35*(5), 2173-2180.

Ripke, S., Neale, B. M., Corvin, A., Walters, J. T., Farh, K.-H., Holmans, P. A., . . . Huang, H. (2014). Biological insights from 108 schizophrenia-associated genetic loci. *Nature, 511*(7510), 421.

Risch, N., & Merikangas, K. (1996). The future of genetic studies of complex human diseases. *Science, 273*(5281), 1516-1517.

Ritterband-Rosenbaum, A., Nielsen, J. B., & Christensen, M. S. (2014). Sense of agency is related to gamma band coupling in an inferior parietal-preSMA circuitry. *Frontiers in human neuroscience, 8*, 510.

Roiser, J. P., Wigton, R., Kilner, J. M., Mendez, M. A., Hon, N., Friston, K. J., & Joyce, E. M. (2013). Dysconnectivity in the frontoparietal attention network in schizophrenia. *Front Psychiatry, 4*, 176. doi:10.3389/fpsyt.2013.00176

Romans, S. E., & Seeman, M. V. (2006). *Women's mental health: A life-cycle approach*: Lippincott Williams & Wilkins.

Rosburg, T., Boutros, N. N., & Ford, J. M. (2008). Reduced auditory evoked potential component N100 in schizophrenia—a critical review. *Psychiatry research, 161*(3), 259-274.

Rösler, L., Rolfs, M., Van der Stigchel, S., Neggers, S. F., Cahn, W., Kahn, R. S., & Thakkar, K. N. (2015). Failure to use corollary discharge to remap visual target locations is associated with psychotic symptom severity in schizophrenia. *Journal of neurophysiology, 114*(2), 1129-1136.

Roth, M. J., Synofzik, M., & Lindner, A. (2013). The cerebellum optimizes perceptual predictions about external sensory events. *Current Biology, 23*(10), 930-935.

Roux, F., Wibral, M., Singer, W., Aru, J., & Uhlhaas, P. J. (2013). The phase of thalamic alpha activity modulates cortical gamma-band activity: evidence from resting-state MEG recordings. *Journal of Neuroscience, 33*(45), 17827-17835.

Ruhrmann, S., Schultze-Lutter, F., Salokangas, R. K., Heinimaa, M., Linszen, D., Dingemans, P., . . . Heinz, A. (2010). Prediction of psychosis in adolescents and young adults at high risk: results from the prospective European prediction of psychosis study. *Archives of general psychiatry, 67*(3), 241-251.

Rummell, B. P., Klee, J. L., & Sigurdsson, T. (2016). Attenuation of responses to self-generated sounds in auditory cortical neurons. *Journal of Neuroscience, 36*(47), 12010-12026.

Sato, M., Mengarelli, M., Riggio, L., Gallese, V., & Buccino, G. (2008). Task related modulation of the motor system during language processing. *Brain and language, 105*(2), 83-90.

Satterthwaite, T. D., Vandekar, S. N., Wolf, D. H., Bassett, D. S., Ruparel, K., Shehzad, Z., . . . Gennatas, E. D. (2015). Connectome-wide network analysis of youth with Psychosis-Spectrum symptoms. *Molecular psychiatry, 20*(12), 1508.

Savoie, F.-A., Thénault, F., Whittingstall, K., & Bernier, P.-M. (2018). Visuomotor prediction errors modulate EEG activity over parietal cortex. *Scientific reports, 8*(1), 1-16.

Schafer, & Marcus. (1973). Self-stimulation alters human sensory brain responses. *Science, 181*(4095), 175-177. doi:10.1126/science.181.4095.175

Schlosser, D. A., Campellone, T. R., Biagianti, B., Delucchi, K. L., Gard, D. E., Fulford, D., . . . Vinogradov, S. (2015). Modeling the role of negative symptoms in determining social functioning in individuals at clinical high risk of psychosis. *Schizophrenia research, 169*(1-3), 204-208.

Schmidt, A., & Borgwardt, S. (2013). Abnormal effective connectivity in the psychosis high-risk state. *NeuroImage, 81*, 119-120.

Schmidt, A., Smieskova, R., Aston, J., Simon, A., Allen, P., Fusar-Poli, P., . . . Borgwardt, S. (2013). Brain connectivity abnormalities predating the onset of psychosis: correlation with the effect of medication. *JAMA psychiatry, 70*(9), 903-912.

Schneider, D. M., Nelson, A., & Mooney, R. (2014). A synaptic and circuit basis for corollary discharge in the auditory cortex. *Nature, 513*(7517), 189-194.

Schultze-Lutter, F., Addington, J., Ruhrmann, S., & Klosterkötter, J. (2007). Schizophrenia proneness instrument, adult version (SPI-A). *Rome: Giovanni Fioriti*.

Schultze-Lutter, F., Debbané, M., Theodoridou, A., Wood, S. J., Raballo, A., Michel, C., . . . Uhlhaas, P. J. (2016). Revisiting the basic symptom concept: toward translating risk symptoms for psychosis into neurobiological targets. *Frontiers in psychiatry, 7*, 9.

Schultze-Lutter, F., Klosterkötter, J., Picker, H., Steinmeyer, E.-M., & Ruhrmann, S. (2007). Predicting first-episode psychosis by basic symptom criteria. *Clin Neuropsychiatry, 4*(1), 11-22.

Schultze-Lutter, F., Klosterkötter, J., & Ruhrmann, S. (2014). Improving the clinical prediction of psychosis by combining ultra-high risk criteria and cognitive basic symptoms. *Schizophrenia research, 154*(1-3), 100-106.

Schultze-Lutter, F., Michel, C., Schmidt, S. J., Schimmelmann, B., Maric, N., Salokangas, R., . . . Raballo, A. (2015a). EPA guidance on the early detection of clinical high risk states of psychoses. *European Psychiatry, 30*(3), 405-416.

Schultze-Lutter, F., Michel, C., Schmidt, S. J., Schimmelmann, B. G., Maric, N. P., Salokangas, R., . . . Raballo, A. (2015b). EPA guidance on the early detection of clinical high risk states of psychoses. *European Psychiatry, 30*(3), 405-416.

Schultze-Lutter, F., Ruhrmann, S., Berning, J., Maier, W., & Klosterkötter, J. (2010). Basic symptoms and ultrahigh risk criteria: symptom development in the initial prodromal state. *Schizophrenia Bulletin, 36*(1), 182-191.

Sheehan, D. V., Lecrubier, Y., Sheehan, K. H., Amorim, P., Janavs, J., Weiller, E., . . . Dunbar, G. C. (1998). The Mini-International Neuropsychiatric Interview (MINI): the development and validation of a structured diagnostic psychiatric interview for DSM-IV and ICD-10. *The Journal of clinical psychiatry*.

Sheffield, J. M., & Barch, D. M. (2016). Cognition and resting-state functional connectivity in schizophrenia. *Neurosci Biobehav Rev, 61*, 108-120. doi:10.1016/j.neubiorev.2015.12.007

Shenton, M. E., Dickey, C. C., Frumin, M., & McCarley, R. W. (2001). A review of MRI findings in schizophrenia. *Schizophrenia Research, 49*(1-2), 1-52.

Sherman, S. M. (2016). Thalamus plays a central role in ongoing cortical functioning. *Nature neuroscience, 19*(4), 533-541.

Sherman, S. M., & Guillery, R. W. (2006). *Exploring the thalamus and its role in cortical function*: MIT press.

Shim, G., Oh, J. S., Jung, W. H., Jang, J. H., Choi, C.-H., Kim, E., . . . Kwon, J. S. (2010). Altered resting-state connectivity in subjects at ultra-high risk for psychosis: an fMRI study. *Behavioral and Brain Functions, 6*(1), 58.

Shin, K. S., Jung, W. H., Kim, J. S., Jang, J. H., Hwang, J. Y., Chung, C. K., & Kwon, J. S. (2012). Neuromagnetic auditory response and its relation to cortical thickness in ultra-high-risk for psychosis. *Schizophrenia research, 140*(1-3), 93-98.

Simon, A. E., Borgwardt, S., Riecher-Rössler, A., Velthorst, E., de Haan, L., & Fusar-Poli, P. (2013). Moving beyond transition outcomes: meta-analysis of remission rates in individuals at high clinical risk for psychosis. *Psychiatry research, 209*(3), 266-272.

Simon, A. E., Dvorsky, D. N., Boesch, J., Roth, B., Isler, E., Schueler, P., . . . Umbricht, D. (2006). Defining subjects at risk for psychosis: a comparison of two approaches. *Schizophrenia research, 81*(1), 83-90.

Simons, C. J., Tracy, D. K., Sanghera, K. K., O'Daly, O., Gilleen, J., Krabbendam, L., & Shergill, S. S. (2010). Functional magnetic resonance imaging of inner speech in schizophrenia. *Biological psychiatry, 67*(3), 232-237.

Sitskoorn, M. M., Aleman, A., Ebisch, S. J., Appels, M. C., & Kahn, R. S. (2004). Cognitive deficits in relatives of patients with schizophrenia: a meta-analysis. *Schizophrenia research, 71*(2-3), 285-295.

Slotema, C. W., Blom, J. D., van Lutterveld, R., Hoek, H. W., & Sommer, I. E. (2014). Review of the efficacy of transcranial magnetic stimulation for auditory verbal hallucinations. *Biological psychiatry, 76*(2), 101-110.

Snitz, B. E., MacDonald III, A. W., & Carter, C. S. (2005). Cognitive deficits in unaffected first-degree relatives of schizophrenia patients: a meta-analytic review of putative endophenotypes.

Sokolov, B. P. (1998). Expression of NMDAR1, GluR1, GluR7, and KA1 glutamate receptor mRNAs is decreased in frontal cortex of "neuroleptic – free" schizophrenics: evidence on reversible up – regulation by typical neuroleptics. *Journal of neurochemistry, 71*(6), 2454-2464.

Sommer, M. A., & Wurtz, R. H. (2004). What the brainstem tells the frontal cortex. I. Oculomotor signals sent from superior colliculus to frontal eye field via mediodorsal thalamus. *J Neurophysiol*.

Sommer, M. A., & Wurtz, R. H. (2008). Brain circuits for the internal monitoring of movements. *Annu. Rev. Neurosci., 31*, 317-338.

Sperry, R. W. (1950a). Neural basis of the spontaneous optokinetic response produced by visual inversion. *Journal of comparative and physiological psychology, 43*(6), 482.

Sperry, R. W. (1950b). Neural basis of the spontaneous optokinetic response produced by visual inversion. *Journal of comparative and physiological psychology, 43*(6), 482-489.

St Clair, D., Xu, M., Wang, P., Yu, Y., Fang, Y., Zhang, F., . . . Sham, P. (2005). Rates of adult schizophrenia following prenatal exposure to the Chinese famine of 1959-1961. *Jama, 294*(5), 557-562.

Stenner, Bauer, Heinze, Haggard, & Dolan. (2015). Parallel processing streams for motor output and sensory prediction during action preparation. *Journal of neurophysiology, 113*(6), 1752-1762.

Stenner, Bauer, M., Sidarus, N., Heinze, H.-J., Haggard, P., & Dolan, R. J. (2014). Subliminal action priming modulates the perceived intensity of sensory action consequences. *Cognition, 130*(2), 227-235.

Stephan, K. E., Friston, K. J., & Frith, C. D. (2009). Dysconnection in schizophrenia: from abnormal synaptic plasticity to failures of self-monitoring. *Schizophrenia bulletin, 35*(3), 509-527.

Sterzer, P., Adams, R. A., Fletcher, P., Frith, C., Lawrie, S. M., Muckli, L., . . . Corlett, P. R. (2018). The predictive coding account of psychosis. *Biological psychiatry, 84*(9), 634-643.

Stone, J. M., Morrison, P. D., & Pilowsky, L. S. (2007). Glutamate and dopamine dysregulation in schizophrenia--a synthesis and selective review. *J Psychopharmacol, 21*(4), 440-452. doi:10.1177/0269881106073126

Strauss, G. P., Pelletier-Baldelli, A., Visser, K. F., Walker, E. F., & Mittal, V. A. (2020). A review of negative symptom assessment strategies in youth at clinical high-risk for psychosis. *Schizophrenia research*.

Su, Q., Yao, D., Jiang, M., Liu, F., Jiang, J., Xu, C., . . . Li, H. (2015). Increased functional connectivity strength of right inferior temporal gyrus in first-episode, drug-naive somatization disorder. *Australian & New Zealand Journal of Psychiatry, 49*(1), 74-81.

Suga, N., & Schlegel, P. (1972). Neural attenuation of responses to emitted sounds in echolocating bats. *Science, 177*(4043), 82-84.

Suga, N., & Shimozawa, T. (1974). Site of neural attenuation of responses to self-vocalized sounds in echolocating bats. *Science, 183*(4130), 1211-1213.

Sullivan. (1927). The onset of schizophrenia. *American Journal of Psychiatry, 84*(1), 105-134.

Sullivan, Kendler, K. S., & Neale, M. C. (2003). Schizophrenia as a complex trait: evidence from a meta-analysis of twin studies. *Archives of general psychiatry, 60*(12), 1187-1192.

Summerfield, C., Egner, T., Greene, M., Koechlin, E., Mangels, J., & Hirsch, J. (2006). Predictive codes for forthcoming perception in the frontal cortex. *Science, 314*(5803), 1311-1314.

Suvisaari, J., Mantere, O., Keinänen, J., Mäntylä, T., Rikandi, E., Lindgren, M., . . . Raij, T. T. (2018). Is it possible to predict the future in first-episode psychosis? *Frontiers in psychiatry, 9*, 580.

Synofzik, M., Lindner, A., & Thier, P. (2008). The cerebellum updates predictions about the visual consequences of one's behavior. *Current Biology, 18*(11), 814-818.

Tamminga, C. A. (2006). The neurobiology of cognition in schizophrenia. *The Journal of clinical psychiatry, 67*(9), e11-e11.

Tang, Y., Wang, J., Zhang, T., Xu, L., Qian, Z., Cui, H., . . . Shenton, M. E. (2019). P300 as an index of transition to psychosis and of remission: data from a clinical high risk for psychosis study and review of literature. *Schizophrenia research*.

Tang, Y., Wang, J., Zhang, T., Xu, L., Qian, Z., Cui, H., . . . Shenton, M. E. (2020). P300 as an index of transition to psychosis and of remission: data from a clinical high risk for psychosis study and review of literature. *Schizophrenia Research, 226*, 74-83.

Thakkar. (2015). Disrupted saccadic corollary discharge in schizophrenia. *Journal of Neuroscience, 35*(27), 9935-9945.

Thomas, M. L., Green, M. F., Hellemann, G., Sugar, C. A., Tarasenko, M., Calkins, M. E., . . . Lazzeroni, L. C. (2017). Modeling deficits from early auditory information processing to psychosocial functioning in schizophrenia. *JAMA psychiatry, 74*(1), 37-46.

Thompson, A. D., Bartholomeusz, C., & Yung, A. R. (2011). Social cognition deficits and the 'ultra high risk'for psychosis population: a review of literature. *Early intervention in psychiatry, 5*(3), 192-202.

Thornicroft, G. (1990). Cannabis and psychosis: is there epidemiological evidence for an association? *The British Journal of Psychiatry, 157*(1), 25-33.

Timm, J., SanMiguel, I., Keil, J., Schröger, E., & Schönwiesner, M. (2014). Motor intention determines sensory attenuation of brain responses to self-initiated sounds. *Journal of cognitive neuroscience, 26*(7), 1481-1489.

Toftdahl, N. G., Nordentoft, M., & Hjorthøj, C. (2016). Prevalence of substance use disorders in psychiatric patients: a nationwide Danish population-based study. *Social psychiatry and psychiatric epidemiology, 51*(1), 129-140.

Tso, I. F., Angstadt, M., Rutherford, S., Peltier, S., Diwadkar, V. A., & Taylor, S. F. (2020). Dynamic causal modeling of eye gaze processing in schizophrenia. *Schizophrenia Research*.

Uhlhaas, Pipa, G., Lima, B., Melloni, L., Neuenschwander, S., Nikolić, D., & Singer, W. (2009). Neural synchrony in cortical networks: history, concept and current status. *Frontiers in integrative neuroscience, 3*, 17.

Van Donkersgoed, R., Wunderink, L., Nieboer, R., Aleman, A., & Pijnenborg, G. (2015). Social cognition in individuals at ultra-high risk for psychosis: a meta-analysis. *PloS one, 10*(10), e0141075.

Van Os, J. (2009). A systematic review and meta-analysis of the psychosis continuum: evidence for a psychosis proneness-persistence-impairment model of psychotic disorder. *Psychological Medicine, 39*(2), 179.

Van Os, J., Linscott, R. J., Myin-Germeys, I., Delespaul, P., & Krabbendam, L. (2009). A systematic review and meta-analysis of the psychosis continuum: evidence for a psychosis proneness–persistence–impairment model of psychotic disorder. *Psychological medicine, 39*(2), 179-195.

Van Tricht, M. J., Nieman, D. H., Koelman, J. T., Mensink, A. J., Bour, L. J., Van der Meer, J. N., . . . De Haan, L. (2015). Sensory gating in subjects at ultra high risk for developing a psychosis before and after a first psychotic episode. *The world journal of biological psychiatry, 16*(1), 12-21.

Van Veen, B. D., Van Drongelen, W., Yuchtman, M., & Suzuki, A. (1997). Localization of brain electrical activity via linearly constrained minimum variance spatial filtering. *IEEE transactions on biomedical engineering, 44*(9), 867-880.

Veling, W., Susser, E., Van Os, J., Mackenbach, J. P., Selten, J.-P., & Hoek, H. W. (2008). Ethnic density of neighborhoods and incidence of psychotic disorders among immigrants. *American Journal of Psychiatry, 165*(1), 66-73.

Von Holst, E. (1954). Relations between the central nervous system and the peripheral organs. *British Journal of Animal Behaviour*.

von Holst, E., & Mittelstaedt, H. (1950). Das reafferenzprinzip. *Naturwissenschaften, 37*(20), 464-476.

Voss, M., Ingram, J. N., Haggard, P., & Wolpert, D. M. (2006). Sensorimotor attenuation by central motor command signals in the absence of movement. *Nature neuroscience, 9*(1), 26-27.

Walsh, L. D., Moseley, G. L., Taylor, J. L., & Gandevia, S. C. (2011). Proprioceptive signals contribute to the sense of body ownership. *The Journal of physiology, 589*(12), 3009-3021.

Wang, H., Guo, W., Liu, F., Wang, G., Lyu, H., Wu, R., . . . Zhao, J. (2016). Patients with first-episode, drug-naive schizophrenia and subjects at ultra-high risk of psychosis shared increased cerebellar-default mode network connectivity at rest. *Scientific reports, 6*, 26124.

Warburton, E., Wise, R. J., Price, C. J., Weiller, C., Hadar, U., Ramsay, S., & Frackowiak, R. S. (1996). Noun and verb retrieval by normal subjects studies with PET. *Brain, 119*(1), 159-179.

Weinberger, D. R. (1987). Implications of normal brain development for the pathogenesis of schizophrenia. *Archives of general psychiatry, 44*(7), 660-669.

Weiss, C., Herwig, A., & Schütz-Bosbach, S. (2011). The self in action effects: selective attenuation of self-generated sounds. *Cognition, 121*(2), 207-218.

Whitford, Ford, J. M., Mathalon, D. H., Kubicki, M., & Shenton, M. E. (2010). Schizophrenia, myelination, and delayed corollary discharges: a hypothesis. *Schizophrenia bulletin, 38*(3), 486-494.

Whitford, Jack, B. N., Pearson, D., Griffiths, O., Luque, D., Harris, A. W., . . . Le Pelley, M. E. (2017). Neurophysiological evidence of efference copies to inner speech. *Elife, 6*, e28197.

Whitford, Mathalon, D., Shenton, M. E., Roach, B., Bammer, R., Adcock, R., . . . Rausch, A. (2011). Electrophysiological and diffusion tensor imaging evidence of delayed corollary discharges in patients with schizophrenia. *Psychological Medicine, 41*(5), 959-969.

Whitford, Oestreich, L. K., Ford, J. M., Roach, B. J., Loewy, R. L., Stuart, B. K., & Mathalon, D. H. (2018). Deficits in cortical suppression during vocalization are associated with structural abnormalities in the arcuate fasciculus in early illness schizophrenia and clinical high risk for psychosis. *Schizophrenia bulletin, 44*(6), 1312-1322.

Winton-Brown, T., Schmidt, A., Roiser, J., Howes, O., Egerton, A., Fusar-Poli, P., . . . Kapur, S. (2017). Altered activation and connectivity in a hippocampal–basal ganglia–midbrain circuit during salience processing in subjects at ultra high risk for psychosis. *Translational psychiatry, 7*(10), e1245-e1245.

Wolpert, & Ghahramani, Z. (2000). Computational principles of movement neuroscience. *Nature neuroscience, 3*(11s), 1212.

Wolpert, Miall, R. C., & Kawato, M. (1998). Internal models in the cerebellum. *Trends in cognitive sciences, 2*(9), 338-347.

Woods, S. W., Walsh, B. C., Addington, J., Cadenhead, K. S., Cannon, T. D., Cornblatt, B. A., . . . Tarbox, S. I. (2014). Current status specifiers for patients at clinical high risk for psychosis. *Schizophrenia research, 158*(1-3), 69-75.

Xia, M., Wang, J., & He, Y. (2013). BrainNet Viewer: a network visualization tool for human brain connectomics. *PloS one, 8*(7), e68910.

Xu, M.-Q., Sun, W.-S., Liu, B.-X., Feng, G.-Y., Yu, L., Yang, L., . . . St. Clair, D. (2009). Prenatal malnutrition and adult schizophrenia: further evidence from the 1959-1961 Chinese famine. *Schizophrenia bulletin, 35*(3), 568-576.

Yoon, Y. B., Yun, J.-Y., Jung, W. H., Cho, K. I. K., Kim, S. N., Lee, T. Y., . . . Kwon, J. S. (2015). Altered fronto-temporal functional connectivity in individuals at ultra-high-risk of developing psychosis. *PloS one, 10*(8), e0135347.

Yung, A. R., & McGorry, P. D. (1996). The prodromal phase of first-episode psychosis: past and current conceptualizations. *Schizophrenia bulletin, 22*(2), 353-370.

Yung, A. R., McGorry, P. D., McFarlane, C. A., Jackson, H. J., Patton, G. C., & Rakkar, A. (1996). Monitoring and care of young people at incipient risk of psychosis. *Schizophrenia Bulletin, 22*(2), 283-303.

Yung, A. R., McGorry, P. D., McFarlane, C. A., Jackson, H. J., Patton, G. C., & Rakkar, A. (2004). Monitoring and care of young people at incipient risk of psychosis. *Focus, 22*(1), 283-174.

Yung, A. R., Yuen, H. P., McGorry, P. D., Phillips, L. J., Kelly, D., Dell'Olio, M., . . . Stanford, C. (2005). Mapping the onset of psychosis: the comprehensive assessment of at – risk mental states. *Australian and New Zealand Journal of Psychiatry, 39*(11 – 12), 964-971.

Zagha, E., Casale, A. E., Sachdev, R. N., McGinley, M. J., & McCormick, D. A. (2013). Motor cortex feedback influences sensory processing by modulating network state. *Neuron, 79*(3), 567-578.

Zakzanis, K. K., & Hansen, K. T. (1998). Dopamine D2 densities and the schizophrenic brain. *Schizophrenia research, 32*(3), 201-206.

Zaretsky, M., & ROWELL, C. F. (1979). Saccadic suppression by corollary discharge in the locust. *Nature, 280*(5723), 583-585.

Zatorre, R. J., Bouffard, M., Ahad, P., & Belin, P. (2002). Where is' where'in the human auditory cortex? *Nature neuroscience, 5*(9), 905-909.

Zatorre, R. J., Evans, A. C., Meyer, E., & Gjedde, A. (1992). Lateralization of phonetic and pitch discrimination in speech processing. *Science, 256*(5058), 846-849.

Zeidman, P., Jafarian, A., Seghier, M. L., Litvak, V., Cagnan, H., Price, C. J., & Friston, K. J. (2019). A guide to group effective connectivity analysis, part 2: Second level analysis with PEB. *Neuroimage, 200*, 12-25.

Ziermans, T. B., Schothorst, P. F., Sprong, M., & van Engeland, H. (2011). Transition and remission in adolescents at ultra-high risk for psychosis. *Schizophrenia research, 126*(1-3), 58-64.